

UNIVERSITÉ DU QUÉBEC

VARIABILITÉ DE LA PRODUCTION PRIMAIRE ET DE L'EXPORTATION DU
CARBONE ORGANIQUE PARTICULAIRE DANS LA ZONE MÉSOPÉLAGIQUE DE
L'OCÉAN ATLANTIQUE NORD-OUEST LORS DU DÉCLIN D'UN BLOOM
PRINTANIER DE DIATOMÉES

THÈSE
PRÉSENTÉE À
L'UNIVERSITÉ DU QUÉBEC À RIMOUSKI
comme exigence partielle
du programme de doctorat en océanographie

PAR
JULIEN POMMIER

OCTOBRE 2007

UNIVERSITÉ DU QUÉBEC À RIMOUSKI
Service de la bibliothèque

Avertissement

La diffusion de ce mémoire ou de cette thèse se fait dans le respect des droits de son auteur, qui a signé le formulaire « *Autorisation de reproduire et de diffuser un rapport, un mémoire ou une thèse* ». En signant ce formulaire, l'auteur concède à l'Université du Québec à Rimouski une licence non exclusive d'utilisation et de publication de la totalité ou d'une partie importante de son travail de recherche pour des fins pédagogiques et non commerciales. Plus précisément, l'auteur autorise l'Université du Québec à Rimouski à reproduire, diffuser, prêter, distribuer ou vendre des copies de son travail de recherche à des fins non commerciales sur quelque support que ce soit, y compris l'Internet. Cette licence et cette autorisation n'entraînent pas une renonciation de la part de l'auteur à ses droits moraux ni à ses droits de propriété intellectuelle. Sauf entente contraire, l'auteur conserve la liberté de diffuser et de commercialiser ou non ce travail dont il possède un exemplaire.

À mon père

Pour nos parties de pêche à pied au Passous, au cours desquelles l'estran, mis à nu selon les humeurs de Madame Marée, fut un formidable terrain de jeu et d'émerveillements.

De ces moments privilégiés j'ai découvert la curiosité ... et tout son cortège de questions.

De ces questions est née une passion.

*C'est en voulant connaître toujours d'avantage qu'on se rend compte
qu'on ne sait pas grand-chose*

(Pierre Dac – *Y'a du mou dans la corde à noeuds*)

C'est curieux chez les marins, ce besoin de faire des phrases

(Francis Blanche – *Les tontons flingueurs*)



(Bill Watterson – *Calvin & Hobbes*)

AVANT-PROPOS

Cette thèse aborde l'étude du devenir de la matière organique lors du déclin d'un bloom printanier de l'océan Atlantique nord-ouest et sa transition vers des conditions de post-bloom. Plus spécifiquement, ce travail traite de la relation entre la production primaire et le flux vertical de carbone organique particulaire dans la zone mésopélagique, deux composantes majeures de la pompe biologique de carbone dans les océans. Cette étude examine, lors d'un suivi lagrangien, le déclin d'une floraison printanière de diatomées afin de comprendre l'impact de la scénescence du bloom sur les flux océan-atmosphère de gaz actifs sur le plan climatique (dioxyde de carbone, CO₂; sulfure de diméthyle, DMS; gaz halogénés). Cette thèse est une contribution à la composante canadienne du programme de recherche international Surface Ocean – Lower Atmosphere Study (SOLAS).

Cette thèse est composée d'une introduction générale en français, de trois chapitres rédigés sous forme d'articles scientifiques en anglais, d'une conclusion générale et perspectives de recherche en français, et de la liste des références.

Le premier chapitre de la thèse décrit les changements dans la production, la biomasse, la structure de taille et la composition spécifique des communautés phytoplanctoniques, lors du déclin du bloom et sa transition vers des conditions de post-bloom. Ces résultats ont fait l'objet d'un article scientifique soumis pour publication dans la revue *Marine Ecology Progress Series* (*Pommier J, Gosselin M, Michel C, Size*

fractionated phytoplankton production and biomass during the decline of the northwest Atlantic spring bloom).

Le second chapitre décrit la variabilité temporelle des flux verticaux de carbone organique particulaire dans la partie supérieure de la zone mésopélagique (50-150 m), lors du déclin du bloom et sa transition vers des conditions de post-bloom. Les résultats de ce chapitre ont été rassemblés dans un second article soumis pour publication dans la revue *Marine Ecology Progress Series* (*Pommier J, Michel C, Gosselin M. Particulate organic carbon export in the upper twilight zone of the northwest Atlantic Ocean during the decline of the spring bloom*).

Le troisième chapitre présente un budget des stocks et des flux de carbone organique particulaire et dissous dans la zone euphotique et la zone mésopélagique pour la période du déclin du bloom. Les résultats de ce budget ont permis la préparation d'un troisième article qui sera soumis pour publication dans une revue à comité de lecture (*Pommier J, Gosselin M, Michel C. Carbon budget in the euphotic and upper twilight zones of the northwest Atlantic Ocean during the decline of the spring bloom*).

La conclusion générale résume les principaux résultats des trois chapitres de la thèse et expose les perspectives de recherche.

Les résultats rapportés dans cette thèse ont fait l'objet de deux affiches scientifiques et de quatre conférences présentées lors de divers congrès nationaux et internationaux (Assemblée générale annuelle Québec-Océan – 2004, 2005; SOLAS Science Meeting, Halifax – 2004; CMOS Congress, Vancouver – 2005; ASLO Summer Meeting, Santiago de Compostella – 2005; ASLO Aquatic Sciences Meeting, Santa Fé – 2007).

REMERCIEMENTS

Quelle que soit son ambition, une thèse de doctorat est tout sauf une entreprise solitaire. Elle ne repose pas sur la seule passion (voire la pure folie ...) d'un individu et son aboutissement implique le soutien d'un grand nombre de personnes que je souhaite, ici, remercier.

Je tiens, pour commencer, à exprimer toute mon estime à mon directeur de recherche, le professeur Michel Gosselin. Merci Michel, pour ton soutien intellectuel, ta grande disponibilité et ton support financier. Parmi les meilleurs souvenirs de mon doctorat figurent ces moments au cours desquels je venais te voir avec mes nombreuses questions de novice. Après m'avoir gratifié d'un « Coudonc, t'as rien appris à l'école 'stie ? », on s'asseyait et tu me donnais un véritable cours d'océanographie. Au fur et à mesure de l'avancement du doctorat, ces moments se sont transformés en de véritables et passionnantes discussions scientifiques. Tu es un excellent professeur Michel, le meilleur que j'ai eu la chance de côtoyer. Tu m'as enseigné des fondements scientifiques essentiels sur lesquels bâtir mon avenir dans le monde de la recherche océanographique. C'est un cadeau inestimable dont je te suis profondément reconnaissant. Je ne serais pas sans te remercier également pour la grande confiance dont tu as su faire montre à mon égard. Tout d'abord en faisant le pari un peu fou qu'un maudit cousin de France pourrait satisfaire les exigences de ce doctorat. Mais aussi en m'envoyant exposer les résultats de nos recherches dans de nombreux congrès nationaux et internationaux.

J'adresse également mes plus sincères remerciements et toute ma gratitude au docteur Christine Michel, co-directrice de cette thèse. Christine, la dynamique, la motivante ! Les rares fois où nous nous sommes rencontrés, cette thèse à fait un incroyable bon en avant. Tu as été un véritable carburant. De nos réunions ont émergé les grandes idées de cette thèse. Je tiens par ailleurs à remercier et exprimer tout mon respect au professeur Maurice Levasseur, examinateur externe de mon comité de thèse. Merci Maurice pour tes conseils scientifiques toujours avisés et judicieux. Merci également d'avoir su m'apporter un support « humain » à travers les exigences professionnelles d'un doctorat.

Je tiens à remercier le professeur Paul Tréguer d'avoir accepté de juger cette thèse en qualité d'examinateur externe. Ayant, par le passé, traîné ma blouse à l'Institut Universitaire Européen de la Mer, je suis très honoré que mes recherches doctorales soient jugées par un professeur de cet institut de recherche. Je remercie également le professeur Jean-Claude Brêthes d'avoir accepté la présidence du jury de ma thèse et, dans un tout autre registre, de m'avoir initié aux concepts fondamentaux (s'il en est) de la dimension Poznave des professeurs Albert Pozne et Jean-Paul Suave.

Un très grand et tout particulier remerciement au docteur Sylvie Roy, pour avoir coordonné avec brio les missions océanographiques SOLAS-SABINA et fait en sorte que celles-ci soient un véritable succès scientifique et une aventure inoubliable, depuis la baignade en pleine mer des Sargasses aux tempêtes automnales dans la mer du Labrador. Merci aussi, et surtout, Sylvie pour ton aide inestimable relative à la prise en charge des pièges à particules sur le terrain. Un grand merci également à Zhi-Ping Mei, Magdalena Różanska et Gitane Caron pour leur aide précieuse sur le terrain. Je remercie par ailleurs les

membres d'équipage de la Garde côtière canadienne dont le professionnalisme, l'efficacité et la sympathie ont fait le succès des missions océanographiques SOLAS-SABINA.

Ce projet de recherche doctorale a généré un important travail d'analyse en laboratoire, dont le grand mérite revient aux personnes suivantes, que je ne remercierai jamais assez : Marylin Gauthier, Mélanie Simard, Diane Bérubé, Dominique Hamel, Gitane Caron, Sylvie Lessard, Caroline Jose et Élise Roussel-Garneau.

Merci infiniment aux amis de Riki-sur-mer, qui ont fait de ces 4 (presque 5) années un séjour inoubliable : Fred & Léna, Pierre & Marion, Dothibeau, la gang d'Alternative113 (Marco, VT, Nick), Marion & Brice, Alain Richard @ IMQ, Karine, Seb & Vivi, Marc & Emma, Aurore, Youssouf, Magdalena, Khalida ... et tout particulièrement mes deux « frangins », Yann « El Padré » Alix et Xavier « El Chamal » Mouy, ainsi que Catherine « Maman Cathy » Bédard.

Un remerciement tout particulier à mes parents, Bernard & Christine, à mes soeurs, Marie & Émilie, et à ma douce moitié, Stéphanie, pour leur infaillible confiance, soutien, patience et amour.

Ce projet de recherche doctorale a été soutenu financièrement par les organismes suivants, que je remercie tout particulièrement : le Conseil de recherche en sciences naturelles et en génie (CRSNG) du Canada, la Fondation canadienne pour les sciences du climat et de l'atmosphère (FCSCA), le ministère des Pêches et des Océans (MPO) du Canada, le Fonds québécois de recherche sur la nature et les technologies (FQRNT),

l’Institut des sciences de la mer de Rimouski (ISMER) et le Groupement interinstitutionnel de recherche océanographique du Québec (Québec-Océan).

RÉSUMÉ

La compréhension des processus déterminant l'efficacité de transfert de la matière organique depuis la zone euphotique vers l'océan profond est essentielle afin de mieux appréhender le fonctionnement de la pompe biologique océanique de carbone. Néanmoins, une telle compréhension demeure limitée du fait du manque de connaissances relatives aux processus affectant la matière organique lors de son exportation dans la zone mésopélagique. Dans ce contexte, cette thèse vise à décrire la variabilité des flux de carbone organique particulaire (COP) dans la partie supérieure de la zone mésopélagique (50-150 m) de l'océan Atlantique nord-ouest, lors du déclin du bloom printanier et sa transition vers des conditions de post-bloom. La variabilité des flux de COP est mise en relation avec les changements temporels de la production, la biomasse, la composition spécifique et la structure de taille des communautés phytoplanctoniques.

Cette étude a permis de décrire le déclin de l'un des blooms les plus productifs rapportés pour les eaux ouvertes des latitudes tempérées de l'océan Atlantique Nord, sous l'influence d'une limitation de la production primaire par la disponibilité en nitrate. Durant le déclin du bloom, le gros phytoplancton ($\geq 5 \mu\text{m}$), principalement des diatomées centrales, dominait la production primaire et la biomasse phytoplanctonique. En conditions de post-bloom, le système précédemment étudié a été remplacé par un système productif dominé par les flagellés de petite taille (0,7-5 μm). L'analyse de la contribution relative du petit et du gros phytoplancton à la production et la biomasse phytoplanctonique totale a permis de proposer que la biomasse du petit phytoplancton est préférentiellement broutée par le microzooplancton tandis que celle du gros phytoplancton a tendance à s'accumuler dans la zone euphotique. Cette accumulation de cellules phytoplanctoniques est confirmée par la présence d'un maximum profond de chlorophylle *a* (MPC) au voisinage de la base de la zone euphotique, juste au-dessus de la nutricline, qui s'est maintenu pendant toute la durée de l'étude.

Une diminution des flux verticaux de COP sous la base de la zone euphotique (50 m) a été observée durant toute la durée de l'étude. Cette diminution était corrélée à la diminution de la production du gros phytoplancton. Malgré ces changements, les flux verticaux de COP à 150 m n'ont pas présenté de variations temporelles importantes. L'analyse des profils verticaux de flux de COP avec la profondeur a permis de mettre en évidence la réduction du recyclage de la matière organique dans la zone mésopélagique lors du déclin du bloom. De plus, l'intensité du recyclage de la matière organique dans la zone mésopélagique était positivement corrélée à l'exportation verticale de COP depuis la zone euphotique. Ces résultats démontrent que les communautés hétérotrophes mésopélagiques sont capables de répondre rapidement et proportionnellement aux variations des apports de COP depuis la zone euphotique. Ils mettent également en lumière le rôle déterminant des variations à court terme du recyclage du matériel organique par les organismes hétérotrophes dans la zone mésopélagique en regard à l'efficacité de transfert du COP en profondeur.

Un budget de carbone organique particulaire et dissous a été établi pendant le déclin du bloom. Pendant cette période, 67 % du COP des 150 premiers mètres de la colonne d'eau est resté en suspension alors que 30 % a été recyclé par les hétérotrophes et 3 % a été exporté en dessous de 150 m. Le maintien dans les 150 premiers mètres de la colonne d'eau d'une importante biomasse de COP reflète l'accumulation de cellules phytoplanctoniques au niveau du MPC. Ces résultats témoignent également de l'incapacité des hétérotrophes à utiliser toute la biomasse de carbone organique disponible dans cette couche. Cette difficulté à transformer le carbone organique présent dans les eaux de surface est confirmée par la réduction du recyclage du COP dans la zone mésopélagique lors du déclin du bloom. Le bilan de carbone a permis d'estimer le rapport entre la production primaire totale et la respiration par la communauté hétérotrophe lors du déclin du bloom. Ce rapport est en faveur de l'autotrophie nette du système étudié. Ce résultat est en accord avec le consensus voulant que l'océan Atlantique Nord soit un puits océanique de carbone.

TABLE DES MATIÈRES

AVANT-PROPOS	iii
REMERCIEMENTS.....	vi
RÉSUMÉ	x
TABLE DES MATIÈRES	xii
LISTE DES TABLEAUX	xvi
LISTE DES FIGURES	xviii
INTRODUCTION GÉNÉRALE	1
Réchauffement climatique et émissions anthropiques de CO ₂	1
Rôle des océans dans le cycle du carbone et le climat mondial	3
L'océan Atlantique Nord	4
Les pompes océaniques de carbone	6
La pompe physique (ou pompe de solubilité).....	6
La pompe biologique	8
La production primaire	8
L'exportation de carbone organique	11
Recyclage de la matière organique	18
Efficacité et intensité de la pompe biologique.....	20
Problématique	22
Objectifs.....	24
CHAPITRE I	
SIZE-FRACTIONATED PHYTOPLANKTON PRODUCTION AND BIOMASS DURING THE DECLINE OF THE NORTHWEST ATLANTIC SPRING BLOOM.....	28
RÉSUMÉ	28
ABSTRACT.....	28
1.1 Introduction.....	30
1.2 Materials and methods	32

1.2.1 Sampling	32
1.2.2 Analyses.....	34
1.2.3 Numerical analysis.....	38
1.3 Results.....	38
1.3.1 Physical and chemical environment	38
1.3.2 Phytoplankton abundance and composition	44
1.3.3 Chlorophyll <i>a</i> biomass	45
1.3.4 Primary production	50
1.3.5 Particulate organic carbon	53
1.4 Discussion.....	55
1.4.1 Environmental conditions and phytoplankton nutrient status.....	55
1.4.2 Formation and maintenance of the deep chlorophyll <i>a</i> maximum	57
1.4.3 The decline of the spring diatom bloom	60
1.4.4 Potential fate of large and small phytoplankton cells	62
1.5 Conclusion	64

CHAPITRE II

PARTICULATE ORGANIC CARBON EXPORT IN THE UPPER TWILIGHT ZONE OF THE NORTHWEST ATLANTIC OCEAN DURING THE DECLINE OF THE SPRING BLOOM.....	66
RÉSUMÉ	66
ABSTRACT.....	66
2.1 Introduction.....	68
2.2 Materials and methods	70
2.2.1 Sampling	70
2.2.2 Analyses.....	71
2.3 Results.....	77
2.3.1 Particulate organic carbon sinking fluxes.....	77
2.3.2 Chlorophyll <i>a</i> and phytoplankton cells sinking fluxes	80

2.3.3 Algal and fecal carbon sinking fluxes.....	82
2.4 Discussion.....	85
2.4.1 Linking particle sinking fluxes to epipelagic processes	85
2.4.2 Coupling between primary production and POC sinking export.....	87
2.4.3 Temporal variability in POC recycling in the upper twilight zone.....	90
2.4.4 Mesozooplankton grazing in the upper twilight zone.....	93
2.5 Conclusion	95

CHAPITRE III

CARBON BUDGET IN THE EUPHOTIC AND UPPER TWILIGHT ZONES OF THE NORTHWEST ATLANTIC OCEAN DURING THE DECLINE OF THE SPRING BLOOM	97
RÉSUMÉ	97
ABSTRACT.....	97
3.1 Introduction.....	99
3.2 Materials and methods	101
3.2.1 Sampling	101
3.2.2 Analyses.....	103
3.2.3 Numerical analyses	104
3.2.4 Particulate organic carbon budget.....	107
3.2.5 Dissolved organic carbon budget.....	109
3.3 Results.....	110
3.3.1 Carbon budget in the euphotic zone	114
3.3.2 Carbon budget in the upper twilight zone.....	115
3.4 Discussion.....	115
3.4.1 POC budget.....	115
3.4.2 DOC budget	116
3.4.3 Heterotrophic community respiration.....	120
3.4.4 Ecological significance of the carbon budget	122

CONCLUSION GÉNÉRALE.....	125
RÉFÉRENCES	134

LISTE DES TABLEAUX

CHAPITRE I

SIZE-FRACTIONATED PHYTOPLANKTON PRODUCTION AND BIOMASS DURING THE DECLINE OF THE NORTHWEST ATLANTIC SPRING BLOOM

Table 1. Daily variations in the water column structure: depth of the surface mixed layer (Z_{mix}), depth of the 0.2% surface PAR (Z_{eu}), depth of the nutricline (Z_{nutr}), average temperature and salinity in the surface mixed layer (SML) and between Z_{mix} and Z_{eu} ($Z_{\text{mix}}-Z_{\text{eu}}$). Standard deviations of temperature and salinity are indicated in parentheses when applicable.....	39
Table 2. Daily variations in the integrated molar ratio of dissolved inorganic nitrogen (DIN) to phosphate (DIN:PO ₄) and to silicic acid (DIN:Si(OH) ₄) averaged over the surface mixed layer (SML) and between the depth of the surface mixed layer and the base of the euphotic zone ($Z_{\text{mix}}-Z_{\text{eu}}$). Standard deviations are indicated in parentheses.....	44
Table 3. Temporal variations in total chlorophyll <i>a</i> (chl <i>a</i>) sinking velocity at depths of 50% and 5% surface PAR. ND: No data available	48

CHAPITRE II

PARTICULATE ORGANIC CARBON EXPORT IN THE UPPER TWILIGHT ZONE OF THE NORTHWEST ATLANTIC OCEAN DURING THE DECLINE OF THE SPRING BLOOM

Table 1. Characteristics of the free-drifting particle interceptor trap moorings and of the upper water column in the northwest Atlantic in spring 2003. The depths of the euphotic zone (Z_{eu}) and of the surface mixed layer (Z_{mix}) are from Pommier et al. (ms-a, Chapitre I)	73
Table 2. Carbon sinking fluxes of the three major phytoplankton groups and of fecal pellet carbon attributed to copepods and appendicularians below the base of the euphotic zone (below Z_{eu}) and at 150 m throughout the study period. The percent contributions (%) of total phytoplankton carbon and total fecal pellet carbon to the total particulate organic carbon sinking fluxes are also reported.....	84

CHAPITRE III

CARBON BUDGET IN THE EUPHOTIC AND UPPER TWILIGHT ZONES OF THE NORTHWEST ATLANTIC OCEAN DURING THE DECLINE OF THE SPRING BLOOM

Table 1. Definition, units and constant value (when applicable) of the variables used in the carbon budget for the euphotic and upper twilight zones. NA is not applicable.....	105
Table 2. Daily rates of total primary production (PP), particulate primary production (P_{POC}) and phytoplankton dissolved organic carbon release (P_{DOC}) integrated over the euphotic zone and of vertical sinking fluxes of particulate organic carbon at 50 and 150 m (F_{50m} and F_{150m} , respectively) during a Lagrangian study of the decline of a spring bloom in the northwest Atlantic Ocean in 2003. The daily rates of each variable were summed from days 1 to 6 to estimate total values for the Lagrangian study period. The sinking fluxes on days 1, 3 and 5 (italics) were estimated from the regressions between F_{50m} and P_{POC} and between F_{150m} and P_{POC} which were computed from values on days 2, 4 and 6. See Materials and methods for more details.....	111
Table 3. Concentrations of particulate (POC) and dissolved (DOC) organic carbon integrated over the euphotic zone and the upper twilight zone of the northwest Atlantic Ocean at the beginning (day 1) and the end (day 7) of a Lagrangian study of the decline of the spring bloom in 2003. The semi-labile (DOC_{SL}) and labile (DOC_L) fractions of the total DOC stock (DOC_T) are indicated. Minimum and maximum estimates of bacterial respiration on labile DOC (R_{DOC_L}) from days 1 to 7 were calculated based on bacterial growth efficiencies of 34% (Rivkin & Legendre 2001) and 5% (del Giorgio & Cole 2000), respectively. See Materials and Methods for more details on estimates of DOC fractions and bacterial respiration.....	112

LISTE DES FIGURES

INTRODUCTION GÉNÉRALE

- Fig. 1.** Représentation schématique des pompes océaniques de carbone. La pompe physique, ou pompe de solubilité, assure la dissolution du CO₂ atmosphérique dans les eaux océaniques de surface, sous l'influence de la température et du gradient de pression partielle de CO₂. Le carbone inorganique dissous dans les eaux de surface est ensuite exporté vers l'océan profond lors de la plongée des eaux de surface au sein de cellules de convection. La pompe biologique résulte, quant à elle, de l'action combinée de la photosynthèse phytoplanctonique dans la zone euphotique, de l'exportation de matériel organique vers l'océan profond et du recyclage de la matière organique au sein des réseaux trophiques pélagiques. Source: Bopp et al. (2002). Reproduit avec l'autorisation de l'auteur 7
- Fig. 2.** Représentation schématique du « Mandala » de Margalef selon lequel la turbulence détermine la concentration en nutriments du milieu et la succession écologique d'espèces phytoplanctoniques depuis les diatomées de grande taille, à stratégie démographique de type r, vers les flagellés de petite taille, à stratégie démographique de type K. Redessinée d'après Margalef (1997) 12
- Fig. 3.** Modèle dichotomique de l'export de matériel biogénique en fonction de la taille des cellules phytoplanctoniques et de singularités de l'environnement hydrodynamique D'après Legendre & Le Fèvre (1989) 14

CHAPITRE I

SIZE-FRACTIONATED PHYTOPLANKTON PRODUCTION AND BIOMASS DURING THE DECLINE OF THE NORTHWEST ATLANTIC SPRING BLOOM

- Fig. 1.** Location of the sampling sites from 25 April (day 1) to 01 May (day 7) during a Lagrangian study of a water mass in the northwest Atlantic Ocean in spring 2003. On 14 May (day 20), the ship went back to the latitude/longitude position occupied on day 1 33
- Fig. 2.** Contour plots for (a) sigma-t (kg m⁻³), (b) temperature (°C), and (c) salinity in the upper 80 m of the northwest Atlantic Ocean throughout the Lagrangian study period (days 1 to 7) and on days 19 to 21 40

Fig. 3. Temporal variations of the temperature–salinity diagrams of the upper 350 m of the water column throughout the Lagrangian study period (days 1 to 7) and on day 20.....	41
Fig. 4. Temporal variations in the average concentrations of (a) nitrate+nitrite ($\text{NO}_3 + \text{NO}_2$), (b) ammonium (NH_4), (c) phosphate (PO_4) and (d) silicic acid ($\text{Si}(\text{OH})_4$) integrated over the surface mixed layer depth (Z_{mix}) and between Z_{mix} and the base of the euphotic zone ($Z_{\text{mix}} - Z_{\text{eu}}$) (average \pm standard deviation).....	43
Fig. 5. Vertical profiles of size-fractionated chlorophyll <i>a</i> (chl <i>a</i>) concentration throughout the study period. B_L : biomass of large phytoplankton cells ($\geq 5 \mu\text{m}$), B_S : biomass of small phytoplankton cells ($0.7\text{--}5 \mu\text{m}$), B_T : total chl <i>a</i> biomass (i.e. $B_L + B_S$), Z_{mix} : depth of the surface mixed layer, Z_{eu} : depth of the euphotic zone.....	46
Fig. 6. Temporal variations in the size-fractionated chlorophyll <i>a</i> (chl <i>a</i>) concentration (a, b) and primary production (c, d) integrated over the surface mixed layer depth (Z_{mix}) (a, c) and between Z_{mix} and the base of the euphotic zone (b, d). B_L : biomass of large phytoplankton cells ($\geq 5 \mu\text{m}$), B_S : biomass of small phytoplankton cells ($0.7\text{--}5 \mu\text{m}$), P_L : particulate production of large phytoplankton cells ($\geq 5 \mu\text{m}$), P_S : particulate production of small phytoplankton cells ($0.7\text{--}5 \mu\text{m}$), P_{DOC} : dissolved organic carbon release rate. Bars in c) and d) represent the standard deviation of total production (i.e. $P_L + P_S + P_{\text{DOC}}$)	47
Fig. 7. Vertical profiles of size-fractionated primary production throughout the study period. P_L : particulate production of large phytoplankton cells ($\geq 5 \mu\text{m}$), P_S : particulate production of small phytoplankton cells ($0.7\text{--}5 \mu\text{m}$), P_T : total production (particulate and dissolved production), Z_{mix} : depth of the surface mixed layer, Z_{eu} : depth of the euphotic zone.....	49
Fig. 8. Temporal variations in the particulate primary production normalized to total chlorophyll <i>a</i> (chl <i>a</i>) biomass of large ($P_L:B_L$) and small ($P_S:B_S$) phytoplankton cells integrated over the surface mixed layer depth (Z_{mix}) and between Z_{mix} and the base of the euphotic zone ($Z_{\text{mix}} - Z_{\text{eu}}$)	52
Fig. 9. Vertical profiles of the ratio of particulate organic carbon to total chlorophyll <i>a</i> (POC:chl <i>a</i>) throughout the study period. Z_{mix} : depth of the surface mixed layer, Z_{eu} : depth of the euphotic zone	54

CHAPITRE II

PARTICULATE ORGANIC CARBON EXPORT IN THE UPPER TWILIGHT ZONE OF THE NORTHWEST ATLANTIC OCEAN DURING THE DECLINE OF THE SPRING BLOOM

- Fig. 1.** Location of the drifting buoy from day 1 (25 April) to day 7 (01 May) during a Lagrangian study of a water mass in the northwest Atlantic Ocean in spring 2003. On day 20 (14 May), the ship went back to the latitude/longitude position occupied on day 1. Filled circles indicate the sampling days during which concomitant measurements of primary production and particulate organic material sinking fluxes were made 72
- Fig. 2.** Vertical profiles of temperature (T, solid line), salinity (S, short-dashed line) and sigma-t (σ_t , long-dashed line) in the upper 400 m of the water column on day 4 (28 April 2003) of a Lagrangian study of a water mass in the northwest Atlantic Ocean. The horizontal dashed lines indicate the depths of the shallowest (50 m) and deepest (150 m) particle interceptor traps 74
- Fig. 3.** Temporal changes in the vertical profiles of particulate organic carbon (POC) sinking flux from 50 m to 150 m (mean \pm standard deviation). For each day, the symbols represent the observed data; the curve is a moving average ($n = 2$) 78
- Fig. 4.** Temporal changes in (a) size-fractionated particulate primary production integrated over the euphotic zone depth based on measurements reported in Pommier et al. (ms-a, Chapitre I), (b) particulate organic carbon (POC) sinking flux below the base of the euphotic zone (below Z_{eu} , i.e., at 50 m from days 2 to 6 and at 75 m on day 20) and at 150 m and (c) export ratio below Z_{eu} and at 150 m. Mean values and standard deviations are presented for each variable. In (a), the production values of small (P_S : 0.7–5 μm) and large (P_L : $\geq 5 \mu\text{m}$) phytoplankton cells are indicated 79
- Fig. 5.** Temporal changes in (a) chlorophyll *a* (chl *a*) sinking fluxes, (b) the ratio of chl *a* to total pigment (i.e., chl *a* + pheopigments) and (c) the sinking flux of phytoplankton cells below the base of the euphotic zone (below Z_{eu} i.e., at 50 m from days 2 to 6 and at 75 m on day 20) and at 150 m. Mean values and standard deviations are presented for each variable. In (c), the percent contribution of diatoms to the total phytoplankton cell sinking fluxes below Z_{eu} (open circles) and at 150 m (filled circles) are also indicated 81

- Fig. 6.** Temporal changes in (a) intact phytoplankton carbon sinking fluxes, (b) the percent contribution of the three major phytoplankton groups (Diat: diatoms, Dinofl: dinoflagellates, Other fl: other flagellates) to total phytoplankton carbon sinking fluxes and (c) fecal pellet carbon sinking fluxes below the base of the euphotic zone (below Z_{eu} , i.e., at 50 m from days 2 to 6 and at 75 m on day 20) and at 150 m. In (a), mean values and standard deviations are presented. For each sampling day in (b), the left and right stacked bars are relative to the flux below Z_{eu} and at 150 m, respectively..... 83

CHAPITRE III

CARBON BUDGET IN THE EUPHOTIC AND UPPER TWILIGHT ZONES OF THE NORTHWEST ATLANTIC OCEAN DURING THE DECLINE OF THE SPRING BLOOM

- Fig. 1.** Location of the drifting buoy from 25 April (day 1) to 01 May 2003 (day 7) during a Lagrangian study of the decline of the spring bloom in the northwest Atlantic Ocean 102

- Fig. 2.** Budget of dissolved and particulate organic carbon in the euphotic and upper twilight zones of the northwest Atlantic Ocean during a Lagrangian study conducted from 25 April (day 1) to 01 May 2003 (day 7). 113

INTRODUCTION GÉNÉRALE

Selon la Convention-cadre des Nations-Unies sur le changement climatique (CCNUCC), on entend par changement climatique le changement du climat attribuable directement ou indirectement aux activités humaines, altérant la composition de l'atmosphère mondiale et venant s'ajouter à la variabilité naturelle du climat observée au cours de périodes comparables. Le terme changement climatique, tel qu'utilisé par le Groupe d'experts intergouvernemental sur l'évolution du climat (GIEC), désigne quant à lui le changement du climat dans le temps, qu'il soit dû à la variabilité naturelle ou bien provoqué par les activités humaines. Quelles qu'en soient les nuances, ces définitions ont en commun la prise de conscience de la place de l'homme dans la biosphère et de ses impacts sur son environnement.

Réchauffement climatique et émissions anthropiques de CO₂

Selon le dernier rapport du GIEC (IPCC 2007), le réchauffement du système climatique est sans équivoque. Un nombre croissant d'observations nous donne aujourd'hui une image d'ensemble d'une planète qui se réchauffe, reflétant la modification à la hausse du bilan radiatif à la surface de la Terre au cours du siècle dernier. De 1906 à 2005, la température moyenne à la surface du globe (i.e. moyenne de la température de l'air près de la surface du sol et de la température de surface de la mer) s'est accrue de 0.76°C (IPCC 2007). Cette augmentation de la température de surface est la plus forte du dernier millénaire (Mann & Jones 2003), la dernière décennie étant la plus chaude enregistrée

depuis 1850, date à partir de laquelle on dispose d'enregistrements de la température de surface (IPCC 2007). Depuis la seconde moitié du vingtième siècle, ce signal thermique s'est ressenti dans les 8000 premiers mètres de la troposphère (IPCC 2001). Une augmentation de la charge thermique a également été détectée dans l'ensemble des bassins océaniques jusqu'à 3000 m de profondeur (Levitus et al. 2000, Barnett et al. 2001).

La modification à la hausse du bilan radiatif terrestre est très vraisemblablement imputable à l'augmentation des concentrations atmosphériques de gaz à effet de serre d'origine anthropique (IPCC 2007). Parmi ceux-ci, le dioxyde de carbone (CO_2) joue un rôle majeur. Il explique en particulier 32 % du réchauffement climatique contemporain (Mann et Lazier 1996). Depuis 1750 (début de l'ère industrielle), les concentrations atmosphériques de CO_2 ont augmenté d'environ 36 %, passant de 278 à 379 ppm (IPCC 2007), et dépassent aujourd'hui largement la gamme de variations naturelles des 420 000 dernières années (Petit et al. 1999). L'émission annuelle de CO_2 anthropique vers l'atmosphère pour la décennie 1980 a été estimée à $7,1 \pm 1,1 \text{ Pg C}$ (Sarmiento & Gruber 2002). On estime qu'environ 75 % de ces émissions sont liés à l'exploitation de combustibles fossiles, le reste étant imputable, pour l'essentiel, aux modifications de l'utilisation des sols, plus particulièrement au déboisement. Près de la moitié des émissions annuelles de CO_2 anthropique ($3,2 \pm 2 \text{ Pg C}$) est accumulée dans l'atmosphère, la différence étant captée par les puits de carbone continental ($1,9 \pm 1,6 \text{ Pg C}$) et océanique ($2,0 \pm 0,9 \text{ Pg C}$) (Sarmiento et al. 2000, Sarmiento & Gruber 2002). Alors qu'une grande incertitude demeure quant à l'importance du puits de carbone continental, les océans sont

considérés comme le principal puits de carbone à l'échelle de la planète et leur importance dans le cycle global du carbone est aujourd'hui sans équivoque.

Rôle des océans dans le cycle du carbone et le climat mondial

De par leurs interactions avec l'atmosphère, les océans sont des régulateurs majeurs de la composition atmosphérique et donc du climat. Recouvrant 72 % de la surface de la Terre, ils constituent une composante majeure du système climatique, échangeant avec l'atmosphère d'importantes quantités de chaleur, d'eau, de gaz et de moment (Bigg et al. 2003). Les échanges thermiques entre l'océan et l'atmosphère permettent une redistribution de la chaleur emmagasinée à l'équateur vers les pôles et sont à la base de la circulation thermohaline, mécanisme majeur de régulation des conditions climatiques à la surface du globe (Bigg et al. 2003). Les océans jouent également un rôle important dans la modulation annuelle, décennale et millénaire de la concentration atmosphérique de dioxyde de carbone (Raven & Falkowski 1999). Sous l'action de la pompe de solubilité, de la pompe biologique et de la pompe de carbonate (Volk & Hoffert 1985, Longhurst & Harrison 1989, Longhurst 1991), des échanges actifs de CO₂ se produisent entre l'atmosphère et l'océan. En absorbant environ un tiers des émissions anthropiques de ce gaz, les océans constituent l'un des puits majeurs de carbone atmosphérique. On estime que les océans ont contribué à l'absorption de 26 % à 44 % des émissions anthropiques de CO₂ depuis le début l'ère industrielle (Tans et al. 1990). La production primaire nette océanique (i.e. la fixation photosynthétique de carbone inorganique dissous et sa transformation en matière organique par le phytoplancton marin) permet la formation annuelle de 45-50 Pg de carbone

organique dont 16 Pg sont exportés chaque année vers l'océan profond (Falkowski et al. 1998). Ces flux de carbone sont assurés par une biomasse phytoplanctonique d'environ 1 Pg de carbone, soit 0,2 % de la biomasse photosynthétique mondiale (Falkowski et al. 1998). Le réservoir océanique de carbone total (carbone organique et inorganique, dissous et particulaire) est aujourd'hui estimé à environ 38 000 Pg, soit près de 60 fois le réservoir atmosphérique (Watson & Orr 2003). Ainsi, la moindre perturbation des processus biogéochimiques et physiques liés au cycle océanique du carbone peut profondément modifier la concentration atmosphérique de CO₂ (Watson et Orr 2003).

L'océan Atlantique Nord

En regard au rôle crucial des océans dans le cycle global du carbone, l'océan Atlantique Nord revêt une importance particulière. Bordé par les continents nord-américain et européen, il est l'océan le plus exposé aux émissions anthropiques de CO₂ (Koeve & Ducklow 2001). Cet océan est l'une des zones océaniques les plus productives de l'océan mondial (Harrison et al. 1993). Sathyendranath et al. (1995) y ont estimé la production primaire annuelle à 10,5 Pg C. Il représente le plus important puits océanique de carbone de l'hémisphère Nord (Gruber et al. 2002). L'absorption annuelle de carbone anthropique y a été estimée entre 0,7 ± 0,1 Pg C (Gruber et al. 2002) et 1,0 Pg C (Doney et al. 2000) soit près de la moitié du puits de carbone océanique mondial. Il constitue également l'un des sites prépondérants de formation d'eau profonde (mers du Labrador, du Groenland et de Norvège) gouvernant la circulation thermohaline et régissant la pompe de solubilité (Siegenthaler & Sarmiento 1993).

L'océan Atlantique Nord est un également un vaste bassin océanique au niveau duquel sont observées de grandes variations saisonnières des conditions atmosphériques, thermiques et lumineuses. Celles-ci se traduisent dans l'océan par la succession d'une période hivernale de fort mélange vertical de la colonne d'eau, assurant l'apport de nutriments depuis l'océan profond vers la zone euphotique, et de la stratification progressive des eaux de surface au printemps, assurant le maintien des cellules phytoplanctoniques au-dessus de la profondeur critique (Sverdrup 1953, Smetacek & Passow 1990). Cette saisonnalité marquée des conditions océanographiques de l'océan Atlantique Nord se traduit, aux latitudes tempérées et subpolaires, par le développement au printemps d'une importante floraison phytoplanctonique (ou bloom), dominée par les diatomées de grande taille (Colebrook 1979) et qui constitue l'un des événements les plus remarquables de l'océan mondial (Ducklow & Harris 1993, Koeve & Ducklow 2001).

L'océan Atlantique Nord représente donc un terrain idéal en regard à l'étude de l'influence des océans sur le cycle général du carbone. À cet égard, les programmes de recherche WOCE (World Ocean Circulation Experiment) et JGOFS (Joint Global Ocean Flux Study) ont constitué les premières initiatives internationales d'envergure visant à comprendre les processus biogéochimiques et physiques liés au cycle du carbone océanique et leurs influences sur les concentrations atmosphériques de CO₂ et le climat. Ils ont en particulier permis d'améliorer considérablement les connaissances relatives au fonctionnement des pompes océaniques de carbone.

Les pompes océaniques de carbone

Les échanges de CO₂ entre l'océan et l'atmosphère sont régis par un ensemble de processus physicochimiques et biologiques déterminant les pompes physique et biologique de carbone (Fig. 1).

La pompe physique (ou pompe de solubilité)

Elle assure la solubilisation de CO₂ atmosphérique dans les eaux océaniques de surface, sous le contrôle de la température et du gradient de pression partiel de CO₂ entre l'atmosphère et l'océan (Takahashi 1989). Le CO₂, une fois dissous dans l'eau de mer (CO_{2-aq}), réagit avec celle-ci pour former de l'acide carbonique (H₂CO₃), des ions bicarbonate (HCO₃⁻) et carbonate (CO₃²⁻) selon l'équation 1 :



Cet équilibre complexe entre le CO₂ atmosphérique et les différentes formes ioniques du CO₂ aqueux défini le système de carbonate qui assure le rôle tampon de l'eau de mer en lui conférant un pH relativement stable compris entre 8,0 et 8,3 et pouvant atteindre temporairement une valeur de 9 lors d'une floraison phytoplanctonique (Mann & Lazier 1996). En déterminant l'orientation de la chaîne de réaction du système de carbonates, le pH de l'eau de mer contrôle ainsi la pression partielle de CO₂ dans les eaux de surface et donc le flux océan-atmosphère de CO₂.

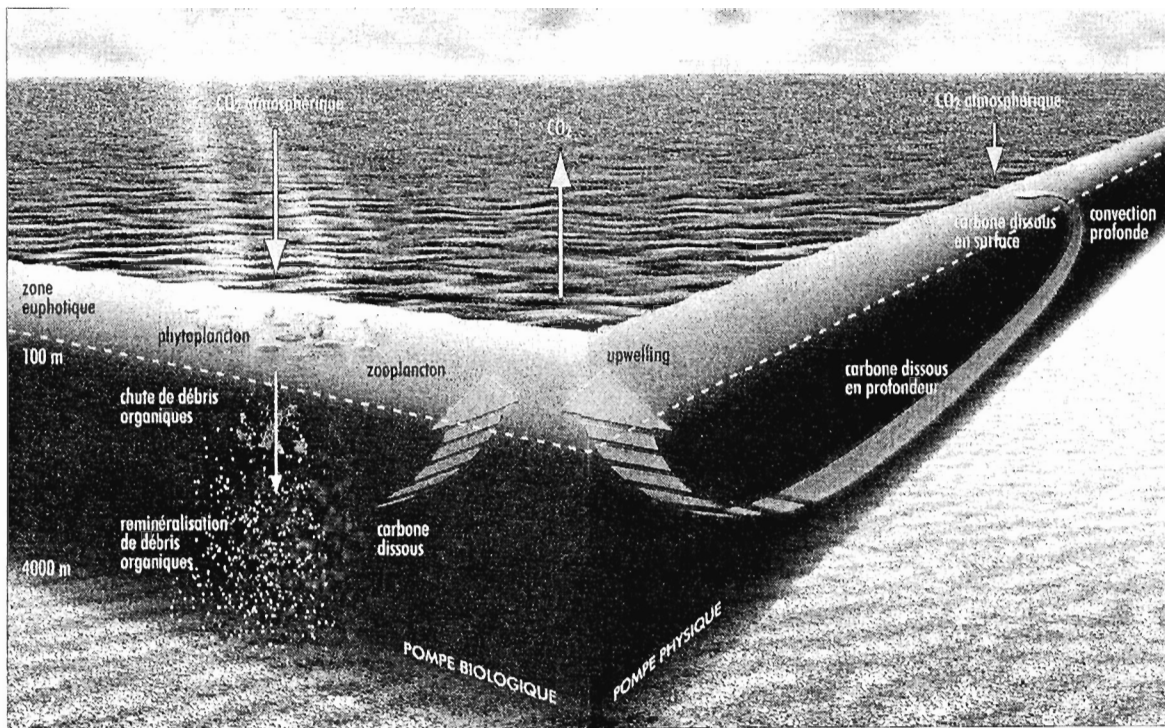


Fig. 1. Représentation schématique des pompes océaniques de carbone. La pompe physique, ou pompe de solubilité, assure la dissolution du CO₂ atmosphérique dans les eaux océaniques de surface, sous l'influence de la température et du gradient de pression partielle de CO₂. Le carbone inorganique dissous dans les eaux de surface est ensuite exporté vers l'océan profond lors de la plongée des eaux de surface au sein de cellules de convection. La pompe biologique résulte, quant à elle, de l'action combinée de la photosynthèse phytoplanctonique dans la zone euphotique, de l'exportation de matériel organique vers l'océan profond et du recyclage de la matière organique au sein des réseaux trophiques. Source : Bopp et al. (2002). Reproduit avec l'autorisation de l'auteur

La pompe de solubilité est particulièrement importante aux latitudes polaires et subpolaires de l'océan mondial où la faible température des eaux de surface permet de dissoudre une grande quantité de CO₂. De plus, les mers des hautes latitudes (mers de Ross et de Weddell en Antarctique, mers du Labrador, du Groenland et de Norvège dans l'Atlantique Nord) sont des lieux importants de plongée des eaux de surface formant les masses d'eau intermédiaires et profondes. Cette plongée des eaux de surface est à la base de

la circulation thermohaline et permet la séquestration d'une grande quantité de carbone inorganique dissous dans la circulation océanique profonde.

La pompe biologique

La pompe biologique de carbone est la résultante de trois processus permettant d'entretenir un gradient vertical de carbone inorganique dissous (CID) favorable au flux de CO₂ depuis l'atmosphère vers les eaux de surface. Ces processus sont : (1) la production photosynthétique de carbone organique, (2) l'exportation du matériel organique vers l'océan profond, et (3) le recyclage de la matière organique lors de son exportation.

La production primaire

La photosynthèse phytoplanctonique au sein de la zone euphotique assure la fixation de carbone inorganique dissous dans la matière organique selon l'équation 2 :



où la molécule « CH₂O » est l'élément de base des glucides. La photosynthèse phytoplanctonique assure ainsi la production primaire de matière organique, à la base des réseaux alimentaires pélagiques.

Deux facteurs majeurs limitent la photosynthèse, et donc la production primaire : (1) la lumière, qui fournit la source d'énergie nécessaire à la photolyse de l'eau (première phase, dite « lumineuse », de la photosynthèse) et (2) la disponibilité en nutriments. De

manière générale, aux latitudes tempérées et subpolaires de l'océan Atlantique Nord, la limitation de la photosynthèse par la lumière intervient principalement durant la période précédant le bloom printanier, lorsque le mélange vertical est tel qu'il entraîne les cellules phytoplanctoniques en deçà de la profondeur critique (Sverdrup 1953, Smetacek & Passow 1990). La limitation de la photosynthèse par la lumière peut également intervenir à la base de la zone euphotique. À cet égard, l'augmentation de la concentration intracellulaire en chlorophylle représente un moyen par lequel les cellules phytoplanctoniques, au voisinage de la base de la zone euphotique, peuvent s'acclimater aux faibles intensités lumineuses et éventuellement contribuer à la formation du maximum profond de chlorophylle (Cullen 1982). La limitation de la photosynthèse par les nutriments dans l'Atlantique Nord intervient principalement à la fin du bloom printanier, lorsque la croissance du phytoplancton est limitée par la pauvreté des eaux de surface en azote et en silicium dissous (Platt et al. 1992, Sieracki et al. 1993, Falkowski et al. 1998, Leblanc et al. 2005). Du fait des apports éoliens (depuis le désert saharien) et fluviaux, la production primaire au sein de l'Atlantique Nord ne serait pas limitée par le fer (Falkowski et al. 1998). Cependant, ce paradigme a été remis en cause par Blain et al. (2004) selon lesquels la production des diatomées aux latitudes tempérées de l'Atlantique du nord-est peut être co-limitée par le fer et le silicium dissous. De plus, au sein de systèmes dominés par les cyanobactéries diazotrophes (libres, en colonies ou endosymbiontes), tels que rencontrés aux latitudes tropicales et subtropicales, la production primaire est limitée par la disponibilité en fer et en phosphate (Michaels et al. 2001, Karl et al. 2003, Mills et al. 2004).

La source d'azote supportant la production primaire est déterminante pour la pompe biologique océanique de carbone. Ainsi, au sein de systèmes où le mélange vertical saisonnier de la colonne d'eau injecte une grande quantité de nutriments profonds dans la zone euphotique, la production primaire est dite « nouvelle » et la source d'azote préférentiellement utilisée par le phytoplancton est le nitrate, d'origine allochtone (Dugdale & Goering 1967, Eppley & Peterson 1979). Au sein de tels systèmes, le phytoplancton de grande taille (microphytoplancton) domine la communauté phytoplanctonique. Le bloom printanier de diatomées aux latitudes tempérées et subpolaires de l'océan Atlantique Nord est caractéristique de tels systèmes. Au-delà des nitrates régénérés en profondeur, la production nouvelle peut également être supportée par d'autres sources allochtones d'azote, tels l'apport atmosphérique d'ammonium, de nitrate, d'ammoniac et d'azote organique dissous (Paerl 1985, Legendre & Gosselin 1989, Prospero et al. 1996) et la fixation d'azote moléculaire atmosphérique (N_2) par les cyanobactéries diazotrophes (Carpenter & Romans 1991). À l'opposé, au sein de systèmes fortement stratifiés, le mélange vertical est trop faible pour permettre l'injection de nutriments depuis les profondeurs océaniques vers la zone euphotique. La production primaire au sein de tels systèmes est dite « régénérée », car le phytoplancton utilise l'ammonium, source autochtone d'azote régénérée sur place par les organismes hétérotrophes (Dugdale & Goering 1967, Eppley & Peterson 1979). La production régénérée favorise la dominance de cellules phytoplanctoniques de petite taille (pico- et nanophytoplancton) et est prépondérante aux latitudes tropicales et subtropicales. La distinction entre production nouvelle et régénérée, existe non seulement à l'échelle spatiale (e.g. latitudes tempérées et subpolaires *versus* latitudes tropicales et subtropicales

de l'océan Atlantique Nord) mais aussi temporelle. Ainsi, lors du bloom printanier de l'Atlantique Nord, les diatomées de grande taille, à stratégie démographique de type *r*, profitent des concentrations élevées de nitrates apportés dans la zone euphotique lors du fort mélange vertical hivernal et la production nouvelle domine. Suite au bloom, le système évolue progressivement vers des conditions de post-bloom oligotrophes estivales où les eaux de surface sont alors fortement stratifiées, la communauté phytoplanctonique est dominée par les flagellés de petite taille, à stratégie démographique de type *K*, et la production régénérée est prépondérante (Lochte et al. 1993, Sieracki et al. 1993). Cette évolution temporelle illustre les deux extrêmes d'une succession écologique définissant le « Mandala » de Margalef (Margalef 1958, 1997) selon lequel les forçages physique (turbulence) et chimique (quantité de nutriments, nature de la source d'azote disponible) déterminent la composition spécifique et la structure de taille des communautés phytoplanctoniques (Fig. 2). Néanmoins, le paradigme de la dominance des flagellés dans les milieux stratifiés (Margalef 1958, Estrada et al. 1987) a été remis en cause par la découverte de populations de dinoflagellés de grande taille se maintenant dans des milieux fortement turbulents comme les upwellings ou les zones frontales (Smayda 2002).

L'exportation de carbone organique

Par son effet sur la structure de taille des communautés phytoplanctoniques, la nature de la production primaire (nouvelle *versus* régénérée) influence de différentes manières l'exportation de carbone biogène dans les océans (Legendre & Le Fèvre 1989, 1995). Selon le concept de production nouvelle (Dugdale & Goering 1967, Eppley & Peterson 1979),

dans un système à l'équilibre, l'importation dans la zone euphotique de nitrate depuis les profondeurs océaniques doit être balancée par l'exportation de matière organique depuis la zone euphotique vers l'océan profond. Ainsi le ratio de la production nouvelle à la production primaire totale d'un système, ou *f*-ratio, est une indication de son potentiel d'exportation du carbone organique.

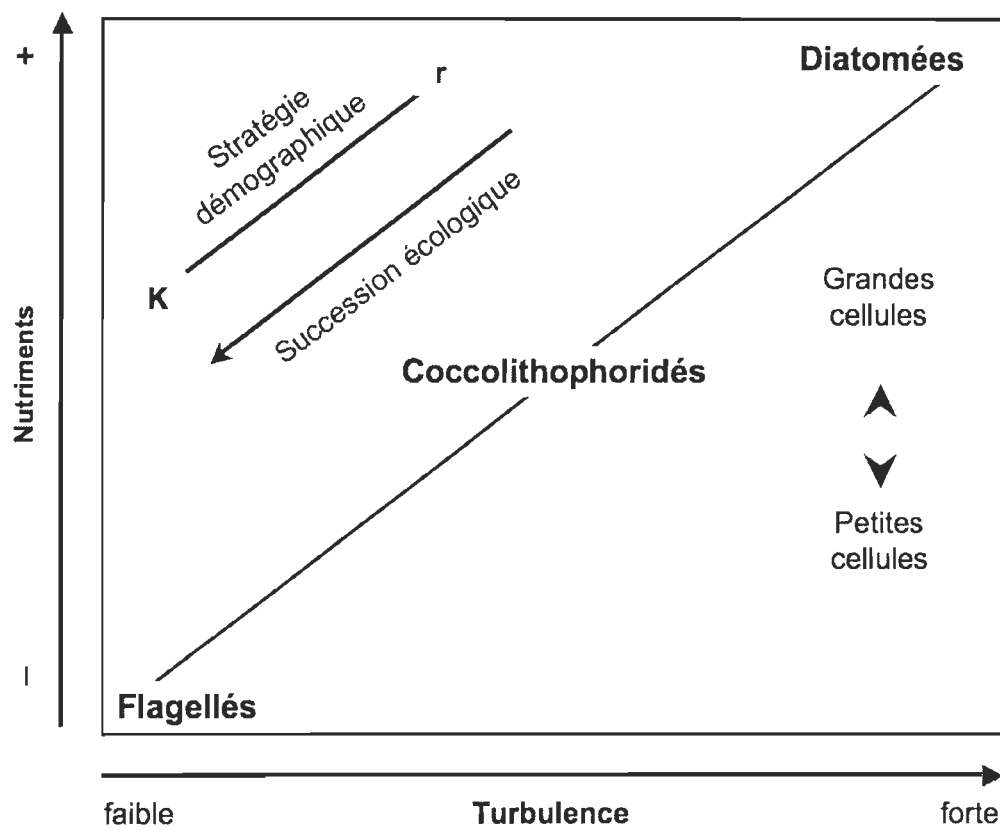


Fig. 2. Représentation schématique du « Mandala » de Margalef selon lequel la turbulence détermine la concentration en nutriments du milieu et la succession écologique d'espèces phytoplanctoniques depuis les diatomées de grande taille, à stratégie démographique de type *r*, vers les flagellés de petite taille, à stratégie démographique de type *K*. Redessinée d'après Margalef (1997)

Le concept de production nouvelle *versus* régénérée est également à la base du modèle dichotomique de contrôle hydrodynamique de la rétention et de l'exportation de la matière organique, via la structure de taille des communautés phytoplanctoniques (Legendre & Le Fèvre 1989). Selon ce modèle (Fig. 3), les systèmes à fort hydrodynamisme favorisent la production nouvelle et le développement de cellules phytoplanctoniques de grande taille à fort potentiel d'exportation. À l'inverse, les systèmes à faible hydrodynamisme et fortement stratifiés sont en faveur d'une production régénérée et de cellules phytoplanctoniques de petite taille à faible potentiel d'exportation, privilégiant ainsi la rétention et le recyclage de la matière organique dans les eaux de surface au sein de la boucle microbienne (Cho & Azam 1988, Legendre & Le Fèvre 1995, Legendre & Rassoulzadegan 1996). Entre ces deux extrêmes, la variabilité des conditions hydrodynamiques donne lieu à différentes situations contrôlant le potentiel d'exportation et de rétention de la matière organique. En regard au potentiel d'exportation d'un système, la nitrification, i.e. l'oxydation bactérienne de l'ammonium en nitrate, revêt une importance particulière. Du fait de l'inhibition par la lumière des bactéries nitrifiantes, ce processus a longtemps été considéré comme négligeable au sein de la zone euphotique. Néanmoins, il est aujourd'hui reconnu que la nitrification dans la colonne d'eau a lieu majoritairement au voisinage de la base de la zone euphotique (Zehr & Ward 2002), là où le phytoplancton est limité par la lumière et ne peut entrer en compétition avec les bactéries pour la ressource en ammonium (Ward 2000). La nitrification à la base de la zone euphotique aurait des implications potentielles majeures, bien que celles-ci demeurent encore incertaines, en regard à la nature de la production primaire. Ainsi, la production phytoplanctonique supportée par le nitrate issu de ce

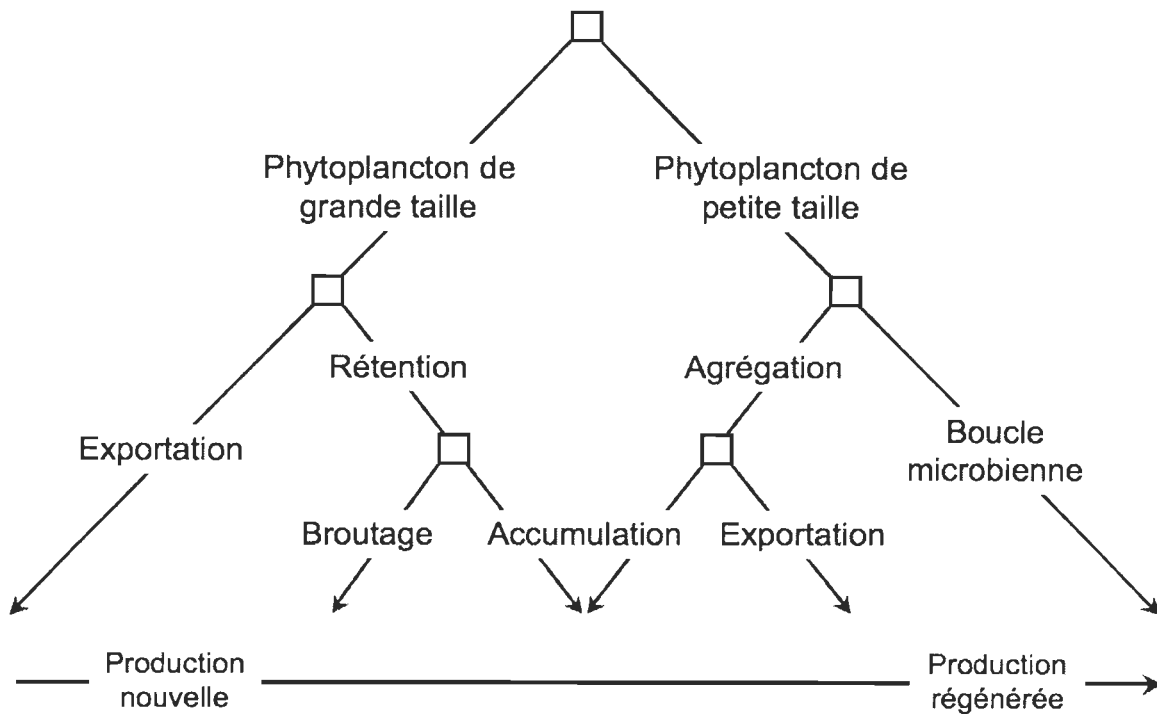


Fig. 3. Modèle dichotomique de l'export de matériel biogénique en fonction de la taille des cellules phytoplanctoniques et de singularités de l'environnement hydrodynamique D'après Legendre & Le Fèvre (1989)

processus peut être nouvelle, lorsque la nitrification à lieu au-dessous de la zone euphotique) ou bien régénérée, quand la nitrification à lieu dans la zone euphotique (Ward 2000). La nitrification dans la zone euphotique induirait ainsi une surestimation de la production nouvelle, et donc du potentiel d'exportation du système, via la prise de nitrate recyclé dans la zone euphotique (Fernandez & Raimbault 2007).

Les systèmes dominés par les cyanobactéries diazotrophes constituent également un cas particulier en regard au potentiel d'exportation du carbone organique. La fixation d'azote moléculaire atmosphérique (N_2) par ces organismes engendre une production de matière organique dont les rapports stœchiométriques sont supérieurs aux rapports de Redfield (Redfield et al. 1963), notamment dans la matière organique dissoute. Dans de telles circonstances, dites de « carbon overconsumption », la matière organique est fortement enrichie en carbone, comparativement au phosphore et à l'azote (Kahler et Koeve 2001, Körtzinger et al. 2001). Le devenir de cette matière organique riche en carbone (i.e. exportation ou respiration) revêt ainsi une importance particulière en regard au potentiel de séquestration du carbone au sein des systèmes dominés par les producteurs primaires diazotrophes (Karl et al. 2003). L'exportation annuelle de carbone associée à la fixation d'azote moléculaire atmosphérique (N_2) a été estimée à environ 0,8 Pg C.

L'acquisition de structure minérale, à l'image des frustules siliceux des diatomées, du squelette siliceux des silicoflagellés et des coccolithes calcaires de certaines espèces de prymnésiophycées, favorise l'exportation de matériel organique en augmentant la densité, et donc la vitesse de chute, des cellules phytoplanctoniques et des pelotes fécales et agrégats dans lesquels elles peuvent être incorporées (Armstrong et al. 2002, Francois et al. 2002, Klass & Archer 2002). Ces structures minérales permettent ainsi d'accroître l'efficacité de transfert du carbone organique en profondeur (définie comme le ratio entre le flux de carbone organique en profondeur et le flux de carbone organique exporté depuis la zone euphotique; Francois et al. 2002). Elles offrent également une protection contre la minéralisation de la matière organique (Armstrong et al. 2002). Selon Nelson et al. (1995),

près de 50 % du carbone biogénique exporté, à l'échelle globale, vers l'océan profond est synthétisé par les diatomées. Une meilleure compréhension des facteurs influençant la contribution relative des diatomées à la production primaire totale est ainsi de première importance en regard à l'intensité de la pompe biologique océanique de carbone (Tréguer et al. 1995). Néanmoins, selon Francois et al. (2002), les carbonates joueraient un rôle plus important que la silice biogénique en regard à leur influence sur l'efficacité de transfert du carbone organique vers l'océan profond. Les ornementations de la frustule de certaines espèces de diatomées jouent un double rôle quant à l'exportation de matériel organique particulaire. Elles permettent, d'une part, d'augmenter la surface de la cellule et la friction avec le milieu ambient, réduisant ainsi la vitesse de chute de cellules libres dans la colonne d'eau. Elles favorisent, d'autre part, le maintien des diatomées entre elles pour former des chaînes de cellules et des agrégats cellulaires favorisant ainsi l'exportation de matériel organique particulaire. Les organismes calcifiants, quant à eux, agissent à la fois comme un puits de carbone, via la pompe biologique, et une source de carbone via la pompe de carbonates. Parfois nommée « pompe biologique dure » (en opposition à la pompe biologique classique, dite « molle »), la pompe de carbonate concerne les organismes marins qui se façonnent un squelette de carbonate de calcium (CaCO_3), tels les coccolithophoridés, les foraminifères et les ptéropodes. La pompe de carbonate peut potentiellement contrecarrer l'action de la pompe biologique étant donné que pour chaque atome de carbone fixé au sein d'une molécule de CaCO_3 , une molécule de CO_2 est libérée dans les eaux de surface (Eq. 3).



La formation de particules exopolymériques transparentes (« transparent exopolymeric particles », ou TEP), notamment sous l'influence d'un stress nutritif lors du déclin de bloom de diatomées, permet l'agrégation de matériel organique particulaire (Passow et al. 2001, Passow 2002) et la formation de la « neige marine » (Honjo 1997), favorisant ainsi l'exportation de carbone organique vers l'océan profond. De par leur faible densité, les TEP peuvent également augmenter la flottabilité des agrégats de particules organiques et leur temps de résidence dans les eaux de surface (Kiørboe et al. 1998, Azetsu-Scott & Passow 2004).

Le zooplancton participe également à l'exportation de carbone organique en profondeur, par le biais des migrations nycthémérales dans la colonne d'eau. Morales (1999) a ainsi estimé que l'intensité du transport actif de carbone dans les eaux profondes de l'océan Atlantique par le zooplancton est comparable au transport de carbone résultant de la sédimentation passive des particules. La contribution du zooplancton à l'exportation de matière organique se fait surtout via la production de pelotes fécales, qui représente l'un des vecteurs principaux d'exportation de la matière organique particulière (Turner 2002). Les pelotes fécales du mésozooplancton (e.g. copépodes) sédimentent à des vitesses relativement faibles, de l'ordre de 100 m j^{-1} , favorisant leur ingestion (coprophagie) et fragmentation (coprorhexie) par le zooplancton et leur dégradation par les bactéries (Lorenzen & Welschmeyer 1983, Fortier et al. 1994). Les pelotes fécales du macrozooplancton microphage (e.g. salpes, appendiculaires), en revanche, ont des vitesses

de chutes suffisamment rapides (jusqu'à $>1000 \text{ m j}^{-1}$) pour échapper à la minéralisation, ce qui leur permet d'atteindre, relativement intactes, l'océan profond (Fortier et al. 2004).

L'exportation de la matière organique particulaire a longtemps été considérée comme le seul vecteur de transfert du carbone organique vers l'océan profond. En effet, du fait de sa caractéristique physique, le carbone organique dissous ne peut sédimentter à proprement parler. Néanmoins, la subduction le long de lignes d'isodensité (Hansell & Carlson 2001) et le mélange vertical lié à la convection (Carlson et al. 1994, Emerson et al. 1997) permettent le transfert en profondeur de la matière organique dissoute accumulée dans les eaux de surface par les communautés pélagiques. L'exportation de carbone organique dissous vers l'océan profond représente environ $20 \pm 10\%$ de l'export total de matière organique vers l'océan profond (Hansell 2002).

Recyclage de la matière organique

Les organismes hétérotrophes permettent l'oxydation de la matière organique consommée à des fins métaboliques et entraînent ainsi la libération de carbone organique et inorganique dissous dans le milieu ambiant. Contrairement à la photosynthèse, qui n'a lieu que dans la zone euphotique, le recyclage de la matière organique par broutage et minéralisation est un processus se produisant dans toutes les couches de la colonne d'eau.

Le recyclage de la matière organique au sein des écosystèmes pélagiques demeure la composante la moins connue de la pompe biologique océanique de carbone (del Gorgio & Williams 2005). Elle résulte principalement de l'action des bactéries, du broutage par le zooplancton et de la lyse virale.

Les bactéries assurent la minéralisation de la matière organique via la consommation de carbone organique dissous en suspension dans la colonne d'eau ou bien issu de la solubilisation de la matière organique particulaire (principalement des agrégats et des pelotes fécales) sous l'action d'enzymes exolytiques. Bien souvent, les bactéries dominent la respiration des communautés pélagiques dans la zone euphotique (Rivkin & Legendre 2001). Le mésozooplancton consomme essentiellement du phytoplancton et du microzooplancton. Il est également capable de se nourrir à partir d'agrégats et de pelotes fécales. Le microzooplancton est principalement représenté par les ciliés et les flagellés hétérotrophes. Ces derniers se nourrissent principalement de bactéries, de picophytoplancton et, dans le cas de certains dinoflagellés, de diatomées. Les flagellés hétérotrophes peuvent également consommer la fraction colloïdale de la matière organique dissoute (Tranvik et al. 1993). Les ciliés quant à eux se nourrissent de cellules phytoplanctoniques, de flagellés et, dans le cas des petits ciliés, de bactéries. Dans de nombreux systèmes océaniques, la pression de broutage du microzooplancton est souvent dominante par rapport à celle du mésozooplancton (Calbet & Landry 2004), en particulier lors du bloom printanier de l'océan Atlantique Nord (Burkhill et al. 1993, Harrison et al 1993, Fileman & Leakey 2005, Karayanni et al. 2005). Enfin, la lyse virale des cellules phytoplanctoniques et bactériennes, bien que longtemps sous-estimée, est reconnue aujourd'hui comme un processus majeur de contrôle des flux de carbone au sein des écosystèmes pélagiques (Fuhrman 1999, Wilhelm & Suttle 1999, Suttle 2005).

Les transformations de la matière organique par les organismes hétérotrophes permettent de modifier la taille de celle-ci mais aussi sa biodisponibilité (Legendre &

Rivkin 2005). La modification de la taille de la matière organique intervient principalement lors du « sloppy-feeding » et de la coprophagie/coprhexie par le mésozooplancton, qui permettent de briser les cellules phytoplanctoniques et les pelotes fécales en fragments de plus petites tailles. En contribuant à la solubilisation des agrégats et des pelotes fécales, les bactéries participent également à la modification de taille de la matière organique particulière. La minéralisation de la matière organique est proportionnelle à son temps de résidence dans la colonne d'eau (Tréguer et al. 2003), et donc inversement proportionnelle à sa vitesse de chute. Cette dernière étant proportionnelle à la taille des particules (loi de Stokes), la modification de la taille de la matière organique particulière par les organismes hétérotrophes influence donc le potentiel de rétention (et donc de minéralisation) ou d'exportation du carbone organique. Les transformations de la matière organique par les hétérotrophes influencent également sa minéralisation, via la modification de sa labilité et donc de sa biodisponibilité. D'une part, la fragmentation de la matière organique particulière, via le broutage par le zooplancton ou l'action des exoenzymes bactériennes et des enzymes digestives des brouteurs, permet de libérer dans le milieu des composés dissous labiles utilisables par les bactéries. D'autre part, la matière organique dissoute devient de plus en plus réfractaire du fait de la consommation préférentielle de composés labiles et semilabiles par les bactéries (Legendre & Rivkin 2005).

Efficacité et intensité de la pompe biologique

Un concept fondamental en regard à l'analyse de la pompe biologique océanique de carbone réside dans la distinction entre son efficacité et son intensité. La capacité du

phytoplancton à épuiser les nutriments des eaux de surface définit l'efficacité de la pompe biologique de carbone (E_{PB}), dont l'expression mathématique est résumée par l'équation 4 (Sarmiento & Gruber 2006) :

$$E_{PB} = \frac{C_{prof} - C_{surf}}{C_{prof}} \quad \text{Eq. 4}$$

où C_{prof} et C_{surf} symbolisent les concentrations en nutriments dans l'océan profond et dans les eaux de surface, respectivement. Ainsi, dans un système dont les eaux de surface sont épuisées en nutriments comparativement aux eaux océaniques profondes, l'efficacité de la pompe biologique est proche de 100 %. À l'inverse, un système dont les concentrations en nutriments dans les eaux de surface sont comparables à celles des eaux profondes, l'efficacité de la pompe biologique est proche de zéro.

L'intensité de la pompe biologique de carbone est définie, quant à elle, en regard à la valeur absolue du flux vertical de carbone organique. Ainsi, la pompe biologique est plus intense dans un système où le flux vertical de carbone organique particulaire est de $250 \text{ mg m}^{-2} \text{ j}^{-1}$ que dans un système où ce flux est de $70 \text{ mg C m}^{-2} \text{ j}^{-1}$.

Une pompe biologique efficace n'implique pas nécessairement que celle-ci soit intense, et réciproquement (Sarmiento & Gruber 2006). Ainsi, la pompe biologique des zones de glace marginale de l'océan Austral est intense mais peu efficace. À l'inverse, la pompe biologique au niveau des gyres subtropicaux est peu intense mais très efficace.

Problématique

Les résultats obtenus lors du programme JGOFS offrent aujourd’hui une image plus approfondie du fonctionnement de la pompe biologique océanique de carbone et ont permis le développement de modèles du cycle biogéochimique du carbone océanique, à l’image du modèle Pelagic Interaction Scheme for Carbon and Ecosystem Studies (PISCES; Aumont & Bopp 2006). De tels modèles de la biogéochimie océanique, lorsque ceux-ci sont intégrés à des modèles de circulation générale ou à des modèles couplés océan-atmosphère (Marti et al. 2005), permettent de tenir compte du rôle crucial des processus biogéochimiques océaniques dans la prévision de l’évolution du climat planétaire. Néanmoins, la capacité prédictive de tels modèles demeure encore limitée du fait de nombreuses incertitudes relatives au manque de connaissances, bien que nettement améliorées depuis JGOFS, mais encore insuffisantes, du fonctionnement de la pompe biologique de carbone et de sa réponse aux changements climatiques (Boyd & Doney 2003).

Jusqu’à présent, les programmes océanographiques visant à l’étude de la pompe biologique océanique de carbone se sont principalement consacrés à la description des processus influençant la production primaire (son intensité et sa nature, i.e. nouvelle ou régénérée) et le recyclage au sein de la zone euphotique, ainsi qu’à la quantification du flux vertical de carbone organique dans l’océan profond (Honjo 1996). Une telle approche est légitime en ce sens que l’export vertical de carbone organique au-dessous de la profondeur de séquestration (ou de ventilation, i.e. la pycnocline permanente) représente le processus le plus pertinent en regard au piégeage de carbone atmosphérique dans la circulation océanique profonde pour de longues périodes de temps (plusieurs siècles). La connaissance

actuelle de la pompe biologique océanique de carbone se rapporte donc principalement au couplage entre les processus épipélagiques (zone euphotique) et l'océan profond.

C'est sur cette base qu'ont été développés de nombreux algorithmes reliant le flux de carbone organique particulaire (COP) à la profondeur (Martin et al. 1987) et/ou la production primaire totale (Eppley & Peterson 1979, Suess 1980, Betzer et al. 1984, Pace et al. 1987, Wassman 1990), la structure de taille de la production et de la biomasse phytoplanctonique (Tremblay et al. 1997) et le flux de carbonates (Armstrong et al. 2002, Francois et al. 2002). Cependant, la plupart de ces algorithmes ne représente pas de manière adéquate les processus de recyclage affectant la matière organique lors de son exportation (Boyd & Trull 2007), en particulier dans la zone mésopélagique (Ducklow et al. 2001).

La zone mésopélagique, ou « twilight zone », représente cette portion de la colonne d'eau comprise entre la base de la zone euphotique et une profondeur d'environ 1000 m (Buesseler et al. 2007b). La zone mésopélagique comprend la zone disphotique, au sein de laquelle l'intensité lumineuse est trop faible pour la photosynthèse mais suffisante pour influencer la vision des organismes (Warrant 2000, Herring 2002). En dessous de cette zone disphotique se trouve la zone aphotique. La zone mésopélagique est considérée comme le lieu d'un intense recyclage de la matière organique. On estime ainsi que près de 90 % de la matière organique particulière provenant de la zone euphotique seraient recyclés dans la zone mésopélagique avant d'atteindre la pycnocline permanente (Tréguer et al. 2003). Le carbone inorganique dissous issu de la minéralisation de la matière organique exportée dans la zone mésopélagique peut être ventilé vers l'atmosphère sur une échelle de temps relativement courte (jour ou mois) et est donc d'une importance capitale pour la

balance métabolique des océans (i.e. autotrophie nette *versus* hétérotrophie nette). La zone mésopélagique représente donc une couche intermédiaire cruciale de la colonne d'eau déterminant le couplage entre la zone euphotique et l'océan profond. Une meilleure connaissance des processus influençant le flux vertical de matière organique dans la zone mésopélagique, et donc l'intensité de la pompe biologique océanique de carbone, est nécessaire à la compréhension et la modélisation du cycle biogéochimique du carbone.

Dans ce contexte, et dans la continuité du programme JGOFS, plusieurs programmes et réseaux de recherches ont été mis en place, tels que Integrated Marine Biogeochemistry and Ecosystem Research (IMBER), Vertical Transport In the Global Ocean (VERTIGO) ou Surface Ocean–Lower Atmosphere Study (SOLAS), afin d'améliorer la compréhension de la pompe biologique océanique de carbone, en regard, notamment, à l'importance de la zone mésopélagique et son influence sur les flux océan-atmosphère de CO₂.

Objectifs

Cette thèse a été réalisée dans le cadre de l'Étude des interactions biogéochimiques air-mer dans l'Atlantique Nord (Study of Air-sea Biogeochemical Interactions in the North Atlantic, SABINA) qui est une composante du programme de recherche canadien SOLAS. Dans le cadre de SABINA, un suivi lagrangien du déclin d'une floraison printanière de diatomées de l'océan Atlantique du nord-ouest a été réalisé, afin d'étudier l'influence du déclin de cette floraison (ou bloom) sur la production et les échanges océan-atmosphère de gaz actifs sur le plan climatique, dont le CO₂.

Dans le contexte de ce suivi lagrangien, l'objectif central de cette thèse est d'étudier la relation entre la production primaire et l'exportation de carbone organique particulaire (COP) dans la partie supérieure de la zone mésopélagique (50-150 m), lors du déclin du bloom et sa transition vers des conditions de post-bloom. Une telle étude est nécessaire en regard à l'importance reconnue, mais mal comprise, de la zone mésopélagique dans la régulation du flux vertical de COP (et donc de l'intensité de la pompe biologique) et la biogéochimie des eaux océaniques de surface et de subsurface. Cette étude est la première détaillant les variations temporelles à court terme des flux verticaux de COP dans la zone mésopélagique en relation avec la production phytoplanctonique aux latitudes tempérées de l'océan Atlantique Nord. De plus, cette étude comble le manque de données relatives aux flux verticaux de COP aux latitudes tempérées et subpolaires de l'océan Atlantique du nord-ouest, ces flux ayant été, à l'exception des résultats reportés par Harrison et al. (1993), principalement mesurés dans la partie orientale de ce bassin océanique (Honjo 1997, Antia et al. 2001). Enfin, la phase de déclin du bloom est particulièrement intéressante car elle constitue une fenêtre temporelle déterminante pour le devenir de la matière organique formée lors du bloom, à savoir le broutage, la minéralisation dans les eaux de surface ou l'exportation en profondeur. La phase de déclin du bloom est donc cruciale en regard à l'intensité de la pompe biologique de carbone. Or, la majorité des études relatives au bloom printanier de l'océan Atlantique Nord se sont consacrées à la description des processus responsables du déclenchement et du développement de ce bloom. Le déclin du bloom printanier n'a été que peu étudié jusqu'à présent et son influence sur la biogéochimie

océanique, en général, et sur la pompe biologique de carbone, en particulier, demeure mal connue (Ducklow 1989).

Le premier chapitre de la thèse décrit les changements dans la structure de taille de la production et de la biomasse du phytoplancton durant le déclin du bloom printanier et sa transition vers des conditions de post-bloom. Ce travail a permis de tester l'hypothèse selon laquelle le déclin du bloom de diatomées est associé à une limitation en nutriments et s'accompagne du remplacement des diatomées par une communauté phytoplanctonique dominée par les flagellés de petite taille. Pour ce faire, les concentrations en nutriments (nitrate + nitrite, ammonium, phosphate et silicium dissous), la production et la biomasse du petit ($0,7\text{-}5 \mu\text{m}$) et du gros ($\geq 5 \mu\text{m}$) phytoplancton et la composition spécifique de la communauté phytoplanctonique ont été mesurés dans la zone euphotique. De plus, le devenir potentiel de la biomasse phytoplanctonique a été estimé à partir de la structure de taille des communautés phytoplanctoniques selon l'approche de Tremblay & Legendre (1994).

Le second chapitre aborde le changement des flux verticaux de COP dans la partie supérieure de la zone mésopélagique (50-150 m) lors du déclin du bloom et sa transition vers des conditions de post-bloom. Ce travail a permis de tester l'hypothèse voulant que le déclin du bloom s'accompagne à court terme d'une augmentation des flux verticaux de COP dans la zone mésopélagique. De plus, ce travail a permis de tester l'hypothèse selon laquelle les changements dans la structure de taille des communautés phytoplanctoniques,

entre la période de déclin du bloom et des conditions de post-bloom, s'accompagne d'une réduction de l'exportation de COP dans la zone mésopélagique. À cet effet, les flux verticaux de COP ont été mesurés à 5 profondeurs dans la zone mésopélagique (50, 75, 100, 125 et 150 m) et leur variation temporelle a été mise en relation avec les changements dans l'activité et la structure de taille des producteurs primaires décrits dans le chapitre 1.

Dans le troisième chapitre, un budget de carbone organique particulaire (COP) et dissous (COD) au sein des zones euphotique et mésopélagique a été établi pour la période du déclin du bloom. Après s'être focalisé sur la variabilité à court terme de la production primaire et des flux de COP (objectifs 1 et 2), ce travail vise à obtenir une vision globale des stocks et des flux de carbone au sein des 150 premiers mètres de la colonne d'eau pour l'ensemble de la période d'étude du déclin du bloom. Ce budget a été construit à partir des mesures de production primaire, des flux de COP, des stocks de COP et de COD et d'estimations de la respiration des communautés pélagiques basées sur des données de la littérature. Il a permis de déterminer l'importance relative de l'exportation de COP et du recyclage de la matière organique dans le système étudié. La comparaison de la production totale mesurée et de la respiration totale estimée a également permis d'établir la balance métabolique (i.e. autotrophie nette *versus* hétérotrophie nette) au sein des 150 premiers mètres de la colonne d'eau lors du déclin du bloom.

CHAPITRE I

SIZE-FRACTIONATED PHYTOPLANKTON PRODUCTION AND BIOMASS DURING THE DECLINE OF THE NORTHWEST ATLANTIC SPRING BLOOM

RÉSUMÉ

La structure de taille de la production et de la biomasse phytoplanctonique a été étudiée lors d'un suivi lagrangien, d'une durée de 7 jours, du déclin d'un bloom printanier et durant des conditions de post-bloom dans l'océan Atlantique nord-ouest. L'épuisement des nutriments dans les eaux de surface a conduit à la limitation de la production primaire par la disponibilité en nitrate et au déclin de l'un des blooms les plus productifs rapportés pour les eaux ouvertes de l'océan Atlantique Nord. La production et la biomasse phytoplanctonique dans la zone euphotique ont diminué de $2720 \text{ à } 300 \text{ mg C m}^{-2} \text{ j}^{-1}$ et de $361 \text{ à } 121 \text{ mg chl } a \text{ m}^{-2}$, respectivement. Lors du déclin du bloom, le gros phytoplancton ($\geq 5 \mu\text{m}$), en majorité des diatomées centrales, dominait la production primaire ($\geq 50 \%$) et la biomasse chlorophyllienne ($\geq 82 \%$) dans la zone euphotique. En condition de post-bloom, le petit phytoplancton ($0,7\text{-}5 \mu\text{m}$), en majorité des flagellés, dominait la production primaire (79 %) et contribuait pour 45 % à la biomasse chlorophyllienne totale. Au cours de la période d'étude, un maximum profond de chlorophylle *a* (MPC), correspondant à un maximum d'abondance et de biomasse phytoplanctonique, s'est développé au niveau de la base de la zone euphotique. La formation et le maintient du MPC est expliqué par la sédimentation des cellules phytoplanctoniques au niveau de la base de la zone euphotique, à proximité de la nutricline, où les cellules algales acclimatées aux faibles intensités lumineuses ont maintenu des faibles vitesses de chute. La croissance du phytoplancton en profondeur a également eu lieu de manière épisodique. L'analyse de la contribution relative du petit et du gros phytoplancton à la production et la biomasse phytoplanctonique totales a mis en évidence le contrôle de la biomasse du petit phytoplancton par le microzooplancton et l'accumulation du gros phytoplancton dans la zone euphotique au niveau du MPC.

ABSTRACT

The size structure of phytoplankton production and biomass was surveyed during a 7-day Lagrangian study of the decline of the spring phytoplankton bloom in the northwest Atlantic Ocean and during post bloom conditions. Well-stratified and almost nutrient depleted surface waters led to nitrogen limitation of phytoplankton production and to the decline of one of the most productive bloom ever reported for the open North Atlantic Ocean. Total phytoplankton production and biomass decreased from $2720 \text{ to } 300 \text{ g C m}^{-2} \text{ d}^{-1}$ and from $361 \text{ to } 121 \text{ mg chl } a \text{ m}^{-2}$, respectively. Large phytoplankton cells

($\geq 5 \mu\text{m}$), mainly centric diatoms, were dominant throughout the Lagrangian study period and represented $\geq 50\%$ of total production and $\geq 82\%$ of total chlorophyll *a* (chl *a*) biomass in the euphotic zone. During post bloom conditions, small phytoplankton cells ($0.7\text{--}5 \mu\text{m}$), mainly flagellates, represented up to 79% of total phytoplankton production and 45% of total chl *a* biomass. Throughout the study period, a deep chl *a* maximum (DCM), which corresponded to a maximum in phytoplankton biomass and abundance, developed at the base of the euphotic zone. The formation and maintenance of the DCM is explained by the settling of the phytoplankton biomass at the base of the euphotic zone near the nutricline, where photoacclimated cells maintained low sinking velocities. Phytoplankton growth at depth also occurred sporadically. The analysis of the relative contribution of small and large phytoplankton cells to total primary production and biomass revealed that small phytoplankton cells were probably removed by microzooplankton grazing whereas large algal cells accumulated in the euphotic zone, mainly at the DCM.

1.1 Introduction

The coupling between primary production in surface waters and carbon export to depth has received much attention in recent years. This coupling plays a key role in determining the strength and efficiency of the biological carbon pump in sequestering carbon dioxide into the deep ocean, and thus its potential mitigation of increases in atmospheric CO₂ (Sarmiento & Gruber 2006).

A first step towards understanding the coupling between primary and export production is the investigation of the size structure of phytoplankton production and biomass. The relative contribution of small versus large cells to phytoplankton production and biomass plays a key role in energy transfer throughout pelagic food webs by influencing the fate of primary produced material, i.e. whether organic carbon will be recycled *in-situ*, transferred to upper trophic levels or exported to depth via sedimentation (Legendre & Le Fèvre 1989, Bury et al. 2001). Based on this premise, Tremblay & Legendre (1994) have shown that the potential export of biogenic carbon through sedimentation, grazing, or advection can be predicted from the size structure of phytoplankton production and biomass.

The spring phytoplankton bloom at temperate and subpolar latitudes in the North Atlantic Ocean is one of the most productive of the World Ocean. As in other productive regions, the spring bloom in the North Atlantic Ocean constitutes a major biogeochemical event that contributes significantly to the sinking flux of particles to the deep ocean (Honjo 1996). The development of the North Atlantic spring bloom, from winter light limitation to late spring nutrient limitation of phytoplankton growth, has been extensively studied (e.g.

Riley et al. 1949, Sverdrup 1953). Apart from nutrient limitation of primary production, the sedimentation of particles has also been suggested as an important mechanism by which phytoplankton blooms terminate (Legendre 1990). Indeed, at temperate and subpolar latitudes of the North Atlantic Ocean, temporal uncoupling between phytoplankton (typically large diatoms) growth and zooplankton grazing can result in the massive sedimentation of organic material at the end of the bloom (Parsons & Lalli 1988, Honjo & Manganini 1993). The declining phase of the bloom is therefore of particular interest to address the potential fate of the biogenic carbon that accumulated in the euphotic zone during the bloom period.

However, phytoplankton dynamics during the declining phase of the spring bloom have yet to be studied (Harrison et al. 1993). Therefore, little is known of the interactions between environmental conditions, phytoplankton size structure and the fate of biogenic carbon during the decline of the northwest Atlantic spring bloom at temperate latitudes. The objectives of our study were: (1) to investigate changes in the size structure of phytoplankton production and biomass during the decline of the spring bloom and its transition towards post-bloom conditions in the temperate northwest Atlantic Ocean; and (2) to assess the potential fate (i.e. *in situ* recycling or export from the euphotic zone) of the different phytoplankton size fractions, using the approach developed by Tremblay & Legendre (1994). It was hypothesized that large phytoplankton would rapidly sink out of the euphotic zone after the spring bloom and that the production and biomass would then be dominated by small phytoplankton.

1.2 Materials and methods

1.2.1 Sampling

Sampling was carried out aboard the CCGS *Hudson* in the northwest Atlantic Ocean off the Scotian Shelf (Station L; water depth: 3500 m; Fig. 1) on eight occasions from 25 April to 14 May 2003, as part of the Canadian Surface Ocean–Lower Atmosphere Study (C-SOLAS). From 25 April to 01 May 2003 (days 1 to 7), we conducted a Lagrangian study of a water mass within which a phytoplankton bloom had developed (Fig. 1). According to SeaWiFS satellite imagery of the sampling area, the sampling period was associated with decreasing chlorophyll *a* (chl *a*) concentrations in surface waters (Forget et al. 2007). The water mass under investigation was tracked using a CAST ARGOS drifter (Seimac Smart CAT PTT/GPS transmitter) equipped with a 15-m long Holey Sock tubular drogue centered at a depth of 15 m in the water column. Water samples were collected every day at dawn close to the drifting buoy using a rosette-type sampler equipped with 24 10-l Scripps bottles, a CTD probe (Sea-Bird SBE 9) and an *in situ* fluorometer (WSD-818P). From 13 to 15 May (days 19 to 21), the station occupied on day 1 was revisited. On 14 May (day 20), seawater samples were collected to assess potential chemical and biological changes that could have occurred at that location after the decline of the spring bloom.

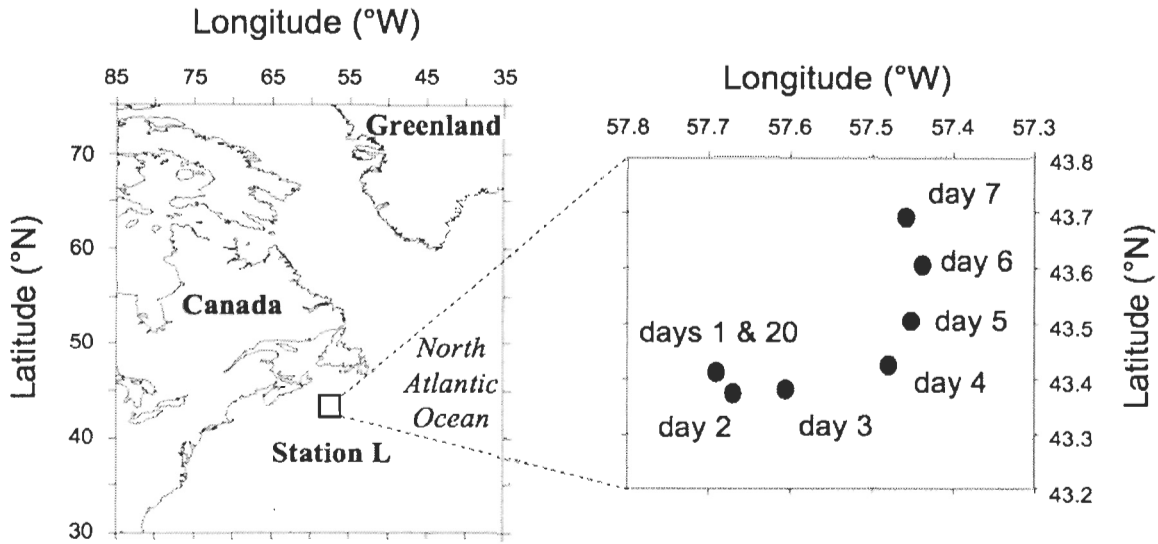


Fig. 1. Location of the sampling sites from 25 April (day 1) to 01 May (day 7) during a Lagrangian study of a water mass in the northwest Atlantic Ocean in spring 2003. On 14 May (day 20), the ship went back to the latitude/longitude position occupied on day 1

Prior to sampling, a vertical profile of irradiance (PAR: photosynthetically active radiation, 400–700 nm) was obtained with a PNF-300 radiometer (Biospherical InstrumentsTM). From this profile, the diffuse light attenuation coefficient (K_d) and the depth of the euphotic zone (depth of 0.2% surface PAR) were calculated. Samples were then collected at seven optical depths (100, 50, 30, 15, 5, 1 and 0.2% of surface PAR), at the depth of maximum chl *a* concentration and at four depths below the euphotic zone (75, 100, 150 and 200 m). Subsamples for subsequent analyses were drawn from the Scripps bottles into acid-washed Nalgene bottles according to Knap et al. (1996).

1.2.2 Analyses

Temperature, salinity and pressure were measured over the water column depth with the CTD probe and averaged over 1-db intervals (ca. 1 m). The depth of the surface mixed layer (Z_{mix}) was determined as the depth of the shallowest extreme curvature of density and temperature profiles using the MATLAB script provided in Lorbacher et al. (2006). This method allows a more accurate determination of Z_{mix} than methods based on a critical threshold value, e.g. Δ -criterion and gradient based methods (Lorbacher et al. 2006). Temperature (T) and salinity (S) profiles from the surface to 350 m, from which T-S diagrams were constructed, were used as proxies to track the water mass under investigation.

Samples for dissolved inorganic nutrients ($\text{NO}_3 + \text{NO}_2$, NH_4 , Si(OH)_4 and PO_4) were filtered through precombusted (450°C for 5 h) Whatman GF/F glass fiber filters and the filtrate collected in 5-ml acid washed polycarbonate cryovials, except for NH_4 samples, which were stored in 50 ml polypropylene centrifugation tubes. $\text{NO}_3 + \text{NO}_2$, Si(OH)_4 and PO_4 samples were stored in liquid nitrogen for later analyses in the laboratory with an Alpkem FS III autoanalyzer. NH_4 samples were analyzed aboard the ship by spectrophotometry (Ultrospec II, LKB Biochrom) according to the alternative method of Solórzano (1969) adapted by Parsons et al. (1984). The depth of the nutricline was determined by visual inspection of the vertical profiles of each nutrient, based on the shallowest extreme curvature of near-surface nutrient profiles.

Particulate organic carbon (POC) concentrations were determined from subsamples filtered onto precombusted 21 mm Whatman GF/F glass fiber filters. Filters were stored in Petri dishes at -20°C until analysis, using a PerkinElmer Model 2400 Elemental Analyzer.

Subsamples for chl *a* determination were filtered onto 25 mm Whatman GF/F filters (total algal biomass: B_T , $\geq 0.7 \mu\text{m}$) and onto 25 mm Poretics 5 μm polycarbonate membranes (biomass of large phytoplankton cells: B_L , $\geq 5 \mu\text{m}$). Concentrations of chl *a* and pheopigments were measured aboard the ship with a Turner Designs 10-005R fluorometer, after 18-h extractions in 90% acetone at 4°C in the dark (Parsons et al. 1984). The chl *a* biomass of small phytoplankton cells (B_S , 0.7–5 μm) was obtained by subtracting B_L from B_T .

Phytoplankton samples collected at the depths of 50% surface PAR and maximum chl *a* concentration were preserved with acidic Lugol (0.4% final concentration; Parsons et al. 1984). Cells were identified and enumerated using the standard inverted microscope method (phase contrast illumination; Utermöhl 1931, Lund et al. 1958).

Chl *a* sinking velocities were measured from days 2 to 20 on samples collected at the 50% and 5% surface PAR depths using settling columns (10 cm diameter and 54 cm height; Bienfang 1981). The samples were well mixed before being poured into the settling columns (SETCOL) so that the initial distribution of particles was homogenous. The initial chl *a* concentration in the sample was measured before the particles were allowed to settle in the dark at a temperature close to that *in situ*. After a settling period of 6 h, the top and bottom fraction of the column were collected and filtered onto Whatman GF/F filters. The

total chl *a* concentration in each fraction was then measured as described above and the chl *a* sinking velocity (m d^{-1}) was calculated according to Bienfang (1981).

Primary production rates were measured at the seven optical depths using the ^{14}C -uptake method (Parsons et al. 1984, Gosselin et al. 1997). Two light and one dark 500 ml Nalgene polycarbonate bottles were filled with seawater from each light level and inoculated with 10 μCi of $\text{NaH}^{14}\text{CO}_3$. The dark bottles contained 250 μl of 0.02 M 3,4-dichlorophenyl-1,1-dimethylurea (DCMU) (Legendre et al. 1983). The total amount of radioisotope in each bottle was determined immediately after inoculation by pipetting 50 μl subsamples into 10 ml of Ecolume scintillation cocktail (ICNTM) containing 50 μl of ethanolamine.

The bottles containing the ^{14}C -isotope were placed in a Plexiglas deck incubator set up on a black board and equipped with tubes wrapped with neutral density screens (LEE Filters) to simulate irradiance at the sample collection depth. Tubes simulating $\leq 30\%$ PAR were wrapped with one layer of blue filter to mimic vertical changes in spectral quality. Running seawater pumped from a depth of about 5 m circulated through the incubator to maintain the temperature at that of the upper mixed layer. Incubations of 8 to 10 h were carried out from sunrise to sunset. Water temperature within the incubators was regularly checked during the incubation. At the end of the incubation, 3 ml of seawater was taken from each bottle and transferred into borosilicate scintillation vials, acidified with 500 μl of 6N HCl and left open on a lab rotator in a fume hood for at least 4 h in order to release inorganic carbon prior to the measurement of total organic carbon production (P_T). The same treatment was applied to another 3 ml subsample that was filtered through a Whatman

GD/X glass fiber syringe filter (nominal pore size of 0.7 μm) to measure the release rate of dissolved organic carbon (P_{DOC}). These samples were then neutralized with 500 μl of 6N NaOH before adding 15 ml of scintillation cocktail. Total particulate organic carbon production (P_{POC}) was measured on 250 ml samples filtered onto Whatman GF/F filters. The remaining 244 ml were filtered onto Poretics 5- μm polycarbonate membranes to measure the production by large phytoplankton cells (P_L , $\geq 5 \mu\text{m}$). The filters were rinsed with filtered seawater before being removed from the filtration system and were placed in borosilicate scintillation vials. Filters were then acidified with 100 μl of 0.5 N HCl and left to evaporate overnight under the fume hood to remove any ^{14}C that had not been incorporated (Lean & Burnison 1979). After that period, scintillation cocktail was added to the vials, which were then stored in a dry and dark room before counting in the laboratory. Counting was performed on a Beckman LS 6500 liquid scintillation counter about one month after sample collection. Production rate of total, particulate and dissolved organic carbon were calculated according to Parsons et al. (1984) using a value of $25000 \text{ mg C m}^{-3}$ as the concentration of dissolved inorganic carbon and a factor of 1.05 to correct for the lower uptake of ^{14}C compared to ^{12}C (Knap et al. 1996). Values from the dark bottles were subtracted from corresponding light values based on the premise that the measured dark fixation of ^{14}C is due solely to bacterial processes occurring similarly in light and dark bottles (Li et al. 1993). The 8–10 h production rates were extrapolated to daily production using the continuous surface PAR measurements made with a 2π light sensor (LI-COR) placed on the upper deck of the ship close to the incubator. The production of small phytoplankton cells (P_S , 0.7–5 μm) was obtained by subtracting P_L from P_{POC} .

1.2.3 Numerical analysis

Concentrations of inorganic nutrients, POC and chl a as well as the primary production rate were integrated over the surface mixed layer (SML), the depth of which we will refer to as Z_{mix} , and between Z_{mix} and the base of the euphotic zone ($Z_{\text{mix}}-Z_{\text{eu}}$) using trapezoidal integration. For inorganic nutrients, an average integrated value over Z_{mix} and $Z_{\text{mix}}-Z_{\text{eu}}$ was estimated by dividing the integrated nutrient concentration by the integration depth of integration. Data were analyzed with non-parametric methods (Sokal & Rohlf 1995). Wilcoxon's signed ranks test was used to compare paired variates and to compare ratios with their respective critical values. Kendall's coefficient of ranks correlation (τ) was used to infer the relationship between two variables. Statistical tests were performed with the STATISTICA 6 software (StatSoft Inc.).

1.3 Results

1.3.1 Physical and chemical environment

Daily changes in the physical properties of the water column are presented in Table 1. The depth of the surface mixed layer (Z_{mix}) ranged from 10 m on day 1 to 26 m on day 6 and was 6 m on day 20 (Table 1). The depth of 0.2% surface PAR, i.e. the base of the euphotic zone (Z_{eu}), significantly increased from 40 to 50 m throughout the Lagrangian study period and was 60 m on day 20 (Kendall's τ correlation between Z_{eu} and the sampling day, $p < 0.01$). Z_{mix} was consistently shallower than Z_{eu} throughout the study period (days 1 to 7 and day 20), with an average value of 16 m for Z_{mix} and 47 m for Z_{eu} (Table 1).

Table 1. Daily variations in the water column structure: depth of the surface mixed layer (Z_{mix}), depth of the 0.2% surface PAR (Z_{eu}), depth of the nutricline (Z_{nutr}), average temperature and salinity in the surface mixed layer (SML) and between Z_{mix} and Z_{eu} ($Z_{\text{mix}}-Z_{\text{eu}}$). Standard deviations of temperature and salinity are indicated in parentheses when applicable

Day	Date	Z_{mix} (m)	Z_{eu} (m)	Z_{nutr} (m)	Temperature (°C)		Salinity	
					SML	$Z_{\text{mix}}-Z_{\text{eu}}$	SML	$Z_{\text{mix}}-Z_{\text{eu}}$
1	25 April	10	40	45	2.7 (0.01)	2.3 (0.21)	32.7 (0.00)	32.8 (0.07)
2	26 April	12	43	43	2.8 (0.01)	2.2 (0.23)	32.7 (0.00)	32.8 (0.06)
3	27 April	11	40	45	3.0 (0.02)	2.4 (0.26)	32.7 (0.00)	32.8 (0.06)
4	28 April	23	45	45	2.9 (0.19)	2.0 (0.11)	32.7 (0.01)	32.8 (0.06)
5	29 April	19	45	45	3.0 (0.01)	2.4 (0.25)	32.6 (0.00)	32.8 (0.06)
6	30 April	26	50	40	3.2 (0.01)	2.6 (0.36)	32.7 (0.01)	32.9 (0.07)
7	01 May	18	50	40	3.4 (0.01)	2.2 (0.63)	32.7 (0.00)	32.8 (0.06)
20	14 May	6	60	40	5.1 (0.01)	3.9 (0.91)	32.9 (0.00)	33.0 (0.06)

The depth of the nutricline (Z_{nutr}), determined from the vertical profiles of $\text{NO}_3 + \text{NO}_2$, PO_4 and $\text{Si}(\text{OH})_4$, was very similar to that of Z_{eu} from days 1 to 5, with a mean value of 45 m and was shallower than Z_{eu} from days 6 to 20, with a mean value of 40 m (Table 1). Similar temperature and salinity were measured in the surface waters from days 1 to 7 (Table 1, Figs. 2 & 3).

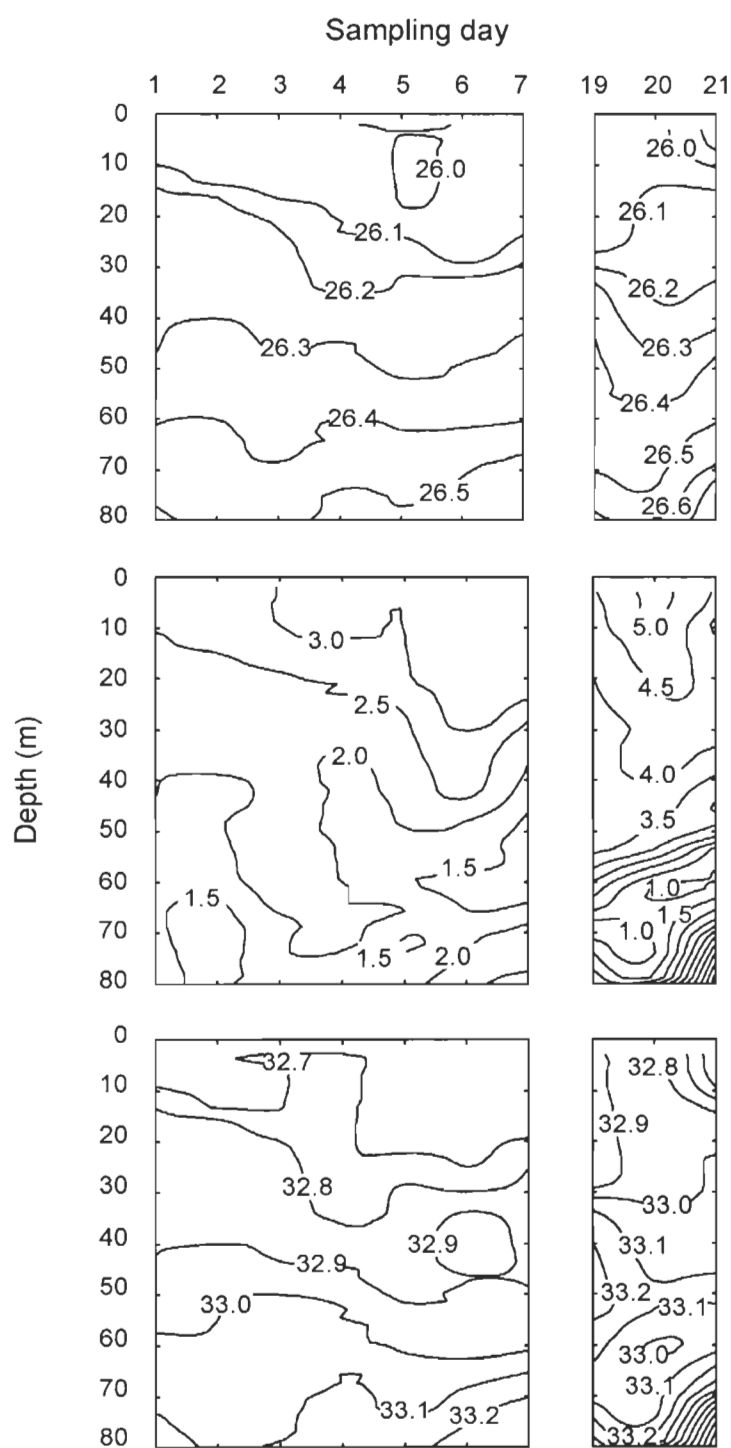


Fig. 2. Contour plots for (a) sigma-t (kg m^{-3}), (b) temperature ($^{\circ}\text{C}$), and (c) salinity in the upper 80 m of the northwest Atlantic Ocean throughout the Lagrangian study period (days 1 to 7) and on days 19 to 21

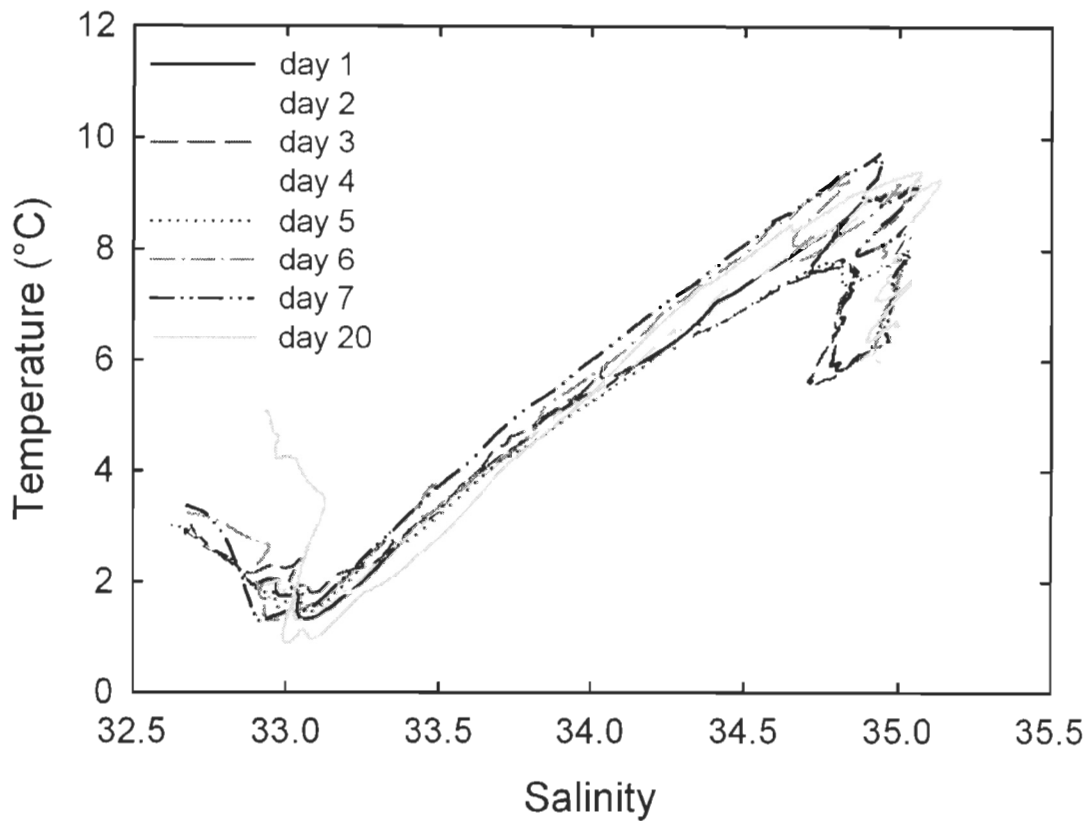


Fig. 3. Temporal variations of the temperature–salinity diagrams of the upper 350 m of the water column throughout the Lagrangian study period (days 1 to 7) and on day 20

On day 20, the vertical profiles of temperature and salinity and the T-S diagrams revealed warmer and more saline waters in the upper 60 m of the water column (Table 1, Figs. 2 & 3).

From days 1 to 20, the integrated concentrations of inorganic nutrients averaged over Z_{mix} were very low, ranging from 0.01 to 0.12 μM for $\text{NO}_3 + \text{NO}_2$, from 0.02 to 0.15 μM

for NH_4 , from 0.07 to 0.20 μM for PO_4 and from 0.27 to 0.72 μM for Si(OH)_4 (Fig. 4). During the same period, nutrient concentrations were significantly higher in $Z_{\text{mix}}\text{-}Z_{\text{eu}}$ than in the SML (Wilcoxon's signed ranks tests, $p < 0.01$), except for Si(OH)_4 from days 1 to 5, with integrated concentrations ranging from 0.04 to 1.51 μM for $\text{NO}_3 + \text{NO}_2$, from 0.09 to 0.33 μM for NH_4 , from 0.07 to 0.26 μM for PO_4 and from 0.38 to 0.94 μM for Si(OH)_4 (Fig. 4). The integrated concentrations of $\text{NO}_3 + \text{NO}_2$, PO_4 and Si(OH)_4 , averaged over Z_{mix} and $Z_{\text{mix}}\text{-}Z_{\text{eu}}$, were all significantly lower than the wintertime concentrations in the euphotic zone reported in the World Ocean Atlas for that region (i.e. $\text{NO}_3 + \text{NO}_2$: 5 μM ; PO_4 : 1 μM ; Si(OH)_4 : 4 μM ; Conkright et al. 2002) integrated over the same depths (Wilcoxon's signed ranks tests, $p < 0.01$). Temporal changes in nutrient concentrations throughout the study period were less pronounced in the SML than in $Z_{\text{mix}}\text{-}Z_{\text{eu}}$ (Fig. 4). The integrated concentrations of inorganic nutrients averaged over $Z_{\text{mix}}\text{-}Z_{\text{eu}}$ were positively correlated with the daily variability of the ratio of Z_{eu} to Z_{nutr} (Kendall's τ correlations, $p < 0.01$). $\text{NO}_3 + \text{NO}_2$, NH_4 and PO_4 concentrations in $Z_{\text{mix}}\text{-}Z_{\text{eu}}$ were significantly lower on day 3 than on day 2 (Wilcoxon's signed ranks tests, $p < 0.01$) and $\text{NO}_3 + \text{NO}_2$ and PO_4 concentrations in that layer were at their lowest from days 3 to 5 (Fig. 4a-c). In $Z_{\text{mix}}\text{-}Z_{\text{eu}}$, all nutrient concentrations significantly increased from day 5 onwards (Kendall's τ correlations between nutrient concentrations and the sampling day, $p < 0.01$), reaching maximum values on day 20 (Fig. 4). The molar ratio of DIN (i.e. $\text{NO}_3 + \text{NO}_2 + \text{NH}_4$) to PO_4 was significantly lower than the Redfield ratio of 16N:1P (Redfield et al. 1963) throughout the study period (Table 2), both within the SML and $Z_{\text{mix}}\text{-}Z_{\text{eu}}$ (Wilcoxon's signed ranks tests, $p < 0.01$). The

molar ratio of DIN to $\text{Si}(\text{OH})_4$ in the SML was significantly lower than the reference value of 1.1N:1Si (Brzezinski 1985) (Wilcoxon's signed ranks test, $p < 0.01$; Table 2).

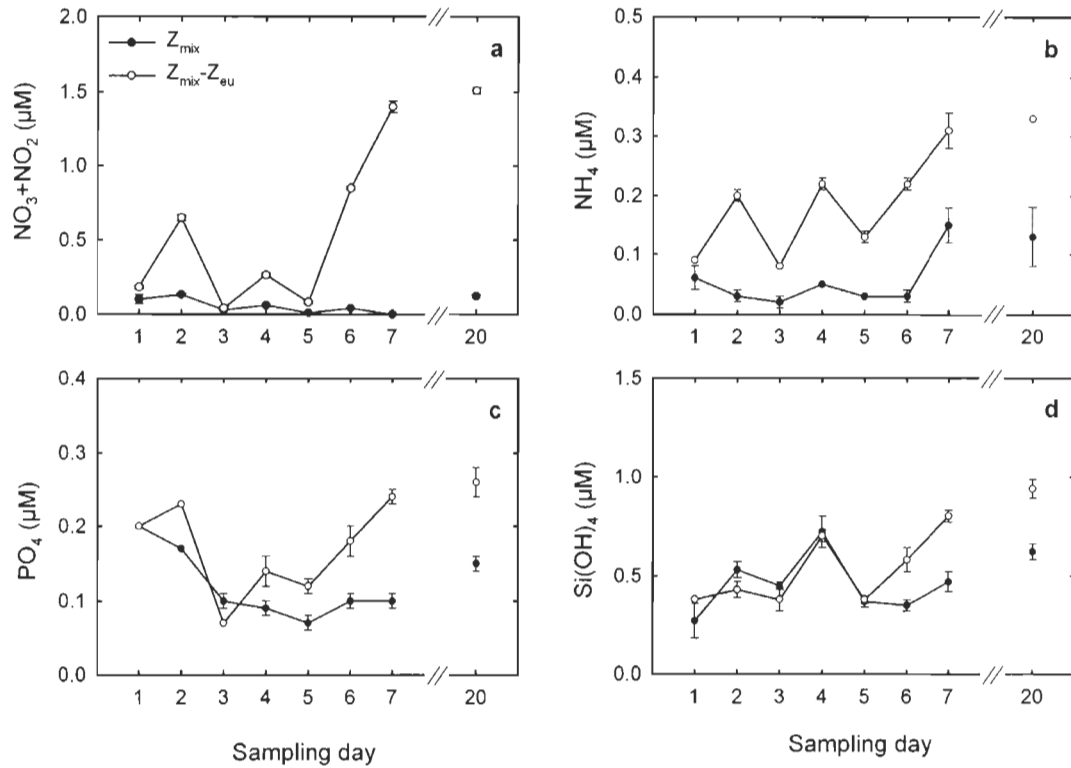


Fig. 4. Temporal variations in the average concentrations of (a) nitrate+nitrite ($\text{NO}_3 + \text{NO}_2$), (b) ammonium (NH_4), (c) phosphate (PO_4) and (d) silicic acid ($\text{Si}(\text{OH})_4$) integrated over the surface mixed layer depth (Z_{mix}) and between Z_{mix} and the base of the euphotic zone ($Z_{\text{mix}} - Z_{\text{eu}}$) (average \pm standard deviation)

In $Z_{\text{mix}} - Z_{\text{eu}}$, the DIN to $\text{Si}(\text{OH})_4$ ratio did not deviate significantly from the 1.1:1 ratio throughout the study period, although values lower than this ratio were observed from days 3 to 5 (Wilcoxon's signed ranks test, $p < 0.01$) (Table 2).

Table 2. Daily variations in the integrated molar ratio of dissolved inorganic nitrogen (DIN) to phosphate (DIN:PO₄) and to silicic acid (DIN:Si(OH)₄) averaged over the surface mixed layer (SML) and between the depth of the surface mixed layer and the base of the euphotic zone (Z_{mix}-Z_{eu}). Standard deviations are indicated in parentheses

Day	DIN:PO ₄ (mol:mol)		DIN:Si(OH) ₄ (mol:mol)	
	SML	Z _{mix} -Z _{eu}	SML	Z _{mix} -Z _{eu}
1	0.80 (0.25)	1.35 (0.05)	0.59 (0.27)	0.71 (0.03)
2	0.94 (0.12)	3.70 (0.13)	0.30 (0.04)	1.98 (0.20)
3	1.00 (0.28)	1.71 (0.14)	0.11 (0.02)	0.32 (0.06)
4	1.22 (0.14)	3.43 (0.51)	0.15 (0.02)	0.69 (0.04)
5	0.57 (0.08)	1.75 (0.22)	0.11 (0.01)	0.55 (0.06)
6	0.70 (0.12)	5.94 (0.67)	0.20 (0.03)	1.84 (0.19)
7	1.50 (0.34)	7.13 (0.42)	0.32 (0.07)	2.14 (0.12)
20	1.67 (0.42)	7.08 (0.55)	0.40 (0.10)	1.96 (0.11)

1.3.2 Phytoplankton abundance and composition

At the 50% light level depth (i.e. 5–10 m), phytoplankton abundance decreased from 0.89×10^3 to 0.43×10^3 cells m⁻³ from days 1 to 7, respectively, and increased to 1.4×10^3 cells m⁻³ on day 20. At the depth of the chl *a* maximum (i.e. 40–50 m; see Fig. 5), cell abundances were up to three times higher than at the 50% light level, ranging from 0.88×10^3 to 1.62×10^3 cells m⁻³ throughout the Lagrangian study period, and increased to 2.98×10^3 cells m⁻³ on day 20. In the SML, centric diatoms (mainly species of the genera *Chaetoceros* and *Thalassiosira*) dominated the phytoplankton assemblage from days 1 to 5 whereas small unidentified flagellates were dominant from days 6 to 7 and on day 20. At the depth of the chl *a* maximum, centric diatoms dominated the phytoplankton assemblage

from days 1 to 7 whereas prymnesiophytes (mainly species of the genera *Chrysochromulina* and *Phaeocystis*) and small unidentified flagellates (2–5 µm) dominated on day 20.

1.3.3 Chlorophyll *a* biomass

Daily changes in the vertical profiles of size-fractionated phytoplankton biomass are presented in Fig. 5. Maximal total chl *a* biomass (B_T) in the SML decreased from 6.5 to 1.0 mg m⁻³ during the Lagrangian study period and was 1.7 mg m⁻³ on day 20. From days 1 to 7, a deep chl *a* maximum (DCM), with total chl *a* concentrations ranging from 8.8 to 16.5 mg m⁻³, was observed at 43–50 m (i.e. at the base of or just below the euphotic zone). On day 20, a chl *a* maximum of 3.2 mg m⁻³ was observed at 40 m (i.e. at the 1% light level depth). The vertical profiles of total chl *a* (B_T) were tightly coupled with the vertical distribution of large phytoplankton cells (B_L). From days 1 to 7, B_L represented more than 65% of the total chl *a* biomass at all stations and all depths. On day 20, however, small phytoplankton cells dominated the total chl *a* biomass ($B_S \geq 55\%$ of B_T) in the upper 30 m whereas large cells were dominant in the rest of the water column ($B_L \geq 51\%$ of B_T). On average, the total integrated chl *a* biomasses over Z_{mix} and over Z_{mix} – Z_{eu} were 47 and 193 mg m⁻², respectively, from days 1 to 7 (Fig. 6a,b). The total chl *a* biomass was lower on day 20 than during the Lagrangian study period (days 1 to 7), with integrated values over Z_{mix} and Z_{mix} – Z_{eu} of 15 and 105 mg m⁻², respectively (Fig. 6a,b). Total chl *a* biomass in the SML showed little daily variability during the study period with a slight decrease from days 1 to 3, an increase on day 4 and a decrease from day 4 onwards (Fig. 6a).

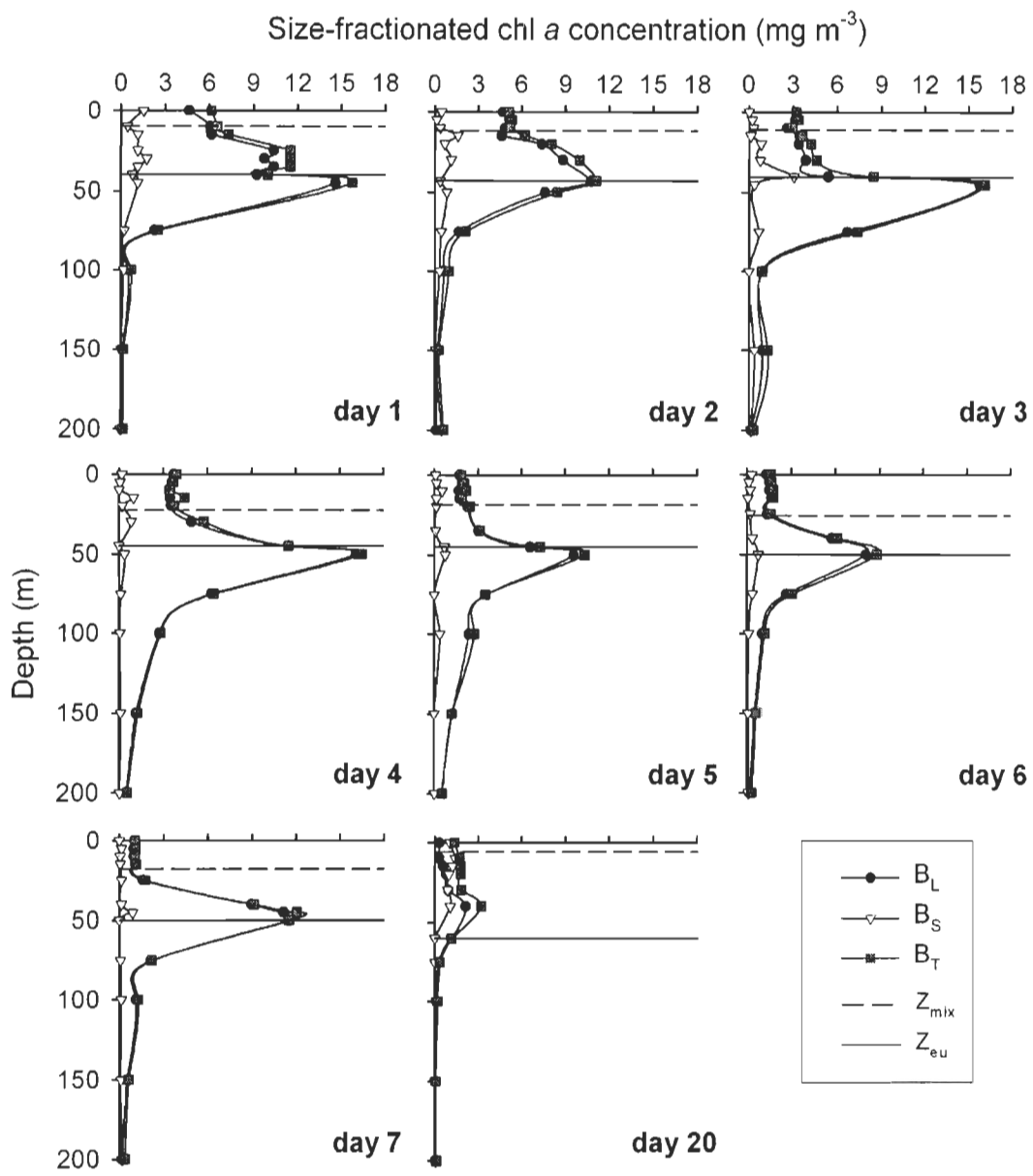


Fig. 5. Vertical profiles of size-fractionated chlorophyll *a* (chl *a*) concentration throughout the study period. B_L : biomass of large phytoplankton cells ($\geq 5 \mu\text{m}$), B_S : biomass of small phytoplankton cells ($0.7\text{--}5 \mu\text{m}$), B_T : total chl *a* biomass (i.e. B_L+B_S), Z_{mix} : depth of the surface mixed layer, Z_{eu} : depth of the euphotic zone

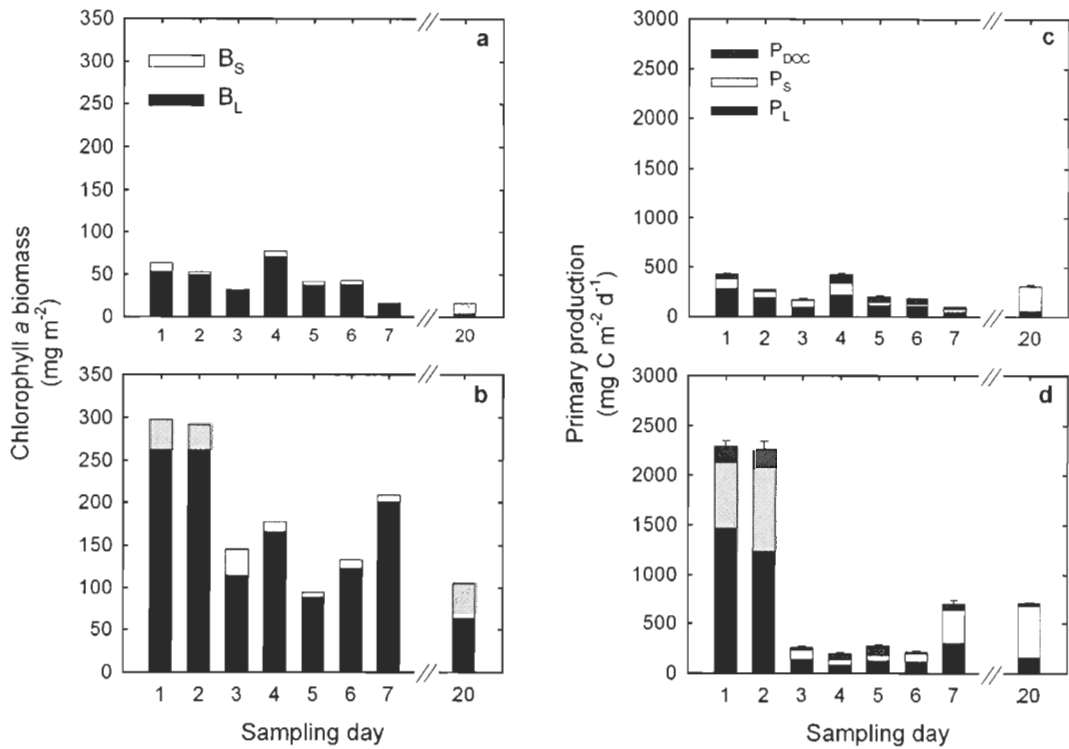


Fig. 6. Temporal variations in the size-fractionated chlorophyll *a* (chl *a*) concentration (a, b) and primary production (c, d) integrated over the surface mixed layer depth (Z_{mix}) (a, c) and between Z_{mix} and the base of the euphotic zone (b, d). B_L : biomass of large phytoplankton cells ($\geq 5 \mu\text{m}$), B_S : biomass of small phytoplankton cells ($0.7-5 \mu\text{m}$), P_L : particulate production of large phytoplankton cells ($\geq 5 \mu\text{m}$), P_S : particulate production of small phytoplankton cells ($0.7-5 \mu\text{m}$), P_{DOC} : dissolved organic carbon release rate. Bars in c) and d) represent the standard deviation of total production (i.e. $P_L + P_S + P_{\text{DOC}}$)

The total chl *a* biomass integrated over $Z_{\text{mix}}-Z_{\text{eu}}$ decreased by ca. 50% from days 2 to 3 (Fig. 6b). It showed pronounced daily variability from days 3 to 6, increased from days 6 to 7 and decreased afterwards (Fig. 6b). Large phytoplankton cells were dominant in both

layers during the Lagrangian study period, contributing $\geq 84\%$ and $\geq 79\%$ of the total chl *a* biomass integrated over Z_{mix} and over $Z_{\text{mix}}-Z_{\text{eu}}$, respectively (Fig. 6a,b). On day 20, large phytoplankton cells were still dominant ($B_L = 60\%$ of B_T) in $Z_{\text{mix}}-Z_{\text{eu}}$, whereas small phytoplankton cells dominated in the SML ($B_S = 79\%$ of B_T). Chl *a* sinking velocities were low during the Lagrangian study, with values ranging from null to 0.40 m d^{-1} and from 0.03 to 0.27 m d^{-1} at the 50% and 5% light depths, respectively (Table 3).

Table 3. Temporal variations in total chlorophyll *a* (chl *a*) sinking velocity at depths of 50% and 5% surface PAR. ND: No data available

Day	50%		5%	
	Depth (m)	Chl <i>a</i> sinking velocity (m d^{-1})	Depth (m)	Chl <i>a</i> sinking velocity (m d^{-1})
1	ND	ND	ND	ND
2	5	0.15	20	0.03
3	5	0.40	20	0.25
4	5	0.12	20	0.17
5	5	0.11	20	0.17
6	5	0.25	25	0.27
7	5	0.06	25	0.10
20	5	0.00	30	0.09

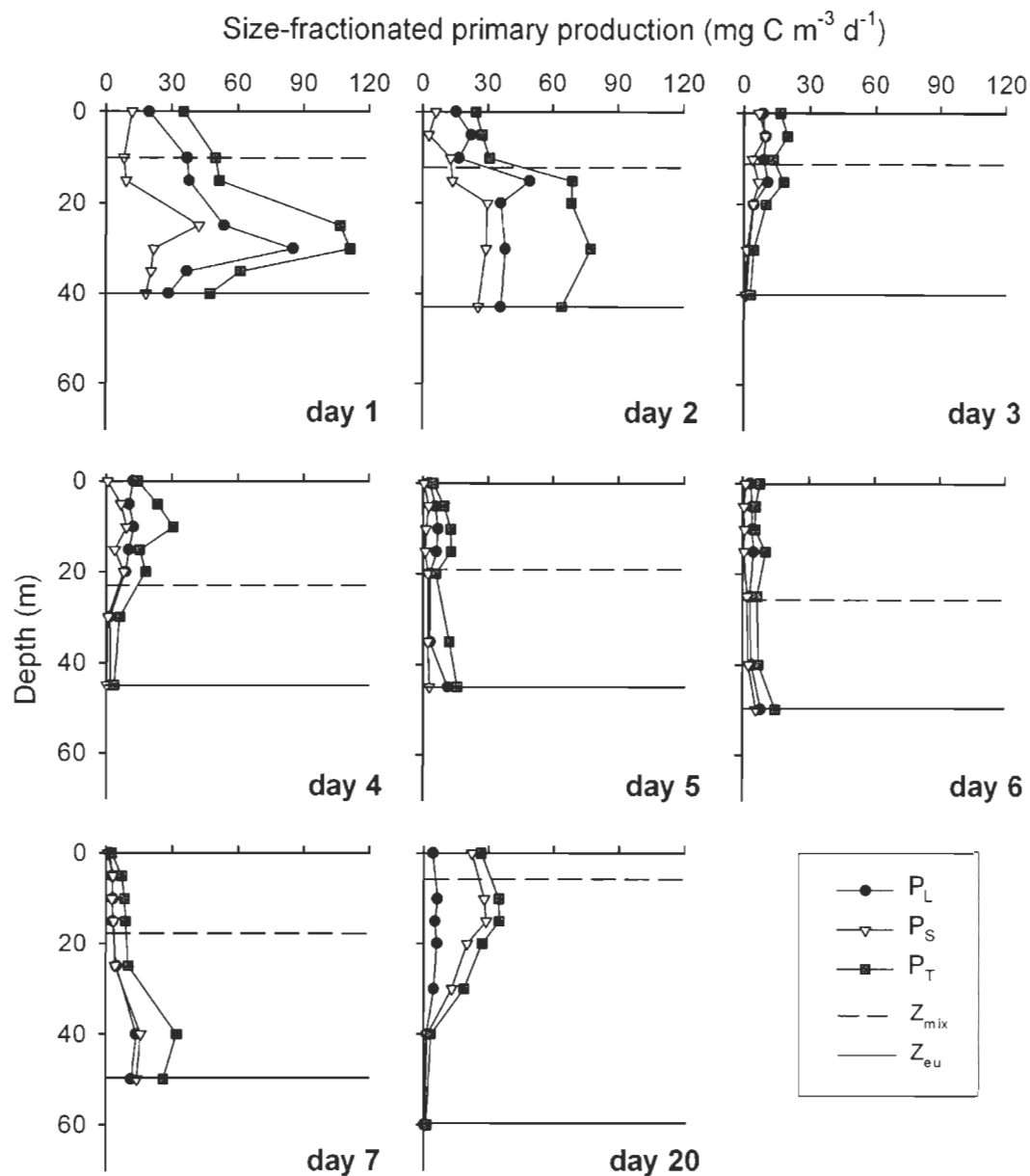


Fig. 7. Vertical profiles of size-fractionated primary production throughout the study period. P_L : particulate production of large phytoplankton cells ($\geq 5 \mu\text{m}$), P_S : particulate production of small phytoplankton cells ($0.7\text{--}5 \mu\text{m}$), P_T : total production (particulate and dissolved production), Z_{mix} : depth of the surface mixed layer, Z_{eu} : depth of the euphotic zone

1.3.4 Primary production

Fig. 7 shows the daily variations in the vertical profiles of size-fractionated primary production. The highest production rates were measured on day 1, with a maximum value of $111 \text{ mg C m}^{-3} \text{ d}^{-1}$ at 30 m. Primary production decreased on day 3, with values $\leq 32 \text{ mg C m}^{-3} \text{ d}^{-1}$ throughout the water column from days 3 to 7. A small increase was observed on day 20, with a maximum value of $35 \text{ mg C m}^{-3} \text{ d}^{-1}$ at 15 m. The lowest production rates ($\leq 15 \text{ mg C m}^{-3} \text{ d}^{-1}$) were measured on day 6 (Fig. 7). Substantial production rates of 47 and $64 \text{ mg C m}^{-3} \text{ d}^{-1}$ were measured at the base of the euphotic zone on days 1 and 2, respectively and maximum production rates were measured at that depth on days 5 and 6 (Fig. 7). Production by large phytoplankton was dominant at all depths from days 1 to 6 (Fig. 7), accounting for 50% to 94% of the total particulate primary production (P_{POC}). The contribution of large phytoplankton cells to P_{POC} was equal to that of small phytoplankton cells at all depths on day 7, whereas production by small phytoplankton cells prevailed (from 55% to 84% of P_{POC}) at all depths on day 20 (Fig. 7). Total integrated primary production rates over Z_{mix} and over $Z_{mix}-Z_{eu}$ ranged from 105 ± 1 to $426 \pm 18 \text{ mg C m}^{-2} \text{ d}^{-1}$ and from 197 ± 13 to $2295 \pm 53 \text{ mg C m}^{-2} \text{ d}^{-1}$, respectively, during the Lagrangian study (days 1 to 7) and were 306 ± 21 and $713 \pm 7 \text{ mg C m}^{-2} \text{ d}^{-1}$, respectively, on day 20 (Fig. 6c,d). Total primary production integrated over Z_{mix} slightly decreased from days 1 to 3, increased on day 4 then decreased until day 7 (Wilcoxon's signed ranks tests, $p < 0.01$; Fig. 6c). It increased again on day 20 (Wilcoxon's signed ranks test, $p < 0.01$; Fig. 6c). Total primary production integrated over $Z_{mix}-Z_{eu}$ was very high on days 1 and 2 ($> 2200 \text{ mg C m}^{-2} \text{ d}^{-1}$). It decreased significantly by about 90%, from days 2 to 3

(Wilcoxon's signed ranks test, $p < 0.01$) and remained fairly constant from days 3 to 6 (Fig. 6d). Total production rates integrated over $Z_{\text{mix}}-Z_{\text{eu}}$ increased significantly from days 6 to 7 (Wilcoxon's signed ranks test, $p < 0.01$) and were similar on days 7 and 20 (Fig. 6d). Production by large phytoplankton cells dominated the integrated P_{POC} in both the SML and $Z_{\text{mix}}-Z_{\text{eu}}$ from days 1 to 6, accounting for from 55% to 81% of P_{POC} (Fig. 6c,d). On day 7, large and small phytoplankton cells contributed equally to the integrated P_{POC} in both the SML and $Z_{\text{mix}}-Z_{\text{eu}}$ (Fig. 6c,d). On day 20, primary production by small phytoplankton cells prevailed and contributed 83% and 77% of the integrated P_{POC} in the SML and in $Z_{\text{mix}}-Z_{\text{eu}}$, respectively (Fig. 6c,d). No significant correlations were found between nutrient concentrations and size fractionated or total primary production in either layer throughout the Lagrangian study period (Kendall's τ correlations, $p > 0.05$).

In the SML, the percentage of total primary production released as extracellular carbon (percent extracellular release, $\text{PER} = P_{\text{DOC}} / P_T \times 100$) increased from 10% to 30% from days 1 to 6. Values of 23% and 1% were measured on days 7 and 20, respectively. In $Z_{\text{mix}}-Z_{\text{eu}}$, PER increased from 7% to 34%, from days 1 to 5, and then progressively decreased to a value of 4% on day 20 (Fig. 6d). Throughout the study period, no significant correlations were found between the concentration of inorganic nutrients and PER, in either the SML or $Z_{\text{mix}}-Z_{\text{eu}}$ (Kendall's τ correlations, $p > 0.05$).

We compared the phytoplankton production normalized to the chl a biomass (P:B ratio) of large phytoplankton cells ($P_L:B_L$) with that of small phytoplankton cells ($P_S:B_S$) in the SML and in $Z_{\text{mix}}-Z_{\text{eu}}$ (Fig. 8). In the SML, $P_L:B_L$ decreased from 5.3 on day 1 to 2.7 mg C mg chl a^{-1} d $^{-1}$ on day 7 and increased to 16.2 mg C mg chl a^{-1} d $^{-1}$ on day 20 (Fig. 8). In

$Z_{\text{mix}}-Z_{\text{eu}}$, $P_L:B_L$ decreased from 5.6 on day 1 to 0.5 mg C mg chl $a^{-1} d^{-1}$ on day 4 and remained ≤ 2.5 mg C mg chl $a^{-1} d^{-1}$ afterwards (Fig. 8). The P:B ratios of large cells were significantly lower than those of small phytoplankton cells in both the SML and in $Z_{\text{mix}}-Z_{\text{eu}}$ (Wilcoxon's signed ranks tests, $p < 0.01$). The temporal changes in $P_S:B_S$ were more pronounced than those of $P_L:B_L$ in both the SML and in $Z_{\text{mix}}-Z_{\text{eu}}$ (Fig. 8).

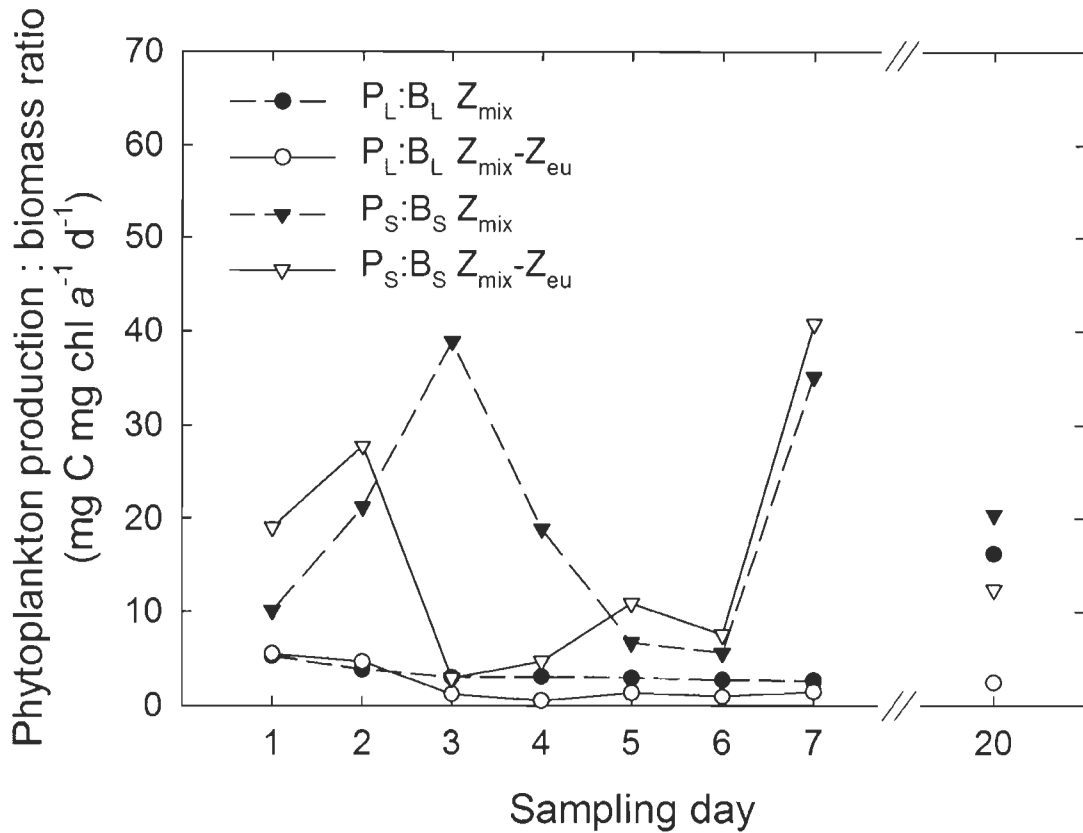


Fig. 8. Temporal variations in the particulate primary production normalized to total chlorophyll a (chl a) biomass of large ($P_L:B_L$) and small ($P_S:B_S$) phytoplankton cells integrated over the surface mixed layer depth (Z_{mix}) and between Z_{mix} and the base of the euphotic zone ($Z_{\text{mix}}-Z_{\text{eu}}$)

1.3.5 Particulate organic carbon

The POC concentration integrated over Z_{mix} ranged from 3.0 to 6.9 g C m⁻² during the Lagrangian study (days 1 to 7) and was 1.7 g C m⁻² on day 20. The integrated POC concentration was consistently higher in $Z_{\text{mix}}-Z_{\text{eu}}$ than in the SML (Wilcoxon's signed ranks tests, $p < 0.01$), ranging from 6.8 to 12.9 g C m⁻² from days 1 to 7 and amounting 8.6 g C m⁻² on day 20. The depth-integrated concentrations of POC were positively correlated with those of total chl α in both the SML and in $Z_{\text{mix}}-Z_{\text{eu}}$ (Kendall's τ correlations, $p < 0.05$).

During the study, the POC:chl α ratio in the euphotic zone ranged from 27 to 204 g:g and consistently decreased with depth (Fig. 9). The POC:chl α ratio averaged over Z_{mix} increased throughout the Lagrangian study, from 71 on day 1 to 194 on day 7 and was 122 on day 20 (Fig. 9). The POC:chl α ratio averaged over $Z_{\text{mix}}-Z_{\text{eu}}$ increased from 42 on day 1 to 74 on day 7 and was 93 on day 20 (Fig. 9). In the SML, this ratio was consistently higher than the value of 40–50 obtained by Lorenzen (1968) for healthy phytoplankton populations (Wilcoxon's signed ranks test, $p < 0.01$). However, in $Z_{\text{mix}}-Z_{\text{eu}}$, it did not deviate significantly from the critical value of Lorenzen (1968) (Wilcoxon's signed ranks test; $p < 0.01$), except on day 20 (Fig. 9).

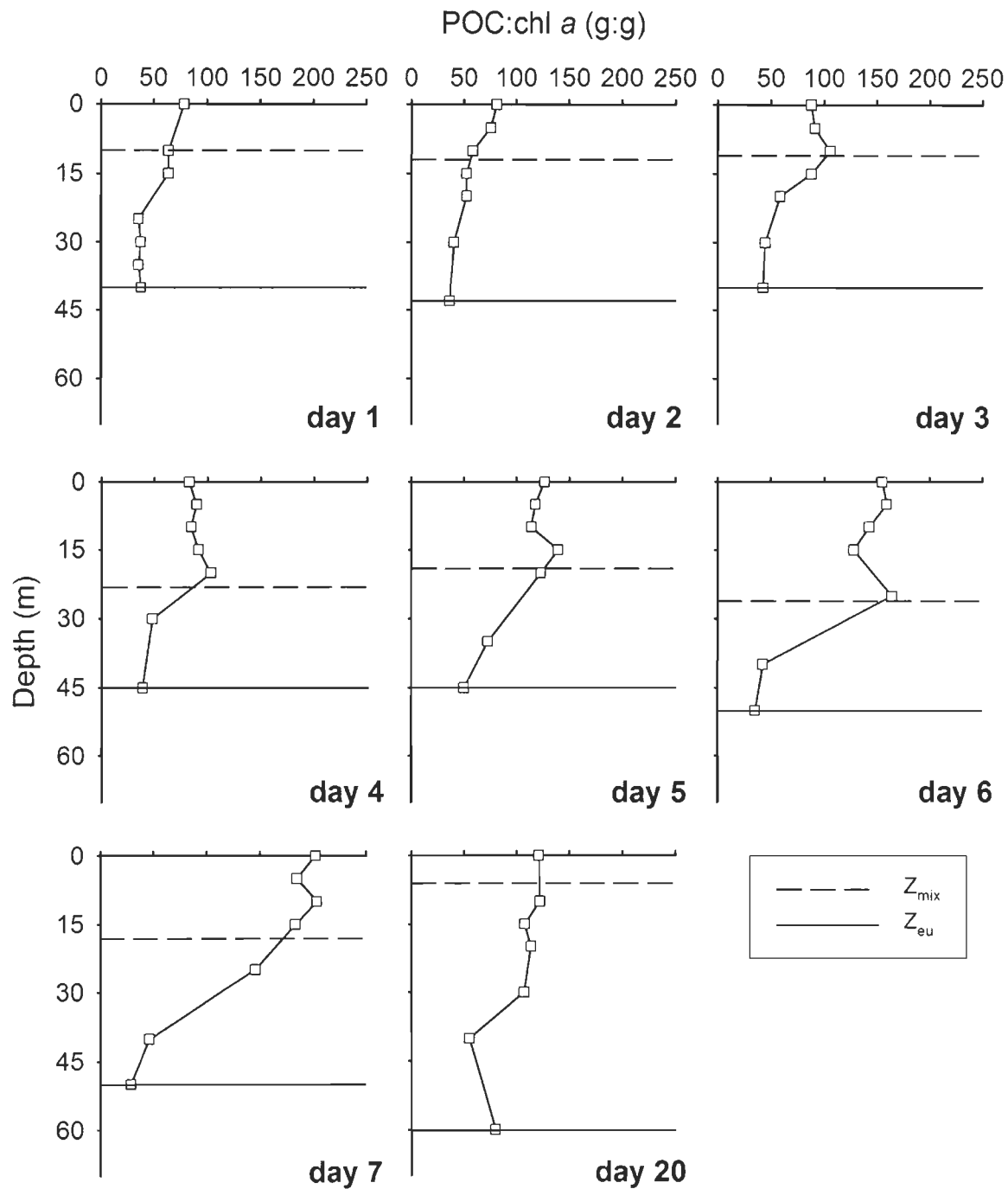


Fig. 9. Vertical profiles of the ratio of particulate organic carbon to total chlorophyll *a* (POC:chl *a*) throughout the study period. Z_{mix} : depth of the surface mixed layer, Z_{eu} : depth of the euphotic zone

1.4 Discussion

1.4.1 Environmental conditions and phytoplankton nutrient status

The surface waters remained well stratified throughout the study period despite stronger wind velocities during the night from days 3 to 4 (average wind speed = 16 m s^{-1}) and from days 5 to 6 (average wind speed = 11 m s^{-1}). The wind event on days 3–4 was echoed by an increased drift distance of the Lagrangian buoy (Fig. 1). According to temperature and salinity profiles (Fig. 2b, c) and to T-S diagrams (Fig. 3), the drifting buoy remained in the same water mass from days 1 to 7, as planned for the Lagrangian sampling design. Thirteen days later (day 20), the presence of warmer and more saline waters in the upper 60 m of the water column suggested that we sampled a different surface water mass than during the Lagrangian study period. However, the sampling station on day 20 was likely representative of post-bloom conditions occurring in the northwest Atlantic Ocean off the Scotian Shelf. The two wind events (days 3–4 and days 5–6) also translated vertically into a deepening of the surface mixed layer, as observed on days 4 and 6. Episodic increases in the mixed-layer depth in response to changes in wind stress are well-known (Mann & Lazier 1996). However, wind-induced turbulence did not extend down to the nutricline or to the DCM and thus did not profoundly impact the structure of the upper water column, which remained well stratified throughout the Lagrangian study period.

The daily variability in nutrient concentrations in $Z_{\text{mix}}-Z_{\text{eu}}$ can be partially explained by variations in the depth of Z_{eu} relative to Z_{nutr} . Since the nutricline was located close to

the base of the euphotic zone, small changes in Z_{eu} led to large variations in nutrient concentrations at the 1% and 0.2% surface PAR depths. This in turn caused pronounced changes in nutrient concentrations integrated over Z_{mix} - Z_{eu} . Indeed, a substantial increase in nutrient concentrations was observed from day 6 onwards when the nutricline was 10 to 20 m shallower than the base of the euphotic zone (Table 1, Fig. 4). Despite these daily variations, nutrient concentrations remained fairly low throughout the study period and well below the average wintertime concentrations in the euphotic zone reported in the World Ocean Atlas for that region ($\text{NO}_3 + \text{NO}_2$: 5 μM ; PO_4 : 1 μM ; Si(OH)_4 : 4 μM ; Conkright et al. 2002). These very low nutrient concentrations reflect consumption by phytoplankton during the bloom. According to Liebig's law of minimum (Liebig 1940) and the reference ratios of 16N:1P (Redfield et al. 1963) and 1.1N:1Si (Brzezinski 1985), nitrogen was the inorganic nutrient in lowest availability for phytoplankton growth (Table 2). Nitrogen limitation of primary producers is a common feature at temperate latitudes of the North Atlantic Ocean in late spring and summer (Parsons & Lalli 1988, Platt et al. 1992).

The euphotic zone is usually viewed as a two-layer system, with the nutricline acting as a boundary between the nutrient-depleted surface layer and deeper waters where low light availability limits phytoplankton growth (Dugdale 1967, Cullen 1982). During this study, the nutricline was located very close to the base of the euphotic zone (Table 1). Moreover, very low nutrient concentrations (Fig. 4), low DIN:PO₄ molar ratios (Table 2), low P:B ratios of the large phytoplankton (< 5 mg C mg chl $a^{-1} d^{-1}$, Fig. 8) and the high POC:chl a ratio (Fig. 9) suggest that diatoms were generally nitrogen limited in the top layer of the euphotic zone (i.e. at depths > 1% surface PAR). The higher P:B ratios of the

small phytoplankton (Fig. 8) suggest that these cells were less nitrogen-stressed than the larger algal cells. In the bottom layer of the euphotic zone (i.e. at depths $\leq 1\%$ surface PAR), the POC:chl α ratios were close to the critical value of 40–50 g:g (Lorenzen (1968) suggesting that the phytoplankton assemblage was light-limited. This two-layer system allowed the development and maintenance of a deep chl α maximum (DCM) at a depth where both light and nutrient availability offered the best compromise for phytoplankton growth and accumulation (Fig. 5).

1.4.2 Formation and maintenance of the deep chlorophyll α maximum

One of the most noticeable features of the Lagrangian study period was the formation and maintenance of a DCM dominated by large phytoplankton cells near the base of the euphotic zone and the nutricline. The post-bloom period was also characterized by the presence of a DCM around the 1% light level depth. This feature is typical of stratified temperate waters in transition from bloom to oligotrophic conditions (Cullen 1982). The DCM can reflect an increase in intracellular chl α concentration due to photoacclimation to low light levels (physiological response) and/or an increase in phytoplankton biomass (population response) by either growth at depth, accumulation along a density structure or changes in cell buoyancy (Cullen 1982). During this study, different mechanisms seem to have played a role in the formation and maintenance of the DCM. As pointed out by Cullen (1982), a chl α maximum does not necessarily correspond to a maximum in phytoplankton biomass, as chl α per cell abundance or per cell volume increases when the cells become shade acclimated (Prézelin 1981). The low POC:chl α ratios measured at the base of the

euphotic zone (27–50 g:g, Fig. 9) during this study demonstrate that photoacclimation indeed occurred at the DCM. However, there was also evidence that the observed DCM did not only reflect shade acclimation but also represented an increase in phytoplankton carbon biomass and abundance. Firstly, vertical profiles showed that maximum POC concentrations (not shown) were always associated with maximum chl α concentrations. Secondly, phytoplankton abundances were three times higher at the DCM than in the SML. Finally, chl α concentration and phytoplankton abundance at the DCM were positively correlated (Kendall's τ correlation, $p < 0.05$). These results confirm that the DCM was associated with the maximum phytoplankton biomass.

During some days, primary production at depth may have contributed to increase phytoplankton biomass at the DCM, as shown by substantial production rates measured at the base of the euphotic zone on days 1, 2 and 7 (Fig. 7). On other days (i.e. days 3-6 and 20), very low production rates at the base of the euphotic zone indicate that growth at depth had a limited influence in the maintenance of the DCM. Hence, phytoplankton growth in the bottom layer of the euphotic zone may explain, in part, the development of the DCM. However, during the Lagrangian study period, the main mechanism involved in the formation of the DCM was probably the sinking of phytoplankton from the nutrient-limited SML and their accumulation at the base of the euphotic zone near the nutricline on days 2 and 3. This is supported by higher chl α sinking velocities in the SML (i.e. at the 50% surface PAR depth) than at the 5% surface PAR depth on days 2 and 3 (Table 3). Similarly, the decrease in chl α concentration in $Z_{\text{mix}}-Z_{\text{eu}}$ between days 2 and 3 coincided with the increase in chl α concentration at the DCM during the same period (Fig. 5). As the

nutricline was very close to the base of the euphotic zone, shade-acclimated cells that settled there could have taken advantage of the upward diffusion flux of nutrients and increased their buoyancy (Bienfang et al. 1983, Bienfang & Harrison 1984). It is interesting to note the concomitant shallowing of the nutricline and of the chl *a* biomass peak from days 6 onwards (Table 1, Fig. 5). Moreover, the DCM was associated with increased vertical stability, as deduced from the vertical profiles of the Brunt-Väisälä frequency (data not shown). These results indicate that environmental and biological factors play an important role in the location of the DCM in the upper water column, as previously suggested by Vandeventer et al. (1987).

The results presented in the previous paragraphs show that a large part of the phytoplankton biomass was retained at the base of the euphotic zone instead of being rapidly exported to depth during the decline of the northwest Atlantic spring bloom. In addition, the DCM was still observed 5 days (i.e. on day 7) and 18 days (i.e. on day 20) after the drastic reduction in primary production (i.e. on day 3). This indicates that the DCM was maintained for a few weeks after the spring bloom. It is also interesting to note that the biomass of large phytoplankton cells remained high in the upper part of the twilight zone (defined here as the layer between the base of the euphotic zone and 200 m) throughout the Lagrangian study, suggesting a significant transfer of phytoplankton biomass from the euphotic zone to the twilight zone. Thirteen days later, almost no phytoplankton biomass remained in the upper part of the twilight zone. Hence, the decay of the spring bloom has a relatively long duration (i.e. between 1 and 2.5 weeks) in the northwest Atlantic.

1.4.3 The decline of the spring diatom bloom

During the two first sampling days of the Lagrangian study, total primary production rates integrated over the entire euphotic zone were 2720 ± 55 and 2522 ± 99 mg C m⁻² d⁻¹, respectively. Assuming a Redfield C:N uptake ratio of 6.6, the maximum potential production rates based on ambient DIN availability in the euphotic zone (Fig. 4a, b) were 790 and 2231 mg C m⁻² d⁻¹ on days 1 and 2, respectively. While, the estimated and measured rates of primary production on day 2 are in fairly good agreement, the estimated production rate on day 1 is about 3.5 times lower than the measured value. This suggests that we underestimated the ambient DIN concentrations or that phytoplankton were utilizing other sources of ambient dissolved nitrogen, such as urea or labile amino acids (McCarthy 1972, Bronk et al. 2007). Varela et al. (2005) measured an average urea concentration of 0.3 μM in the euphotic zone of the northeast Atlantic Ocean. This concentration would have allowed a daily production rate of ca. 1900 mg C m⁻², since one mole of urea contains two atoms of N. This potential organic N source and the ambient DIN would have been sufficient to support the high production rate measured on day 1. A second potential source of dissolved nitrogen for primary production is the internal pool of DIN in phytoplankton cells (Collos & Slawyk 1980, Dortch et al. 1984). The intracellular inorganic nitrogen pool can account for up to 5% of the total cellular nitrogen (Dortch et al. 1984) which, considering an integrated chl *a* concentration of 361 mg m⁻² in the euphotic zone on day 1 (Fig. 6) and a N:chl *a* ratio 0.5 mol:g (Kudo 2003), gives a potential average pool of intracellular inorganic nitrogen in the euphotic zone of 0.2 μM. A third possible source of dissolved nitrogen is nitrogen regenerated by bacteria and microzooplankton

during the incubation, such as ammonium, urea and amino acids (McCarthy 1972, Bronk et al. 2007, Fernández & Raimbault 2007). These results indicate that when all potential sources of nitrogen are considered (including atmospheric nitrogen), nitrogen availability was sufficient to support the high production rates observed during this study.

The production rates measured during the first two days of the study are among the highest values recorded at temperate latitudes of the open North Atlantic Ocean. For example, maximum integrated production rates reported during the NABE experiment in the northeast Atlantic Ocean ranged from 1860 mg C m⁻² d⁻¹ (Lochte et al. 1993) to 1970 mg C m⁻² d⁻¹ (Bury et al. 2001) whereas Harrison et al. (1993) measured production rates up to 1160 mg C m⁻² d⁻¹ at 45°N, 41°W in the northwest Atlantic Ocean in May 1989. Joint et al. (2001) reported maximum integrated production rates up to ca. 1400 mg C m⁻² d⁻¹ during the spring bloom over the northwest European continental shelf break and production rates > 2000 mg C m⁻² d⁻¹ were recorded by Lohrenz et al. (2002) over the shelf-slope front off Cape Hatteras.

Studies on size-fractionated primary production are often limited to estimates of particulate production. However, it is well established that total primary production also comprises a dissolved fraction (Mague et al. 1980) known as the percent extracellular release (PER). During this study, PER varied between 1 and 34% with an average of 14%. These percentages are in good agreement with reported values ≤20% for most marine environments (Nagata 2000). Increases in PER have been reported under nutrient stress, particularly at the end of phytoplankton blooms (Lancelot & Billen 1984). This is consistent with the increase in PER throughout the Lagrangian study period, when nitrogen

was likely limiting primary production, although no significant correlations were found between PER and inorganic nutrient concentrations.

Throughout the Lagrangian study period, both phytoplankton biomass and production were dominated by large cells (Fig. 6). The same pattern was reported by Joint et al. (1993) during the peak of the spring bloom in the northeast Atlantic Ocean. During the Lagrangian study period, large phytoplankton cells were numerically dominated by centric diatoms. Species of the genera *Chaetoceros* and *Thalassiosira* together represented 64–78% and 51–75% of the total diatom abundance at the 50% light level depth and at the DCM, respectively. The low Si(OH)_4 concentrations compared to wintertime values (Si(OH)_4 : 4 μM ; Conkright et al. 2002) are consistent with the development of a diatom population, a common feature of the spring bloom in temperate latitudes of the North Atlantic Ocean (Sieracki et al. 1993). Under post-bloom conditions (day 20), the numerical phytoplankton dominance shifted to small prymnesiophytes and unidentified flagellates. This seasonal change in the phytoplankton community composition has already been reported in the temperate northeast Atlantic in late spring (Sieracki et al. 1993) and is consistent with the dominance of small phytoplankton cells in terms of primary production and their increased contribution to total chl *a* biomass after the spring bloom (Figs. 5 & 7).

1.4.4 Potential fate of large and small phytoplankton cells

Throughout the study period, small phytoplankton cells contributed more to the total particulate primary production ($P_S = 31\text{--}79\%$ of P_{POC} , Fig. 7) than to the total chl *a* biomass ($B_S = 4\text{--}45\%$ of B_T , Fig. 5). On one hand, this unequal contribution of small cells to total

phytoplankton biomass and production could be related to the higher metabolic rates per unit of biomass of the small cells compared to the larger ones (Glover 1980). This reasoning is consistent with our results (Fig. 8). On the other hand, the larger contribution of small phytoplankton cells to total primary production compared to total chl *a* biomass could be interpreted in terms of preferential removal of small phytoplankton cells by microzooplankton grazing, indicative of a top down control of small phytoplankton biomass and of an active microbial food web within the euphotic zone (Tremblay & Legendre 1994). The higher ratio of pheopigments to total pigments (chl *a* + pheopigments) measured in the small phytoplankton size fraction (23–84%) compared to that in the large fraction (11–29%) during the Lagrangian study period (data not shown) supports this hypothesis. Microzooplankton grazing is generally considered as the main predatory pressure on planktonic primary production in many diverse marine systems (Calbet & Landry 2004), in particular during the spring bloom in the North Atlantic Ocean (Harrison et al 1993, Gaul et al. 1999, Karayanni et al. 2005).

Alternatively, large phytoplankton cells made a smaller contribution to the total particulate primary production ($P_L = 21\text{--}72\%$ of P_{POC} , Figs. 6c, d & 7) than to the total chl *a* biomass ($B_L = 55\text{--}96\%$ of B_T , Figs. 5 & 6a, b) throughout the study period. This may be related to the limitation of diatom production by nutrient supply, as previously mentioned. According to the model of Tremblay & Legendre (1994), the smaller contribution of large phytoplankton cells to total primary production than to total chl *a* biomass can also indicate that large phytoplankton cells tend to accumulate in the euphotic zone rather than being grazed by mesozooplankton or exported to depth through sinking.

This interpretation is consistent with the formation and maintenance of a DCM composed of large phytoplankton near the base of the euphotic zone throughout this study and with the temporal uncoupling between phytoplankton growth and mesozooplankton grazing reported during the North Atlantic spring bloom (Parsons & Lalli 1988). We have already discussed the mechanisms explaining the accumulation of large phytoplankton near the base of the euphotic zone, just above the nutricline (see above). The potential POC export from the euphotic zone (POC_E) was estimated using equations 7 ($\text{POC}_E = P_{\text{POC}} \times f$) and 22 ($f = 0.04 + 0.74 \times P_L/P_{\text{POC}}$) in Tremblay et al. (1997), where f is the f -ratio. An average POC_E value of $1.30 \text{ g C m}^{-2} \text{ d}^{-1}$ was estimated for days 1 and 2 whereas an average value of $0.20 \text{ g C m}^{-2} \text{ d}^{-1}$ was estimated for the rest of the study. The former value is about twice as high as the POC sinking flux of 0.67 g C m^{-2} measured with free-drifting sediment traps deployed below the base of the euphotic zone on day 2 (Pommier et al. ms-b, Chapitre II), whereas the latter value is fairly close to the average POC sinking flux of $0.31 \text{ g C m}^{-2} \text{ d}^{-1}$ measured below the base of the euphotic zone for the rest of the study (Pommier et al. ms-b, Chapitre II).

1.5 Conclusion

We captured the decline of one of the most productive spring diatom bloom ever reported for the open North Atlantic Ocean, under nitrogen-limiting conditions. Phytoplankton production and biomass decreased from 2720 to $400 \text{ mg C m}^{-2} \text{ d}^{-1}$ and from 361 to $121 \text{ mg chl } a \text{ m}^{-2}$, respectively, throughout the study period. Large phytoplankton cells ($\geq 5 \mu\text{m}$), which dominated both the production and biomass during the Lagrangian

study, were replaced by small phytoplankton ($0.7\text{--}5\ \mu\text{m}$) 13 days later. The analysis of the size structure of phytoplankton biomass and production (Tremblay & Legendre 1994) revealed that small phytoplankton cells were potentially removed by microzooplankton grazing whereas large algal cells tended to accumulate in the euphotic zone, mainly at the DCM. The formation and maintenance of the DCM involved sedimentation of phytoplankton cells at the base of the euphotic zone near the nutricline, where photoacclimated cells maintained low sinking velocities. In contrast to our working hypothesis, the decline of the bloom was not associated with the rapid sinking of large phytoplankton cells out of the euphotic zone. The fate of the phytoplankton biomass accumulated at the DCM is important in regard to biogeochemical cycling of the North Atlantic spring bloom. Nevertheless, an assessment of this fate requires detailed information about zooplankton grazing, microbial metabolism and vertical sinking fluxes of biogenic material. This is the subject of the second chapter of this thesis.

CHAPITRE II

PARTICULATE ORGANIC CARBON EXPORT IN THE UPPER TWILIGHT ZONE OF THE NORTHWEST ATLANTIC OCEAN DURING THE DECLINE OF THE SPRING BLOOM

RÉSUMÉ

La variabilité des flux verticaux de carbone organique particulaire (COP) et sa relation à la production primaire ont été étudiées dans la partie supérieure de la zone mésopélagique de l'océan Atlantique nord-ouest, durant le déclin d'un bloom printanier de diatomées et sa transition vers des conditions de post-bloom. Le flux de COP sous la base de la zone euphotique (i.e. 50-75 m) a diminué de 674 ± 105 à 281 ± 17 mg C m⁻² j⁻¹ durant le déclin de bloom et représentait 197 ± 2 mg C m⁻² d⁻¹ en conditions de post-bloom. Le flux de COP sous la base de la zone euphotique était positivement corrélé à la production du gros phytoplancton (≥ 5 µm) durant la période d'étude, mettant ainsi en évidence l'importance de la structure de taille du phytoplancton dans le contrôle de l'exportation de COP en depuis la zone euphotique. Néanmoins, le flux de COP à 150 m est demeuré relativement constant durant la période d'étude. L'analyse des profils verticaux de décroissance du flux de COP avec la profondeur a révélé l'augmentation de l'efficacité de transfert du COP à 150 m liée à la diminution du recyclage de la matière organique dans la partie supérieure de la zone mésopélagique lors du déclin du bloom. De plus, le recyclage du COP dans la zone mésopélagique était positivement corrélé au flux de COP sous la base de la zone euphotique durant la période d'étude. Ces résultats suggèrent que les processus de recyclage de la matière organique dans la partie supérieure de la zone mésopélagique répondent rapidement et proportionnellement à la variabilité des apports de matière organique depuis la zone euphotique. Nous avons émis l'hypothèse que la diminution du recyclage de la matière organique dans la zone mésopélagique lors du déclin du bloom a compensé la réduction du flux de COP sous la base de la zone euphotique, tamponnant ainsi les variations temporelles du flux de COP à 150 m. Ces résultats mettent l'accent sur l'importance des variations à court terme du recyclage de la matière organique dans la partie supérieure de la zone mésopélagique en regard à l'efficacité de transfert du carbone organique en profondeur.

ABSTRACT

The variability of particulate organic carbon (POC) sinking flux and its relation to primary production were investigated in the upper twilight zone of the northwest Atlantic Ocean on four occasions during a Lagrangian study of the decline of a spring diatom bloom

and its transition towards post-bloom conditions. POC sinking fluxes below the euphotic zone (i.e. 50–75 m) decreased from 674 ± 105 to 281 ± 17 mg C m⁻² d⁻¹ throughout the senescence of the bloom and further decreased to 197 ± 2 mg C m⁻² d⁻¹ under post-bloom conditions. POC sinking fluxes below the euphotic zone were positively correlated to the production of large phytoplankton cells (≥ 5 µm) throughout the study period, highlighting the importance of the size structure of primary producers in shaping the export of POC from the euphotic zone. In contrast, POC sinking fluxes at 150 m showed little variation throughout the study period. The analysis of the vertical profiles of POC sinking flux revealed the increase in POC transfer efficiency from 50 to 150 m due to the decrease in POC recycling within the upper twilight zone throughout the decline of the bloom. Moreover, POC recycling within the upper twilight zone was positively correlated with POC sinking fluxes below the euphotic zone throughout the study period, suggesting that recycling processes in the upper twilight zone respond rapidly and proportionally to the export of POC from the euphotic zone. It is hypothesized that the concomitant decreases in POC sinking fluxes below the euphotic zone and in POC recycling within the upper twilight zone compensated each other and could explain the fairly constant POC sinking fluxes at 150 m that were observed throughout the study period. Our results shed light on the importance of short-term variability in organic matter recycling within the upper twilight zone for the efficiency of POC export to depth.

2.1 Introduction

Over the last decades, much effort has been put into the understanding of the relationship between primary production and carbon export to depth in the World Ocean. This interest was largely motivated by the need to predict the efficiency of the biological carbon pump (Volk & Hoffert 1985) in sequestering carbon dioxide in the deep ocean and possibly mitigating the increase in anthropogenic emissions of this climate-relevant greenhouse gas in the context of a globally warming climate.

Most of the contemporary knowledge regarding the coupling between primary production and carbon export to depth is derived from time-series particle interceptor traps moored in the deep ocean that measure particle fluxes at weekly to monthly intervals over periods of several months to more than a year (Honjo 1996). These deep-ocean mooring arrays have proved to be very useful tools in relating the magnitude and temporal patterns of deep carbon fluxes with the seasonality of phytoplankton production (Wefer 1989) and the size structure of primary producers (Boyd & Newton 1999). Results from long-term particle interceptor traps have also served as the basis for developing algorithms that seek to model the export of particulate organic carbon to depth (Bishop 1989).

Nevertheless, predictions of deep-sea carbon export from existing algorithms are still subject to uncertainties. These uncertainties are largely attributed to a lack of knowledge on early processes affecting the flux of particles in the twilight zone (i.e., at depths between the base of the euphotic zone and ~1000 m; Buesseler et al. 2007b). The twilight zone, where about 90% of the exported material is thought to be mineralized, is believed to play a critical role in the transfer of biogenic carbon from the ocean surface to the deep ocean

(Angel 1989, Tréguer et al. 2003). While we know from particle interceptor trap data that particulate organic carbon (POC) fluxes decrease rapidly with depth within the twilight zone, we have little knowledge on the processes responsible for this mineralization pattern (Ducklow et al. 2001). It is believed that the strength and variability of processes affecting the transformation of particulate material during its sinking strongly influence the coupling between primary and export production and determine the efficiency of particle export to depth over short spatial and temporal scales (Wassmann 1998). It is also recognized that deep POC fluxes could be predicted with greater reliability if the processes affecting the early export of organic material from the productive layer were better understood (Boyd & Newton 1995).

In temperate and subpolar latitudes of the North Atlantic Ocean, the spring phytoplankton bloom is a major biogeochemical event contributing significantly to the sinking export of particles to the deep ocean (Honjo 1996). In that region of the World Ocean, temporal uncoupling between phytoplankton growth and zooplankton grazing can result in a massive sedimentation of organic material at the end of the spring bloom (Parsons & Lalli 1988, Honjo & Manganini 1993). The decline of the spring bloom is thus of particular interest for the investigation of the short-term variability in the coupling between primary production and early export processes of particulate organic material. However, there is a lack of information on the sinking flux of organic carbon and its coupling with primary production during that particular stage of the spring bloom at temperate latitudes in the North Atlantic Ocean. Moreover, except for the Western North Atlantic Bloom Experiment (40°N , 47°W and 45°N , 41°W ; Harrison et al. 1993), there is a

lack of information on the sinking flux of organic carbon in the temperate western North Atlantic Ocean, as most of the particle flux data in the North Atlantic have been collected in the eastern part of this ocean basin (Antia et al. 2001). Finally, to our knowledge, there is no detailed information about POC sinking fluxes in the twilight zone of the temperate North Atlantic Ocean.

Within this framework, our study aimed at (1) characterizing the sinking flux of particulate organic carbon in the upper twilight zone (i.e., from the base of the euphotic zone down to 150 m) during the declining phase of the spring bloom in the temperate northwest Atlantic Ocean, (2) investigating the coupling between the activity and size structure of primary producers in the euphotic zone and POC export in the upper twilight zone, and (3) assessing the processes affecting the transformation of the sinking material within the upper twilight zone. This study is part of the Canadian Surface Ocean–Lower Atmosphere Study (C-SOLAS) which aims at quantifying the impact of the senescence of the North Atlantic spring bloom on the production and ventilation to the atmosphere of climatically active trace gases.

2.2 Materials and methods

2.2.1 Sampling

Sampling was carried out aboard the CCGS *Hudson* off the Scotian Shelf at station L (water depth ca. 3500 m; Fig. 1) as part of a Lagrangian survey of the decline of the spring bloom in the northwest Atlantic Ocean (Pommier et al. ms-a, Chapitre I). A water mass

within which a phytoplankton bloom had developed was sampled from 25 April (day 1) to 01 May 2003 (day 7). The water mass under investigation was tracked using a CAST ARGOS drifter (Seimac Smart CAT PTT/GPS transmitter) equipped with a 15-meter-long Holey Sock tubular drogue centered at 15 m in the water column. On 14 May 2003 (day 20), the station occupied on day 1 was revisited and samples were collected in order to study the potential biogeochemical changes in the euphotic zone that could have occurred at that sampling location after the decline of the spring bloom and the potential impact of these changes on the sinking fluxes of biogenic material. Concomitant investigations of primary production and particle sinking fluxes were conducted on 26 April (day 2), 28 April (day 4), 30 April (day 6) and 14 May (day 20) 2003.

2.2.2 Analyses

Primary production rates were measured at seven depths within the euphotic zone (100, 50, 30, 15, 5, 1 and 0.2% of surface PAR) using the ^{14}C -uptake method (Parsons et al. 1984, Gosselin et al. 1997) with on-deck in-situ simulated incubations from sunrise to sunset. Primary production rates were integrated over the euphotic zone depth using trapezoidal integration. The production rates of small (P_S : 0.7–5 μm) and large ($P_L \geq 5 \mu\text{m}$) phytoplankton cells were considered. Detailed information about primary production measurements can be found in Pommier et al. (ms-a, Chapitre I).

Free-drifting particle interceptor traps were deployed for periods of 24 hours (Table 1). The traps, which were PVC cylinders with an internal diameter of 10 cm and an aspect ratio (height:diameter) of 7, were deployed at five depths (50, 75, 100, 125 and

150 m) below both the surface mixed layer and the base of the euphotic zone (except for the trap deployed at 50 m on day 20; Table 1). The present manuscript focuses on the sinking fluxes of organic material below the base of the euphotic zone and at 150 m. The vertical structure of the water column, which was characterized using a CTD probe (Sea-Bird SBE 9), revealed that the deepest trap was located within the permanent thermocline (Fig. 2). For each depth, two traps were installed on the mooring line and centered on the sampling depth.

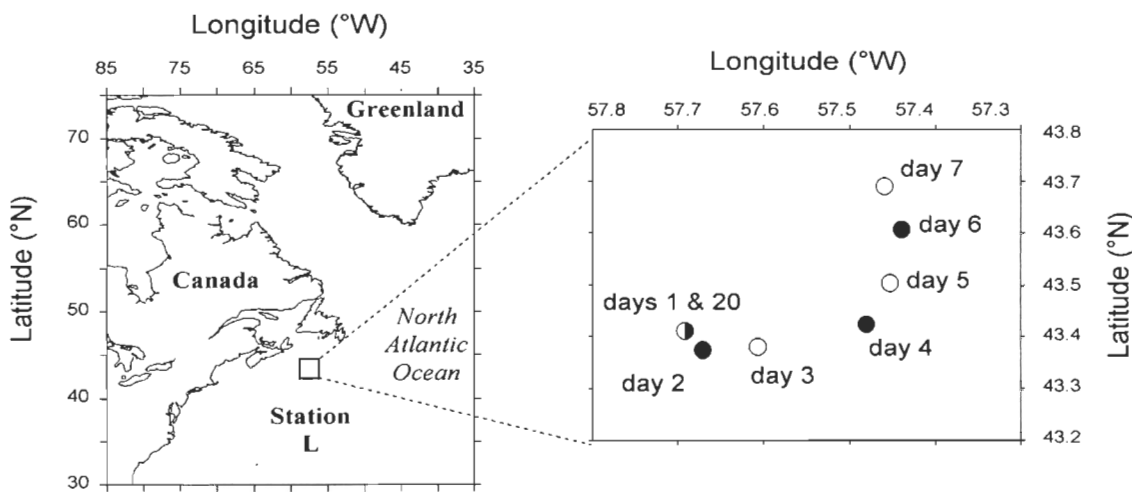


Fig. 1. Location of the drifting buoy from day 1 (25 April) to day 7 (01 May) during a Lagrangian study of a water mass in the northwest Atlantic Ocean in spring 2003. On day 20 (14 May), the ship went back to the latitude/longitude position occupied on day 1. Filled circles indicate the sampling days during which concomitant measurements of primary production and particulate organic material sinking fluxes were made

Table 1. Characteristics of the free-drifting particle interceptor trap moorings and of the upper water column in the northwest Atlantic in spring 2003. The depths of the euphotic zone (Z_{eu}) and of the surface mixed layer (Z_{mix}) are from Pommier et al. (ms-a, Chapitre I)

Day	Date in	Duration (d)	Deployment		Recovery		Distance travelled (km)	Z_{eu} (m)	Z_{mix} (m)
			Latitude (°N)	Longitude (°W)	Latitude (°N)	Longitude (°W)			
2	26 April	0.91	43°21.4	57°37.9	43°21.7	57°34.1	4.3	43	12
4	28 April	1.06	43°24.6	57°28.9	43°28.9	57°28.1	7.5	45	23
6	30 April	0.88	43°37.1	57°25.8	43°40.3	57°28.5	6.9	50	26
20	14 May	0.99	43°21.9	57°42.6	43°20.4	57°41.6	2.4	60	6

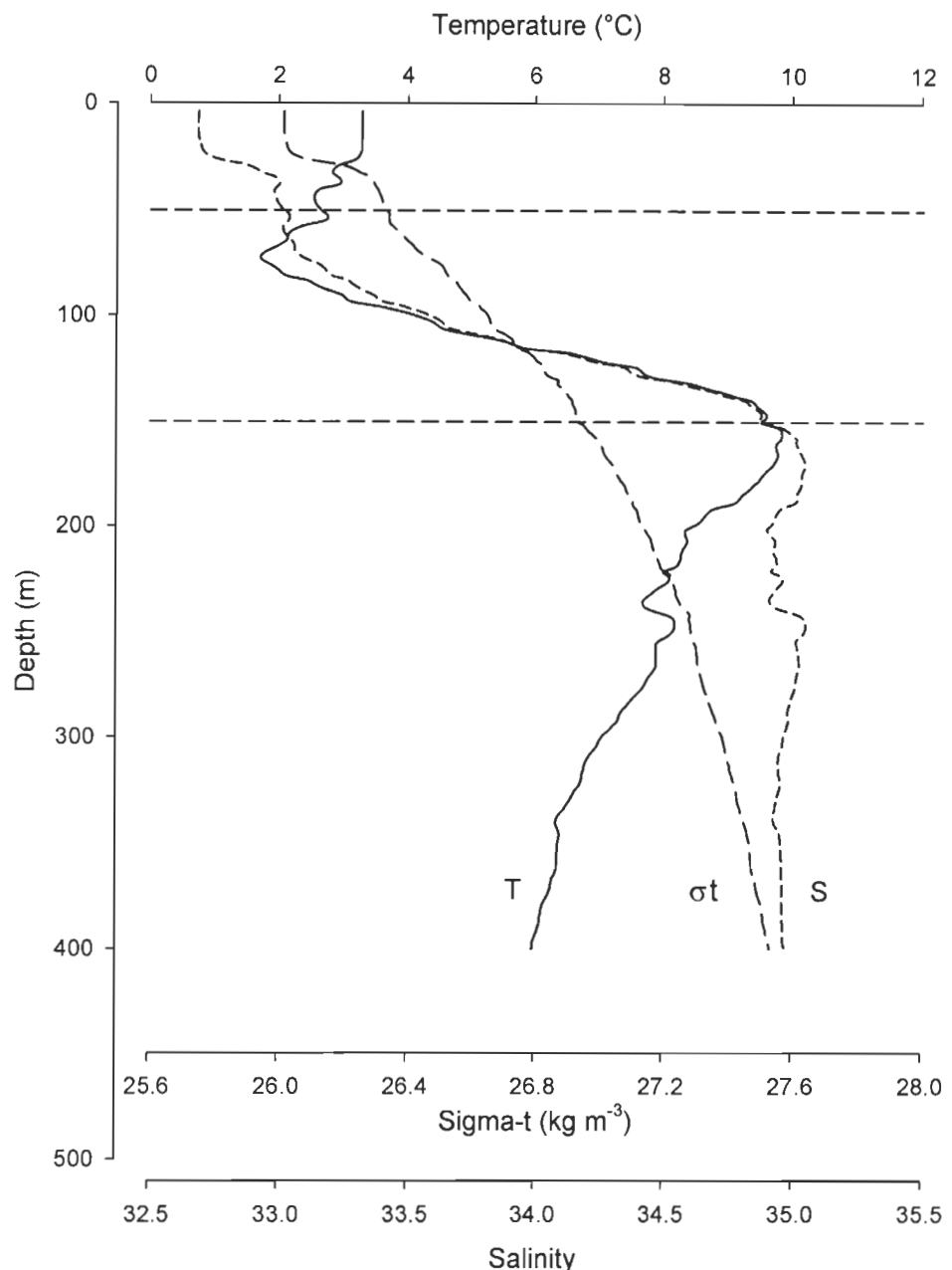


Fig. 2. Vertical profiles of temperature (T, solid line), salinity (S, short-dashed line) and sigma-t (σ_t , long-dashed line) in the upper 400 m of the water column on day 4 (28 April 2003) of a Lagrangian study of a water mass in the northwest Atlantic Ocean. The horizontal dashed lines indicate the depths of the shallowest (50 m) and deepest (150 m) particle interceptor traps

Trap deployment and handling were performed according to Knap et al. (1996) and recommendations from Gardner (2000). The free-drifting particle interceptor traps were surface-tethered with a series of five small buoys so as to dampen wave action and minimize vertical motion on the trap line. Before deployment, the traps were filled with deep seawater that had been pre-filtered through a 0.22 µm Millipore Durapore PVDF membrane and salt was added (to increase salinity by 5) to create a dense layer within the traps. No poison or preservative was added before deployment. Upon recovery, the traps were covered with a tight lid and placed vertically in a dark and cool room for 8 hours. After that sedimentation period, the supernatant was carefully removed and the bottom volume of the trap (900–1000 ml), which was pre-filtered using a 425-µm Nitex mesh to remove large swimmers, was kept in acid-washed Nalgene bottles for subsequent analyses.

Duplicate subsamples for the determination of chlorophyll *a* (chl *a*) and pheopigments (pheo) were filtered onto Whatman GF/F filters and the concentrations of these pigments were measured aboard the ship using a Turner Designs 10-005R fluorometer after a 24-h extraction in 90% acetone at 4°C in the dark (Parsons et al. 1984). Particulate organic carbon concentrations were determined in duplicate with a Perkin-Elmer Model 2400 CHN Analyzer from samples concentrated on pre-combusted (450°C for 5 h) Whatman GF/F filters and kept frozen (-20°C) in Petri dishes before analysis in the laboratory. In order to assess the solubilization of particulate organic material during the deployment period (Kähler & Bauerfeind 2001), dissolved organic carbon (DOC) was measured in the traps before and after deployment using a TOC-5000A Shimadzu analyzer following the procedure explained in Roux et al. (2002). The export ratio (e-ratio, i.e., the

ratio of POC sinking flux at a given depth to particulate primary production integrated over the euphotic zone depth; dimensionless) was calculated based on primary production measurements performed during the trap deployment period. Phytoplankton cells and zooplankton fecal pellets from the traps were collected and analyzed in order to estimate their contribution to the total POC sinking flux. Phytoplankton cells were fixed and preserved in acidic Lugol's solution (Throndsen 1978) and were identified to the lowest possible taxonomic level using the inverted microscope method (Utermöhl 1931, Lund et al. 1958). For each sample, at least 300 cells were counted from the whole sample. Up to 25 cells were measured per enumerated taxon and their biovolumes calculated using appropriate geometric equations (Hillebrand et al. 1999). An average biovolume per taxon was determined and converted into carbon biomass using factors given in Menden-Deuer & Lessard (2000). This carbon biomass, combined with the abundance of cells for each taxon, was used to obtain the contribution of each taxon to the POC sinking flux. The number and size of fecal pellets were also determined in subsamples preserved in hexamine-buffered formaldehyde (2% final concentration) using the inverted microscope. Two types of fecal pellets were identified, assuming a prolate spheroid shape for appendicularian feces and a cylindrical shape for calanoid copepod fecal pellets (Urban et al. 1993). The length and width of complete and broken pellets were measured and the total biovolume of each type of pellet was calculated using the appropriate equations. Biovolumes were then converted into carbon biomass using a factor of $0.057 \text{ mg C mm}^{-3}$ and $0.042 \text{ mg C mm}^{-3}$ for copepod and appendicularian pellets, respectively (González et al. 1994).

2.3 Results

2.3.1 Particulate organic carbon sinking fluxes

POC sinking fluxes progressively decreased with depth on all sampling days (Fig. 3). A progressive weakening of the depth-related decrease in POC sinking fluxes was observed from days 2 to 6, as reflected by the decreasing slopes of the curves of POC sinking fluxes with depth (Fig. 3). From days 2 to 6, particulate primary production decreased ($p < 0.01$; significance was determined using Wilcoxon's signed-ranks test unless otherwise specified) and was dominated by large phytoplankton cells (Fig. 4a). On day 20, particulate primary production increased compared to the previous sampling day (day 6) ($p < 0.01$) but was dominated by small phytoplankton cells (Fig. 4a). From days 2 to 6, POC sinking fluxes below Z_{eu} (i.e., at 50 m) decreased ($p < 0.01$; Fig. 4b) in pace with the decrease in particulate primary production. On day 20, the POC sinking flux below Z_{eu} further decreased ($p < 0.01$; Fig. 4b) whereas primary production increased (Fig. 4a) compared to the previous sampling day. The POC sinking fluxes at 150 m did not vary much between the sampling days (Fig. 4b), showing only a slight but significant increase from days 2 to 4 ($p < 0.05$) and a slight decrease from days 6 to 20 ($p < 0.01$). The export ratio (e-ratio) below Z_{eu} and at 150 m (Fig. 4c) increased from days 2 to 6 and significantly decreased on day 20 ($p < 0.01$). POC sinking fluxes and e-ratios were significantly lower at 150 m than below Z_{eu} ($p < 0.01$) throughout the study period (Fig. 4b, c).

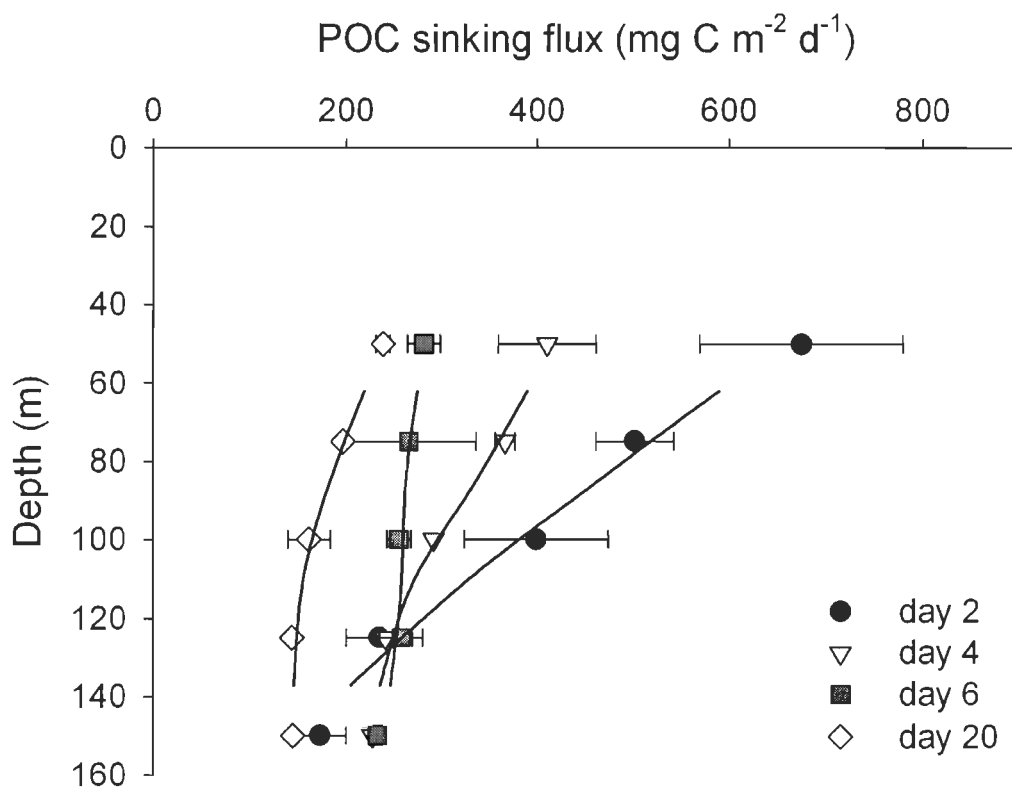


Fig. 3. Temporal changes in the vertical profiles of particulate organic carbon (POC) sinking flux from 50 m to 150 m (mean \pm standard deviation). For each day, the symbols represent the observed data; the curve is a moving average ($n = 2$)

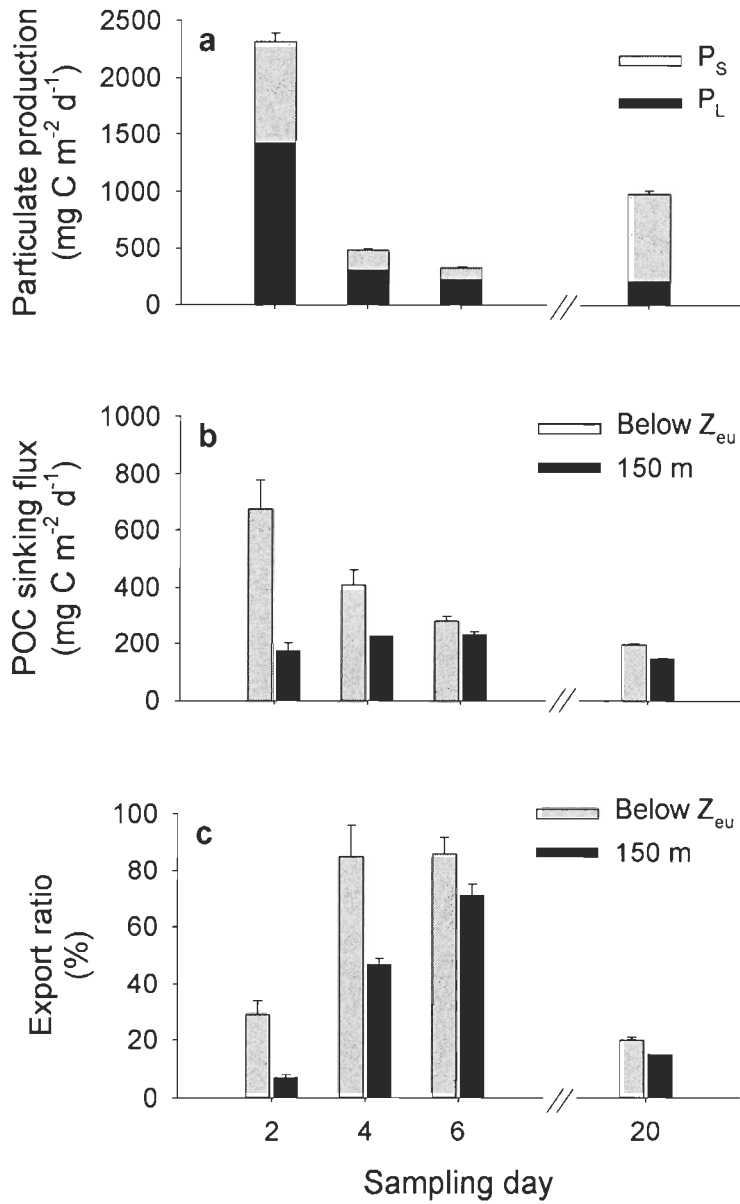


Fig. 4. Temporal changes in (a) size-fractionated particulate primary production integrated over the euphotic zone depth based on measurements reported in Pommier et al. (ms-a, Chapitre I), (b) particulate organic carbon (POC) sinking flux below the base of the euphotic zone (below Z_{eu} , i.e., at 50 m from days 2 to 6 and at 75 m on day 20) and at 150 m and (c) export ratio below Z_{eu} and at 150 m. Mean values and standard deviations are presented for each variable. In (a), the production values of small (P_S : 0.7–5 μm) and large (P_L : $\geq 5 \mu\text{m}$) phytoplankton cells are indicated

2.3.2 Chlorophyll *a* and phytoplankton cells sinking fluxes

Chl *a* sinking fluxes below Z_{eu} progressively decreased ($p < 0.01$) from days 2 to 20 (Fig. 5a). At 150 m, chl *a* sinking fluxes showed little temporal variability, with a small increase observed from days 2 to 4 and a slight decrease afterwards (Fig. 5a). The chl *a* sinking fluxes were significantly lower at 150 m than below Z_{eu} ($p < 0.01$). The percent contribution of chl *a* to total pigment (chl *a* + pheopigments) sinking fluxes below Z_{eu} was $\geq 52\%$ from days 2 to 6 and decreased to 16% on day 20 (Fig. 5b). At 150 m, the percent contribution of chl *a* to total pigment fluxes was $< 38\%$; this percent contribution was significantly lower than that below Z_{eu} throughout the study period ($p < 0.01$). A reduction in the variations of POC sinking fluxes, e-ratios, chl *a* sinking fluxes and chl *a* to total pigment ratios between the two sampling depths was observed from days 2 to 20 (Figs. 4b,c & 5a,b).

Intact phytoplankton cell sinking fluxes below Z_{eu} progressively decreased throughout the study period (Fig. 5c), whereas phytoplankton cell sinking fluxes at 150 m increased from days 2 to 4 and then progressively decreased afterwards (Fig. 5c). On day 2, intact phytoplankton cell sinking fluxes were significantly lower ($p < 0.01$) at 150 m than below Z_{eu} , whereas on day 6, phytoplankton cell sinking fluxes at 150 m were significantly higher than below Z_{eu} ($p < 0.05$). On days 4 and 20, phytoplankton cell sinking fluxes below Z_{eu} and at 150 m did not differ significantly ($p < 0.05$). From days 2 to 6, intact phytoplankton cell sinking fluxes were dominated by diatoms (of the genera *Thalassiosira*, *Chaetoceros* and *Fragilariaopsis*), both below Z_{eu} ($\geq 69\%$ of total cell numbers) and at 150 m ($\geq 53\%$ of total cell numbers) (Fig. 5c). On day 20, the diatom contribution to intact

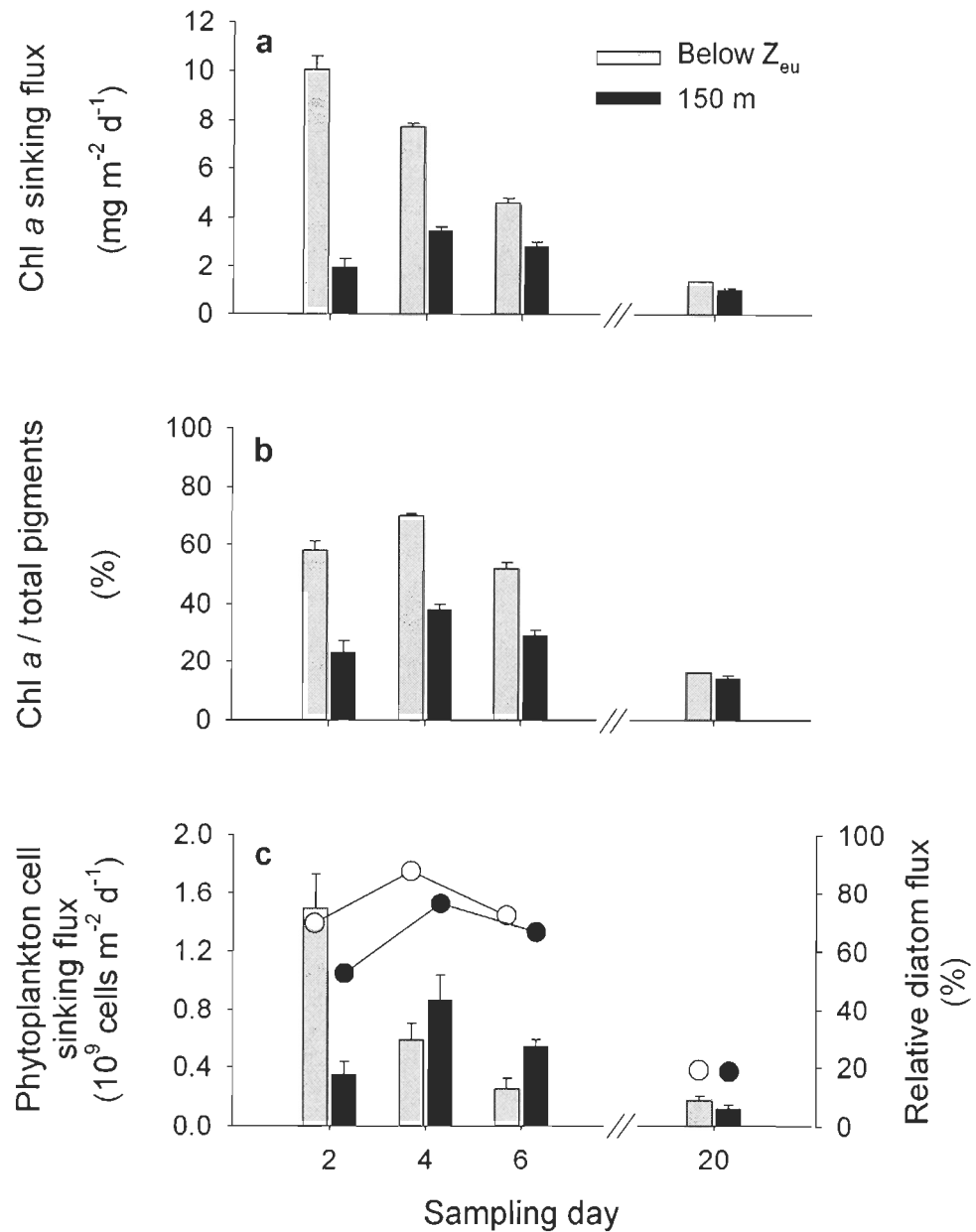


Fig. 5. Temporal changes in (a) chlorophyll *a* (chl *a*) sinking fluxes, (b) the ratio of chl *a* to total pigment (i.e., chl *a* + pheopigments) and (c) the sinking flux of phytoplankton cells below the base of the euphotic zone (below Z_{eu} i.e., at 50 m from days 2 to 6 and at 75 m on day 20) and at 150 m. Mean values and standard deviations are presented for each variable. In (c), the percent contribution of diatoms to the total phytoplankton cell sinking fluxes below Z_{eu} (open circles) and at 150 m (filled circles) are also indicated

phytoplankton cell sinking fluxes below Z_{eu} and at 150 m were reduced to 18% and 19%, respectively (Fig. 5c). Throughout the study period, the contribution of spores and empty frustules to the total diatom sinking flux (i.e., spores + empty frustules + intact diatom cells) was $\leq 50\%$ below Z_{eu} and ranged from 49 to 82% at 150 m.

2.3.3 Algal and fecal carbon sinking fluxes

Sinking carbon fluxes below Z_{eu} from intact phytoplankton and fecal pellets showed opposite temporal patterns, with a progressive decrease of the former and an increase of the latter from days 2 to 20 (Fig. 6a,c). Opposite trends in the temporal changes in the sinking carbon fluxes of phytoplankton and fecal pellets were also observed at 150 m (Fig. 6a,c). On day 2, phytoplankton carbon sinking fluxes were significantly higher ($p < 0.01$) below Z_{eu} than at 150 m (Fig. 6a). From days 4 to 20, phytoplankton carbon sinking fluxes at 150 m were not significantly different ($p < 0.05$) from those below Z_{eu} (Fig. 6a). Diatoms dominated the phytoplankton carbon sinking fluxes from days 2 to 6 (51–97%), both below Z_{eu} and at 150 m (Fig. 6b), while dinoflagellates made a large contribution to the phytoplankton carbon sinking fluxes at both depths (49–81%) on day 20 (Fig. 6b). On day 2, the relative contribution of phytoplankton to the total POC sinking fluxes was lower at 150 m (13%) than below Z_{eu} (22%; Table 2). On days 4 and 6, the relative contribution of phytoplankton to the total POC sinking fluxes was higher at 150 m (36% and 26%, respectively) than below Z_{eu} (19% and 17%, respectively); on day 20, phytoplankton had about the same contribution to the total POC sinking fluxes at both depths (9% below Z_{eu} and 14% at 150 m; Table 2). Fecal pellet carbon fluxes were consistently higher at 150 m

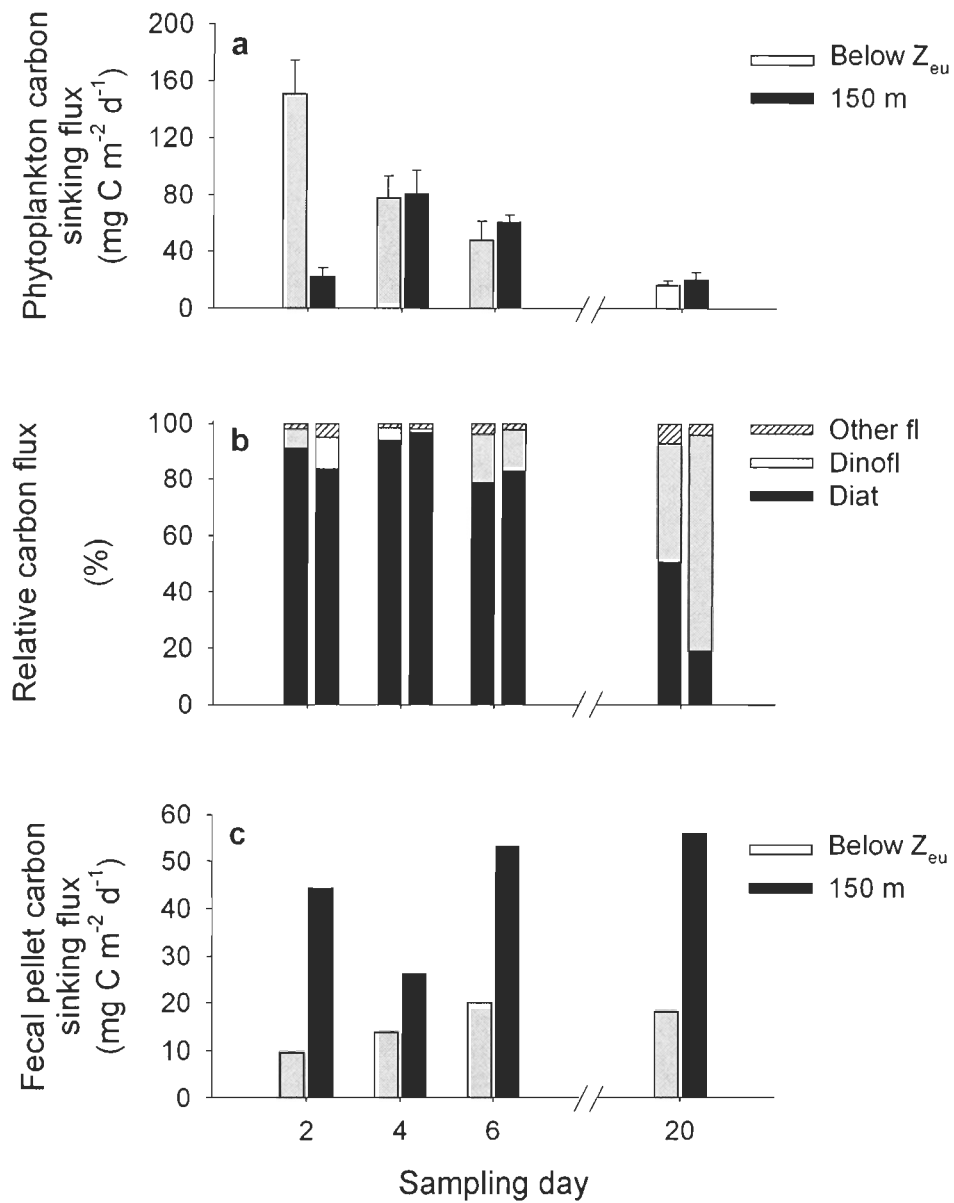


Fig. 6. Temporal changes in (a) intact phytoplankton carbon sinking fluxes, (b) the percent contribution of the three major phytoplankton groups (Diat: diatoms, Dinofl: dinoflagellates, Other fl: other flagellates) to total phytoplankton carbon sinking fluxes and (c) fecal pellet carbon sinking fluxes below the base of the euphotic zone (below Z_{eu} , i.e., at 50 m from days 2 to 6 and at 75 m on day 20) and at 150 m. In (a), mean values and standard deviations are presented. For each sampling day in (b), the left and right stacked bars are relative to the flux below Z_{eu} and at 150 m, respectively

Table 2. Carbon sinking fluxes of the three major phytoplankton groups and of fecal pellet carbon attributed to copepods and appendicularians below the base of the euphotic zone (below Z_{eu}) and at 150 m throughout the study period. The percent contributions (%) of total phytoplankton carbon and total fecal pellet carbon to the total particulate organic carbon sinking fluxes are also reported

Day	Trap depth	Phytoplankton carbon sinking fluxes				Fecal pellet carbon sinking fluxes		
		Diatoms	Dinoflagellates	Other flagellates	%	Copepods	Appendicularians	%
		(mg C m ⁻² d ⁻¹)				(mg C m ⁻² d ⁻¹)		
2	Below Z_{eu}	137.6	10.3	2.8	22	8.0	1.8	1
	150 m	19.1	2.6	1.1	13	27.2	17	26
4	Below Z_{eu}	73.9	3.5	1.0	19	5.3	8.7	3
	150 m	78.9	1.0	1.5	36	15.8	10.4	12
6	Below Z_{eu}	38.0	8.5	1.7	17	9.2	10.9	7
	150 m	50.4	9.0	1.2	26	28.3	24.9	23
20	Below Z_{eu}	8.7	7.2	1.2	9	8.8	9.4	9
	150 m	4.0	16.1	0.8	14	29.6	26.5	39

(26–56 mg C m⁻² d⁻¹) than below Z_{eu} (10–20 mg C m⁻² d⁻¹) throughout the study period (Fig. 6c), as were their percent contributions to the total POC fluxes (12–39% at 150 m and 1–9% below Z_{eu} , respectively; Table 2). Appendicularian feces slightly dominated the fecal carbon sinking fluxes below Z_{eu} throughout the study period (52–62%), except on day 2 (Table 2), while copepod feces were dominant (53–61%) at 150 m (Table 2).

2.4 Discussion

2.4.1 Linking particle sinking fluxes to epipelagic processes

This study was part a 7-day Lagrangian study of the decline, induced by nitrate limitation, of one of the most productive spring blooms ever reported in the open North Atlantic Ocean and its transition towards post-bloom conditions (Pommier et al. ms-a, Chapitre I). Throughout the Lagrangian study period (days 2 to 6), the same water mass containing the bloom patch was effectively tracked (Pommier et al. ms-a, Chapitre I). When we went back to the initial sampling location thirteen days later (day 20), the presence of warmer and more saline waters in the upper 60 m of the water column suggest that we sampled a different surface water mass than during the Lagrangian study period (Pommier et al. ms-a, Chapitre I). However, the sampling station on day 20 was likely representative of post-bloom conditions in the northwest Atlantic Ocean off the continental Scotian Shelf (Forget et al. 2007, Pommier et al. ms-a, Chapitre I). The particle interceptor traps were deployed below the base of the euphotic zone (50–75 m) and below the surface mixed layer (6–26 m; Table 1), so the measured sinking fluxes represented the export of material

sinking out of the euphotic zone. Particle interceptor traps may collect material originating from different areas, so the interpretation of the location and time of origin of the collected particles could be biased (Buesseler et al. 2007a). However, during the Lagrangian study (days 2 to 6), the free-drifting particle interceptor trap array was deployed and drifted in close proximity to the Lagrangian drifting buoy deployed to track the water mass under investigation. Moreover, the trap array was deployed relatively near the euphotic zone and the time scale of trap deployments (24 h) was in phase with that of primary production measurements. Hence, we consider that the particulate primary production rates in the euphotic zone and the POC sinking fluxes in the upper twilight zone measured in our study could be related to one another.

The trapping efficiency of our particle interceptor traps was not estimated during this study. However, the cylindrical shape and aspect ratio (H:D=7) of the traps used in this study have been found to be effective as free-drifting particle interceptor traps (Baker et al. 1988, Knauer & Asper 1989). Similar particle interceptor traps and mooring arrays have been used in other studies (Michel et al. 2002, Caron et al. 2004), and comparisons with flux estimates using ^{234}Th have shown close agreement in estimated carbon fluxes (Th -derived carbon flux = $0.68 + 1.05 \text{ FST flux}$; $n = 13$, $r^2 = 0.89$, $p < 0.001$; Tremblay et al. 2006). The average increase in DOC concentration within the particle interceptor traps during deployment intervals was $11 \pm 6\%$ below Z_{eu} and $10 \pm 5\%$ at 150 m throughout the study period, reflecting the potential loss of particulate organic matter (POM) to the dissolved phase (solubilization; Buesseler et al. 2007a) during trap deployments. Solubilization can result from the diffusion of dissolved organic matter from aggregates,

bacterial degradation of POM, the activity of swimmers, and physical–chemical processes affecting the dissolution of particulate organic matter (Buesseler et al. 2007a). However, there is no standardized method for correcting POC sinking fluxes for solubilization and it is most often ignored in short-term upper ocean flux studies such as the one reported here (Buesseler et al. 2007a). The small increase in DOC in the particle interceptor traps during our study (ca. 10%) indicates low solubilization of POM during the period of trap deployments and suggests that our sinking flux measurements might be slightly underestimated.

2.4.2 Coupling between primary production and POC sinking export

During the decline of the spring bloom, a tight coupling was observed between primary production and POC sinking fluxes below Z_{eu} . Indeed, from days 2 to 6, high and decreasing POC sinking fluxes below Z_{eu} (from 674 to 281 mg C m⁻² d⁻¹; Fig. 4b) were consistent with high and decreasing integrated production rates in the euphotic zone (from 2317 to 326 mg C m⁻² d⁻¹; Fig. 4a). However, during post-bloom conditions (day 20), POC sinking fluxes below Z_{eu} further decreased whereas primary production increased (Fig. 4a,b). On day 20, small phytoplankton cells (mainly unidentified flagellates $\leq 5 \mu\text{m}$) were dominant in terms of primary production (Fig. 4a) and chl *a* biomass (Pommier et al. ms-a, Chapitre I). Small cells have low sinking velocities compared to larger cells (Smayda 1970) and are usually considered to be minor contributors to the sinking export of organic material (Legendre & Le Fèvre 1989), which is in good agreement with the low POC sinking fluxes measured on day 20. Similarly, high POC sinking fluxes observed from days

2 to 6 are consistent with the dominance of large cells (mainly centric diatoms) in terms of primary production (Fig. 4a) and chl *a* biomass (Pommier et al. ms-a, Chapitre I) during that period. Throughout the study period, POC sinking fluxes below Z_{eu} were positively correlated to the production rate of large phytoplankton cells (Kendall's τ coefficient of ranks correlation, $p < 0.05$). These results stress that the size structure of primary producers was more important than the magnitude of primary production in shaping the sinking export of POC from the euphotic zone throughout the study period. Moreover, POC sinking fluxes below Z_{eu} were positively correlated with the sinking fluxes of phytoplankton cells (Fig. 5c) and phytoplankton carbon (Fig. 6a) throughout the study period (Kendall's τ coefficient of ranks correlations, $p < 0.05$), the two latter fluxes being dominated by diatoms (Figs. 5c & 6b). These results are in good agreement with the general understanding that POC export from the euphotic zone is sensitive to ecosystem shifts towards, or away from, the dominance of large cells, particularly diatoms, as part of the phytoplankton assemblage (Boyd & Newton 1999).

POC sinking fluxes measured at 150 m compared well with previous values of 160–260 mg C m⁻² d⁻¹ measured at the same depth during springtime in the temperate northwest Atlantic Ocean (Harrison et al. 1993). Interestingly, POC sinking fluxes at 150 m remained fairly constant throughout the study period despite strong temporal variations in POC sinking fluxes below Z_{eu} (Fig. 4b) and in both the magnitude of primary production and size structure of the primary producers (Fig. 4a). The same trend was also observed in chl *a* sinking fluxes at 150 m, which varied little throughout the study period compared to the temporal changes in the chl *a* sinking fluxes below Z_{eu} (Fig. 5a) and in the magnitude and

size structure of the chl α biomass in the euphotic zone (Pommier et al. ms-a, Chapitre I). In contrast with what has been observed below the base of the euphotic zone, our results emphasize the lack of coupling between primary production and POC sinking export at 150 m throughout the study period. This result is rather unexpected given the premise of organic matter sinking fluxes being positively related to the size structure of pelagic food webs (Legendre & Le Fèvre 1989, Boyd & Newton 1999). According to Buesseler (1998), the changes in POC sinking export to depth are more tightly related to changes in the recycling efficiency of pelagic food webs rather than to changes in the intensity and size structure of primary producers. In line with this, the sinking flux of organic matter at 150 m can be viewed as the result of recycling processes within the twilight zone that affected the exported material from the euphotic zone. Therefore, the fairly constant POC sinking fluxes at 150 m could result from short-term variability in POC recycling within the twilight zone.

One particular aspect that needs to be considered is the potential temporal lag between the sinking export of organic matter below Z_{eu} and that at 150 m. In order to directly relate POC sinking fluxes at 150 m with those in the traps deployed below Z_{eu} (i.e., at 50 m), one would have to assume POM sinking rates of at least 100 m d^{-1} , which is on the order of the sinking velocities of fecal pellets (Lorenzen & Welschmeyer 1983). However, the fecal pellets observed in our samples were mostly broken and highly degraded and fecal carbon represented less than 39% of the total POC sinking fluxes (Table 2). We believe that such degraded fecal material could not have sunk at velocities as high as 100 m d^{-1} during our study. Alternatively, when considering that sinking velocities of particles in the upper ocean typically range from 10 to 50 m d^{-1}

(Sarmiento & Gruber 2006), the particles sinking below Z_{eu} would have reached the 150 m traps in 2 to 10 days. A sinking velocity of 50 m d^{-1} would be consistent with the slight increases observed in chl α and phytoplankton cell sinking fluxes at 150 m from days 2 to 4 (Fig. 5a,c). Nevertheless, these latter increases were minimal. Therefore, although we do not exclude the existence of a potential temporal lag between primary production and the sinking fluxes of organic matter at 150 m, we still surmise that the fairly constant POC sinking fluxes at 150 m were more likely related to short-term variability in POC recycling in the upper twilight zone, as explained below.

2.4.3 Temporal variability in POC recycling in the upper twilight zone

The e-ratios reported in this study (20–86% below Z_{eu} and 7–71% at 150 m; Fig. 4c) compare well with values of 8–79% reported previously by Buesseler et al. (1992) at 75 m in the northeast Atlantic Ocean in springtime. Harrison et al. (1993) reported e-ratios of 26–38% at 150 m in the northwest Atlantic Ocean in springtime. According to Buesseler (1998), most of the open ocean is characterized by e-ratios $\leq 5\text{--}10\%$; e-ratios $\geq 50\%$ are the exception rather than the rule and are usually associated with spring blooms at mid-latitudes. During the decline of the bloom, the increases in the e-ratio, both below Z_{eu} and at 150 m, were concomitant with the decrease in primary production (Fig. 4a,c), which translates into POC from primary producers being exported with a greater efficiency throughout this period. The increase (from 26% on day 2 to 83% on day 6) in the ratio of the POC sinking flux at 150 m to that below Z_{eu} during the decline of the bloom (Fig. 4b) also emphasizes the increase in the transfer efficiency (Buesseler et al. 2007b) of POC

through the upper twilight zone during this period. On day 20, the low e-ratios (20% below Z_{eu} and 15% at 150 m; Fig. 4c) were in good agreement with the dominance of small flagellated cells ($\leq 5 \mu\text{m}$; Pommier et al. ms-a, Chapitre I).

The increase in the transfer efficiency of POC through the upper twilight zone during the decline of the bloom could have been related to the temporal decrease in POC recycling in the upper twilight zone, as deduced from the vertical profiles of POC sinking fluxes (Fig. 3). The decrease in POC sinking fluxes with depth is usually parameterized by the power law function of Martin et al. (1987), according to which $\text{POC}_z = \text{POC}_{100\text{ m}} \times (z/100)^{-b}$ (where POC_z and $\text{POC}_{100\text{ m}}$ are the POC sinking fluxes at depth z and at 100 m, respectively, and b corresponds to the slope of the power law function). In the equation of Martin et al. (1987), b is a key parameter reflecting the strength of organic matter recycling with depth: the larger value of b , the faster the decrease in POC sinking fluxes with depth and the higher the recycling of organic matter (Primeau 2006). Using the approach of Martin et al. (1987), the parameter b was estimated for each day of our study from the slope of the regression between POC sinking fluxes and depth, after a log-log transformation of initial values. On day 2, b was 1.24, which is in good agreement with the value of 1.28 reported for the North Atlantic Ocean by Berelson (2001). On days 4, 6 and 20, b was 0.58, 0.14 and 0.49, respectively. The b values from days 4 to 20 were particularly low considering the values ranging from 0.60 to 1.28 reported by Berelson (2001) for the North Atlantic, Equatorial Pacific and Southern oceans and the Arabian Sea. These low values indicate a low recycling of POC in the upper twilight zone from day 4 onwards, and the temporal decrease in b support the reduction in the recycling of POC within the upper

twilight zone throughout the decline of the spring bloom. The ensuing increase in the transfer efficiency of POC within the upper twilight zone could have compensated for the decrease in POC export below Z_{eu} , thus smoothing the temporal variations in POC sinking fluxes at 150 m from days 2 to 6 (Fig. 4b). Moreover, the parameter b was positively correlated to the POC sinking flux below Z_{eu} throughout the study period (Kendall's τ coefficient of ranks correlation, $p < 0.01$). A positive correlation between b and POC export at 100 m has already been reported by Berelson (2001), who found that intensity of organic matter recycling in the upper 1000 m of the water column is related to the amount of POC exported at 100 m. Our results are in good agreement with those of Berelson (2001) and emphasize that the intensity of POC recycling within the upper twilight zone is proportional to the amount of POC exported from the euphotic zone. Many biological processes in the oceans follow a first-order kinetic, so that the rate of a reaction is proportional to the amount of material present (Boyd & Trull 2007). In line with this, the decrease in POC exported from the euphotic zone from days 2 to 6 could have induced a proportional decrease in the rate of POC recycling by the heterotrophic community within the upper twilight zone. Our results also suggest that the processes of POC recycling in the upper twilight zone responded rapidly to the variability of POC inputs from the euphotic zone, as already reported by Buesseler et al. (2007b) in the northwest Pacific Ocean.

Ultimately, our study shed light on the importance of short-term variability in POC recycling during its sinking through the upper twilight zone for the efficiency of POC export to depth. Our results also emphasize the importance of top-down control in shaping the sinking export of POC to the deep ocean over short time scales, as already reported by

Wassmann (1998). Many biological interactions between the different components of the pelagic food webs can impact the sinking flux of POC, such as zooplankton grazing (including coprophagy/coprorhexy), bacterivory by heterotrophic nanoflagellates, bacterial mineralization of POC and viral lysis of phytoplankton and bacterial cells. Although we did not directly consider these factors, information about mesozooplankton grazing can be deduced from the temporal changes in phytoplankton and fecal POC sinking fluxes, as explained below.

2.4.4 Mesozooplankton grazing in the upper twilight zone

The consistently higher fecal carbon sinking fluxes at 150 m than below Z_{eu} throughout the study period (Fig. 6c) reflect the production of fecal pellets by mesozooplankton within the upper twilight zone. Zooplankton grazing rates were not measured during this study. However, the mesozooplankton ingestion rate (I) can be estimated from the fecal pellet sinking rate measured at 150 m (E), assuming an assimilation efficiency (AE) of 70% (Carlotti et al. 2000) and using the relationship $I = E / (1-AE)$ (Båmstedt et al. 2000). This calculation gives potential ingestion rates of 147, 87 and 177 mg C m⁻² d⁻¹ by the migrating zooplankton population in the upper water column on days 2, 4 and 6, respectively. These ingestion rates could have been underestimated due to potential coprophagy/coprorhexy by the ubiquitous small calanoid copepod *Oithona similis* (Reigstad et al. 2005) which was the most abundant zooplankton species in the upper 100 m of the water column throughout the study period (E. Head, Bedford Institute of Oceanography, pers. comm.). Considering the total particulate primary

production rates of 2317, 481 and 326 mg C m⁻² d⁻¹ on days 2, 4 and 6, respectively (Fig. 4a), the mesozooplankton could have ingested an increasing proportion (from 6 to 54%) of the daily primary production during the decline of the bloom. These values are particularly high compared to previous values of 2.7% (Dam et al. 1993) and < 9% (Harrison et al. 1993) reported for the temperate North Atlantic Ocean during the spring phytoplankton bloom.

On day 2, a large fraction of the sinking phytoplankton in the upper twilight zone was probably grazed by mesozooplankton. This is supported by lower sinking fluxes of chl *a*, phytoplankton cells and phytoplankton carbon at 150 m than below Z_{eu} (Figs. 5b,c & 6a). However, from day 4 onwards, similar sinking fluxes of phytoplankton cells and phytoplankton carbon were measured at both depths (Figs. 5c & 6a) despite consistently higher carbon sinking fluxes of fecal pellets at 150 m than below Z_{eu} (Fig. 6c). This discrepancy may reflect zooplankton vertical migrations (Ducklow et al. 2001), so that mesozooplankton grazing could have occurred at a depth different than that of defecation (e.g., grazing in the euphotic zone and defecation in the upper twilight zone). The consistently higher carbon sinking fluxes of fecal pellets at 150 m than below Z_{eu} , despite similar sinking fluxes of phytoplankton cells and phytoplankton carbon at both depths, could also be attributed to a shift in zooplankton diet from herbivory on day 2 to omnivory from days 4 to 20. A shift from herbivory to omnivory has already been reported for *Calanus finmarchicus* under conditions of low phytoplankton standing stocks in the Gulf of St. Lawrence (Ohman & Runge 1994). Several studies have demonstrated that the feeding behaviour of calanoid copepods can be flexible enough to ingest a mixture of

phytoplankton cells, microzooplankton, detritus and fecal pellets emphasizing their omnivorous feeding behaviour (Lenz 1977, Kleppel 1993). Throughout the study period, less than 53% of the total POC sinking fluxes was composed of intact phytoplankton and fecal pellet (Table 2), suggesting that other sources (e.g., detrital material, marine snow, transparent exopolymers) may have made high contributions to POC sinking fluxes. Detrital material could have contributed substantially to the total POC sinking fluxes in our study, as anamorphous aggregates and degraded fecal material were observed in the particle interceptor traps. Given the abundance of detrital material and the decrease in phytoplankton sinking fluxes throughout the study period, a shift in the mesozooplankton diet from herbivory to omnivory could have occurred during the decline of the bloom, leading to a potential decrease in zooplankton grazing upon phytoplankton cells within the upper twilight zone.

The changes in the sinking fluxes of phytoplankton cells and fecal pellets provided information regarding the potential grazing pressure of mesozooplankton in the upper twilight zone. Nevertheless, more information on the composition and the functioning of the heterotrophic communities in the twilight zone is required to better constrain the decrease in POC recycling in the upper twilight zone observed during our study.

2.5 Conclusion

This study is the first to report the relationship between primary and export production in the upper twilight zone of the temperate northwest Atlantic Ocean. POC sinking fluxes below the bottom of the euphotic zone were high and progressively

decreased during the decline of the bloom and its transition towards post-bloom conditions. Throughout the study period, POC sinking fluxes below the euphotic zone were positively correlated to the production of large phytoplankton cells, stressing the importance of the size structure of phytoplankton communities in shaping the sinking export of POC from the euphotic zone. However, regardless of the variability in POC export from the euphotic zone, fairly constant POC sinking fluxes were measured at 150 m. A positive correlation was found between the sinking flux of POC below the euphotic zone and POC recycling within the upper twilight zone, which led to an increase in POC transfer efficiency at 150 m throughout the study period. It is hypothesized that the concomitant decreases in POC export from the euphotic zone and in POC recycling within the upper twilight zone led to fairly invariant POC sinking fluxes at 150 m. Our results emphasize that although the magnitude and the size structure of primary production may condition the export of POC from the euphotic zone, these variables do not provide reliable information on the efficiency of carbon export to the deep ocean. Our results stress that the recycling processes within the upper twilight zone are very dynamic and can respond rapidly and proportionally to the variability in POC inputs from the euphotic zone. The short-term variability in the recycling of POC within the upper twilight zone appears to be a critical factor governing the transfer efficiency of POC from the euphotic zone to the deep ocean.

CHAPITRE III

CARBON BUDGET IN THE EUPHOTIC AND UPPER TWILIGHT ZONES OF THE NORTHWEST ATLANTIC OCEAN DURING THE DECLINE OF THE SPRING BLOOM

RÉSUMÉ

Un budget de carbone organique particulaire (COP) et dissous (COD) a été établi pour la zone euphotique (≤ 45 m) et la partie supérieure de la zone mésopélagique (45-150 m) de l'océan Atlantique nord-ouest lors d'un suivi lagrangien du déclin d'un bloom printanier de diatomées. Ce budget est basé sur des mesures des concentrations de COP et de COD dans les 150 premiers mètres de la colonne d'eau, de la production primaire dans la zone euphotique, et des flux de COP à 50 et 150 m. Ce budget a révélé que 50 % du COP dans la zone euphotique est resté en suspension dans cette zone tandis que 11 % a été exporté à 50 m. 39 % du COP dans la zone euphotique a été recyclé par le broutage du zooplancton, la lyse virale et/ou d'autres processus de solubilisation. Dans la partie supérieure de la zone mésopélagique, 82 % du COP est resté en suspension, tandis que 7 % a été exporté à 150 m et 11 % a été recyclé. L'importante biomasse de COP accumulée dans les 150 premiers mètres de la colonne d'eau est associée au développement d'un maximum profond de chlorophylle *a* au voisinage de la base de la zone euphotique. Ce budget suggère également que l'activité des hétérotrophes n'était pas suffisante pour utiliser l'importante biomasse de carbone organique accumulée, particulièrement dans la partie supérieure de la zone mésopélagique. La respiration de la communauté hétérotrophe a été estimée entre 5,21 et 5,71 g C m⁻². Le rapport entre la production primaire totale et la respiration de la communauté hétérotrophe était compris entre 1,26 et 1,38, témoignant de l'autotrophie nette du système étudié pour la période du suivi lagrangien. Ce résultat est en accord avec le consensus actuel selon lequel l'océan Atlantique Nord constitue un puits de CO₂ atmosphérique.

ABSTRACT

A budget of particulate (POC) and dissolved (DOC) organic carbon was established for the euphotic (≤ 45 m) and upper twilight (45–150 m) zones of the northwest Atlantic Ocean during a Lagrangian study of the decline of a spring diatom bloom. The budget is based on measurements of DOC and POC stocks in the upper 150 m, primary production rates in the euphotic zone, and particulate organic carbon sinking fluxes at 50 and 150 m. The budget reveals that 50% of the total POC in the euphotic zone remained suspended in that zone whereas 11% was exported to 50 m through sinking. The remaining 39% was

recycled within the euphotic zone through zooplankton grazing, viral lysis and/or other solubilization processes. About 82% of the total POC in the upper twilight zone remained suspended in that zone, whereas 7% was exported through sinking (150 m) and 11% was recycled. The large amount of POC that remained suspended in the upper 150 m is associated with the development of a deep chlorophyll *a* maximum close the base of the euphotic zone. This budget also suggests that heterotrophic activity was not sufficient to utilize the abundant suspended POC, particularly in the upper twilight zone. Heterotrophic community respiration was estimated to vary between 5.21 and 5.71 g C m⁻². This gives a ratio of total primary production to community respiration ranging from 1.26 to 1.38, indicating the net autotrophy of the system under investigation over the study period. These results are in agreement with the general consensus that the North Atlantic spring bloom is acting as a net sink for atmospheric CO₂.

3.1 Introduction

The oceanic carbon cycle has been and remains the focus of many investigations aimed at understanding the biogeochemical dynamics of the upper ocean and its impact on the air-sea exchange of carbon dioxide (CO_2) and other climate-relevant gases. In particular, determining the metabolic balance of epipelagic waters (i.e. whether they are net autotrophic and a sink for atmospheric CO_2 or net heterotrophic and a source of atmospheric CO_2) is essential as this balance ultimately determines the influence of the World Ocean on the carbon budget of the biosphere (del Giorgio & Duarte 2002, del Giorgio & Williams 2005). Large areas of the open ocean have been reported to be net heterotrophic (del Giorgio et al. 1997, Duarte & Agusti 1998, Williams & Bowers 1999); these areas correspond to the central oligotrophic gyres of the oceans where net primary production rates are low and respiration rates exceed photosynthesis (Williams 1998). Alternatively, epipelagic waters of the temperate North Atlantic Ocean are recognized to be net autotrophic (González et al. 2002).

At temperate and subpolar latitudes of the North Atlantic Ocean, the seasonal cycle of mixing and thermal stratification results in a large increase in phytoplankton biomass during springtime known as the North Atlantic spring bloom. This bloom is a basin-wide phenomenon that represents one of the most conspicuous manifestations of the seasonality of biogeochemical processes in the World Ocean; it was intensively investigated during the JGOFS North Atlantic Bloom Experiment (Ducklow & Harris 1993). The spring bloom is usually characterized by the numerical dominance of large diatoms (Colebrook 1982), which are particularly efficient at removing nutrients and associated dissolved inorganic

carbon from surface waters. The biological pump in the temperate North Atlantic is therefore considered highly efficient (Sarmiento et al. 2004). Moreover, due to the temporal uncoupling between phytoplankton growth and mesozooplankton grazing (Parsons & Lalli 1988), the North Atlantic spring bloom is generally associated with high vertical fluxes of particulate organic carbon at the end of the bloom (Honjo & Manganini 1993), so that the biological pump in that region of the World Ocean is strong (Sarmiento et al. 2004). The combination of a strong and efficient biological pump makes the North Atlantic Ocean one of the largest sinks for atmospheric CO₂ in the World Ocean.

Beyond this usual understanding of the North Atlantic spring bloom, several studies have also demonstrated the importance of microzooplankton grazing as a pathway of *in situ* recycling of organic matter during the spring bloom in the northeast (Burkhill et al. 1993, Fileman & Leakey 2005) and the northwest (Harrison et al. 1993) Atlantic Ocean. Determining the fate of the large amount of organic material produced during the spring bloom (i.e. export to depth or *in situ* recycling) is therefore essential when assessing the influence of the bloom on the metabolic balance of the North Atlantic Ocean and its ability to act as a sink or a source of atmospheric CO₂. The declining phase of the bloom represents a critical temporal window during which organic matter could be either exported to depth or recycled within the surface and subsurface waters.

In the two previous chapters of the thesis, we investigated the variability in phytoplankton production and biomass (Chapter I) and in vertical sinking fluxes of particulate organic carbon (Chapter II) during a Lagrangian study of the decline of the spring bloom in the northwest Atlantic Ocean. Based on these results, we developed a

budget of the dissolved and particulate organic carbon fractions in the euphotic and upper twilight zones during the decline of the spring bloom. This budget provides an integrated approach for assessing the organic carbon pathways in the upper 150 m of the water column (i.e. export to depth or *in situ* recycling) during the decline of an intense spring bloom and their relevance to the metabolic balance of the water mass investigated. This study is part of the Canadian Surface Ocean–Lower Atmosphere Study (C-SOLAS), which aimed at quantifying the impact of the senescence of the North Atlantic spring bloom on the production and ventilation to the atmosphere of climatically active trace gases.

3.2 Materials and methods

3.2.1 Sampling

Sampling was carried out aboard the CCGS *Hudson* off the Scotian Shelf at station L (Fig. 1) as part of a Lagrangian survey of the spring bloom decline in the northwest Atlantic Ocean (Pommier et al. ms-a, Chapitre I). A water mass within which a phytoplankton bloom had developed was sampled daily from 25 April (day 1) to 01 May 2003 (day 7). The drifting of the water mass under investigation was tracked by a Lagrangian surface drifting buoy (ARGOS). T-S diagrams from the surface to 350 m revealed that the same water mass was effectively tracked during the Lagrangian study period (Pommier et al. ms-a, Chapitre I). Water column samples were collected with a rosette sampler equipped with 10-liter Scripps bottles, at seven optical depths (100, 50, 30, 15, 5, 1 and 0.2% of surface PAR), at the depth of maximum chlorophyll *a* concentration and at 3 or 4 depths

below the euphotic zone (50, 75, 100 and 150 m). Subsamples for subsequent analyses were taken from the rosette using acid-washed Nalgene bottles according to the JGOFS sampling procedures (Knap et al. 1996) and were pre-screened through a 425 μm Nitex mesh.

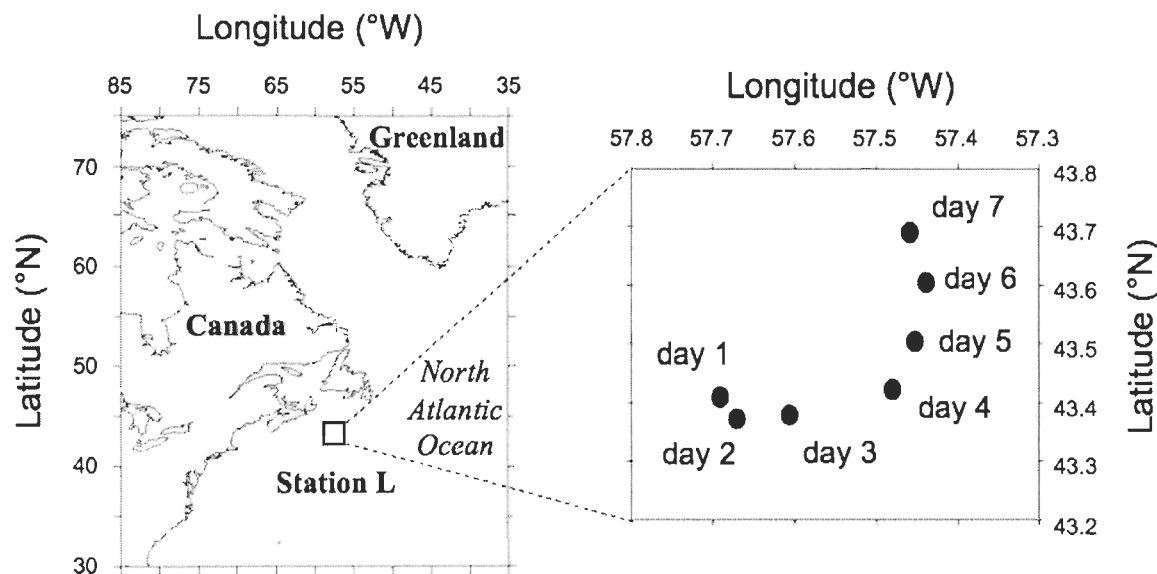


Fig. 1. Location of the drifting buoy from 25 April (day 1) to 01 May 2003 (day 7) during a Lagrangian study of the decline of the spring bloom in the northwest Atlantic Ocean

Free-drifting particle interceptor traps were deployed for periods of 24 h at 50 and 150 m on 26 April (day 2), 28 April (day 4) and 30 April (day 6) in order to collect the sinking flux of particulate organic carbon at these two depths (i.e. $F_{50\text{m}}$ and $F_{150\text{m}}$,

respectively). Trap deployment and handling were performed according to JGOFS protocols (Knap et al. 1996) and recommendations from Gardner (2000). Detailed information on trap specifications, handling and deployment is available in Pommier et al. (ms-b, Chapitre II). The daily vertical sinking fluxes of POC were calculated as $(POC_{trap} \times V_{trap}) / (A_{trap} \times t)$, where POC_{trap} is the concentration of POC in the trap (mg m^{-3}), V_{trap} is the bottom volume of the trap from which POC concentrations were determined (m^{-3}), A_{trap} is the surface area of the trap (in m^{-2}), and t is the duration (in days) of the trap deployment.

3.2.2 Analyses

Primary production rates were measured daily at the seven optical depths using the ^{14}C -uptake method (Parsons et al. 1984, Gosselin et al. 1997) with on-deck *in situ* simulated incubation from sunrise to sunset. Particulate production rates (P_{POC}) were determined in duplicate from samples concentrated on precombusted Whatman GF/F glass fiber filters (nominal pore size of $0.7 \mu\text{m}$). Phytoplankton dissolved organic carbon release rates (P_{DOC}) were determined in duplicate from the filtrate of samples passed through Whatman GD/X glass fiber syringe filters (nominal pore size of $0.7 \mu\text{m}$). Detailed information about primary production measurements can be found in Pommier et al. (ms-a, Chapitre I).

Dissolved organic carbon (DOC) concentrations were measured on days 1 and 7 at discrete depths of the water column. The seawater samples were filtered through precombusted (450°C for 5h) 25 mm Whatman GF/F filter. The filtrate was collected in

5 ml glass storage vials previously cleaned following the protocol of Burdige & Homstead (1994), acidified to ~pH 2 with 50% v/v H₃PO₄ (5 µl ml⁻¹) and covered with Teflon-lined caps. DOC was determined with a TOC-5000A analyzer (Shimadzu, Kyoto, Japan) using the analytical procedure given in Whitehead et al. (2000). Potassium hydrogen phthalate was used to standardize DOC measurements. In addition, samples were systematically checked against low-carbon water (2 µM DOC) and deep Sargasso Sea reference water (44–47 µM DOC) every seven analyses. These seawater DOC reference standards were obtained from Hansell's Certified Reference Materials (CRM) program.

Particulate organic carbon (POC) concentrations were determined at discrete depths of the water column on days 1 and 7 and in the particle interceptor traps on subsamples filtered onto precombusted 21 mm Whatman GF/F filters. Filters were stored in Petri dishes at -20 °C until analysis using a PerkinElmer Model 2400 Elemental Analyzer.

3.2.3 Numerical analyses

The upper water column was divided in two layers: 0–45 m and 45–150 m. The 0–45 m depth interval corresponded closely to the euphotic zone, for which the average depth (Z_{eu}) was 45 m (range: 40 to 50 m) during the study period (Pommier et al. ms-a, Chapitre I). The 45–150 m interval is identified as the upper part of the twilight zone, since the twilight zone is defined as the depth layer between the euphotic zone and 1000 m (Buesseler et al. 2007). Each variable used to establish the carbon budget is described in Table 1.

Table 1. Definition, units and constant value (when applicable) of the variables used in the carbon budget for the euphotic and upper twilight zones. NA is not applicable

Variable	Definition	Units	Constant value
I	Input of particulate and dissolved organic carbon in a specific depth layer (euphotic and upper twilight zone) over the study period	mg C m ⁻²	NA
O	Output of particulate and dissolved organic carbon in a specific depth layer (euphotic and upper twilight zone) over the study period	mg C m ⁻²	NA
$POC_t(z)$	Particulate organic carbon concentration measured at a discrete depth z (m) at time t	mg C m ⁻³	NA
$DOC_T(z)$	Total dissolved organic carbon (DOC) concentration measured at a discrete depth z (m) at time t	mg C m ⁻³	NA
$DOC_R(z)$	Concentration of refractory DOC at a discrete depth z (m) at time t	mg C m ⁻³	540
$DOC_{SL}(z)$	Concentration of semi-labile DOC estimated at a discrete depth z (m) at time t	mg C m ⁻³	NA
$DOC_L(z)$	Concentrations of labile DOC estimated at a discrete depth z (m) at time t	mg C m ⁻³	3% DOC_T
$P_{POC_t}(z)$	Daily particulate primary production rate measured at discrete depths z (m) at time t	mg C m ⁻³ d ⁻¹	NA
$P_{DOC_t}(z)$	Daily phytoplankton DOC release rate measured at discrete depths z (m) at time t	mg C m ⁻³ d ⁻¹	NA
PP	Total primary production in the euphotic zone over the study period	mg C m ⁻²	NA
F_{50m_t} F_{150m_t}	Daily vertical sinking flux of POC at 50 and 150 m at time t	mg C m ⁻² d ⁻¹	NA
L_{POC}	Loss of POC in a specific depth layer over the study period	mg C m ⁻²	NA
L_{DOC_L}	Loss of labile DOC in a specific depth layer over the study period	mg C m ⁻²	NA
R_{DOC_L}	Bacterial respiration on labile DOC in a specific depth layer over the study period	mg C m ⁻²	NA
BGE	Bacterial growth efficiency in a specific depth layer	Dimensionless	0.05–0.34

The suspended POC concentrations on days 1 and 7 were integrated over the euphotic zone and the upper twilight zone using trapezoidal integration ($\int_{0m}^{45\mu} POC_t(z) dz$ and $\int_{45m}^{150\mu} POC_t(z) dz$, respectively, where t is the sampling day).

DOC values from surface waters are most often superimposed on a background of refractory dissolved organic matter (Williams 2000). Therefore, DOC concentrations at discrete depths were corrected by subtracting a value of 45 μM (or 540 mg C m^{-3}), which corresponds to the deep refractory DOC concentration in the sampling area (Hansell 2002). This allowed us to separate the total DOC pool (DOC_T) into the refractory (DOC_R) and labile + semi-labile (DOC_{L+SL}) fractions. Due to its rapid turnover rate, labile DOC usually represents a very small fraction of the total DOC pool in the open ocean, ranging from 0 to 6% (Carlson 2002). A mean value of 3% of the DOC_T was thus used to calculate the labile DOC fraction (DOC_L). DOC_L was then subtracted from DOC_{L+SL} to estimate the semi-labile DOC fraction (DOC_{SL}). The concentrations of DOC_T , DOC_{SL} and DOC_L on days 1 and 7 were then integrated (trapezoidal integration) over the euphotic zone and the upper twilight zone.

The daily rates of particulate primary production (P_{POC}) and of phytoplankton DOC release (P_{DOC}) were integrated over the euphotic zone depth on each sampling day (t) using trapezoidal integration ($\int_{0m}^{45\mu} P_{POC_t}(z) dz$ and $\int_{0m}^{45\mu} P_{DOC_t}(z) dz$, respectively). As the production rates measured on a given day t correspond to a daily rate from t to $t+1$, the integrated production rates measured from days 1 to 6 were summed to obtain the total P_{POC} and P_{DOC}

from days 1 to 7 ($\sum_{t=1}^{t=6 \text{ } 45\mu} P_{POC_t}(z)dz$ and $\sum_{t=1}^{t=6 \text{ } 45\mu} P_{DOC_t}(z)dz$, respectively). $\sum_{t=1}^{t=6 \text{ } 45\mu} P_{POC_t}(z)dz$

and $\sum_{t=1}^{t=6 \text{ } 45\mu} P_{DOC_t}(z)dz$ were summed to get the total primary production in the euphotic zone

(PP) over the study period.

We calculated linear regression equations between F_{50m} and P_{POC} ($F_{50m} = 0.17 \times P_{POC} + 272.86$; $r^2 = 0.93$; $p < 0.05$) and between F_{150m} and P_{POC} ($F_{150m} = -0.03 \times P_{POC} + 242.06$; $r^2 = 0.99$; $p < 0.05$) measured on days 2, 4 and 6 to estimate the POC sinking fluxes at 50 and 150 m on days 1, 3 and 5. As the sediment trap array was deployed for 24 h (i.e. from day t to $t+1$), the POC sinking fluxes from days 1 to 6 were summed to get the total integrated sinking fluxes of POC at 50 and 150 m over the study period ($\sum_{t=1}^{t=6} F_{50m_t}$ and $\sum_{t=1}^{t=6} F_{150m_t}$, respectively).

3.2.4 Particulate organic carbon budget

The carbon budget is based on a mass balance equation that describes the change in suspended POC biomass from days 1 to 7 within a specific depth layer z_1-z_2 (i.e. 0-45 m for the euphotic zone and 45-150 m for the upper twilight zone) as the result of POC input (I) and output (O) processes, as in Eq. 1:

$$\int_{z_1}^{z_2} POC_7(z)dz - \int_{z_1}^{z_2} POC_1(z)dz = I - O \quad (1)$$

Particulate primary production ($\sum_{t=1}^{t=6} \int_{0m}^{45\mu} P_{POC_t}(z) dz$) was assumed to be the main input

of POC to the euphotic zone. Given that the same water mass was sampled during the Lagrangian study period (Pommier et al. ms-a, Chapitre I), potential POC input due to the mixing with a different water mass was assumed to be negligible. Finally, given the location of the sampling station (Fig. 1), any coastal or riverine input of organic carbon was considered negligible. The output term for POC from the euphotic zone comprises: (1) the vertical sinking flux of POC below the base of the euphotic zone ($\sum_{t=1}^{t=6} F_{50m_t}$) and (2) the loss of particulate organic matter through zooplankton grazing, viral lysis and other solubilization processes (L_{POC}). Therefore, the mechanisms responsible for changes in POC stocks in the euphotic zone from days 1 to 7 can be summarized as in Eq. 2:

$$\int_{0m}^{45\mu} POC_7(z) dz - \int_{0m}^{45\mu} POC_1(z) dz = \left(\sum_{t=1}^{t=6} \int_{0m}^{45\mu} P_{POC_t}(z) dz \right) - \left[\left(\sum_{t=1}^{t=6} F_{50m_t} \right) + L_{POC} \right] \quad (2)$$

where each term is as defined above. Note that L_{POC} in Eq. 2 is estimated by resolving the equation.

The same rationale was used for the POC budget in the upper twilight zone. In this zone, the input of POC was the vertical sinking flux of POC at 50 m ($\sum_{t=1}^{t=6} F_{50m_t}$), whereas the output of POC from the upper twilight zone combined the vertical sinking flux of POC

at 150 m ($\sum_{t=1}^{t=6} F_{150m_t}$) and the loss of particulate organic matter in the upper twilight zone (L_{POC}). The mechanisms responsible for changes in POC stocks in the upper twilight zone from days 1 to 7 can be summarized as in Eq. 3:

$$\int_{45m}^{150m} POC_7(z) dz - \int_{45m}^{150m} POC_1(z) dz = \left(\sum_{t=1}^{t=6} F_{50m_t} \right) - \left[\left(\sum_{t=1}^{t=6} F_{150m_t} \right) + L_{POC} \right] \quad (3)$$

where each term is as defined above. Note that L_{POC} in Eq. 3 is estimated by resolving the equation.

3.2.5 Dissolved organic carbon budget

The DOC budget was based on the same rationale as the POC budget (see Eq. 1). Given that refractory DOC (DOC_R) was considered as a constant background, any changes in DOC_T during our study should reflect the dynamics of the labile and semi-labile DOC pools. As a first approach in resolving our DOC budget, simplifications were made regarding the potential input and output of DOC. Firstly, we only considered the dynamics of labile DOC (DOC_L), since its turnover (from hours to days) is particularly relevant to the duration of our study (i.e. 7 days). Secondly, the only input of DOC to the system was assumed to be through P_{DOC} in the euphotic zone. P_{DOC} was assumed to consist only of phytoplankton exudates (Valiela 1995), a source of labile DOC (Christian & Anderson 2002). Thirdly, the output of labile DOC in a specific depth layer (L_{DOC_L}) was entirely

attributed to bacterial consumption (Legendre & Rivkin 2002). L_{DOC_L} was used to estimate the rate of bacterial respiration on labile DOC (R_{DOC_L}) in a specific depth layer as in Eq. 4 (Ducklow 2000):

$$R_{DOC_L} = L_{DOC_L} - BP \quad (4)$$

where BP is the bacterial production. BP is a function of L_{DOC_L} and of the bacterial growth efficiency (BGE) determined as follows $BP \approx L_{DOC_L} \times BGE$ (Carlson 2002). Therefore, R_{DOC_L} was computed as in Eq. 5:

$$R_{DOC_L} = L_{DOC_L} \times (1 - BGE) \quad (5)$$

In order to resolve Eq. 5, two estimates of the bacterial growth efficiency (BGE) were used: (1) an empirical value of 5% for the North Atlantic Ocean (del Giorgio & Cole 2000) and (2) a BGE of 34% estimated from the temperature–growth efficiency relationship of Rivkin & Legendre (2001) and an average temperature of 3.3°C in the upper 150 m.

3.3 Results

The daily rates of total and particulate primary production, of phytoplankton DOC release, and sinking fluxes of POC at 50 and 150 m are presented in Table 2. POC and DOC stocks on days 1 and 7 are shown in Table 3. Based on these data, the budgets of

DOC and POC stocks and fluxes in the euphotic and upper twilight zones are presented in Fig. 2.

Table 2. Daily rates of total primary production (PP), particulate primary production (P_{POC}) and phytoplankton dissolved organic carbon release (P_{DOC}) integrated over the euphotic zone and of vertical sinking fluxes of particulate organic carbon at 50 and 150 m (F_{50m} and F_{150m} , respectively) during a Lagrangian study of the decline of a spring bloom in the northwest Atlantic Ocean in 2003. The daily rates of each variable were summed from days 1 to 6 to estimate total values for the Lagrangian study period. The sinking fluxes on days 1, 3 and 5 (italics) were estimated from the regressions between F_{50m} and P_{POC} and between F_{150m} and P_{POC} which were computed from values on days 2, 4 and 6. See Materials and methods for more details

Day	Date	PP	P_{POC}	P_{DOC}	F_{50m}	F_{150m}
		(mg C m ⁻² d ⁻¹)				
1	25 April	2720	2510	210	712	167
2	26 April	2522	2317	205	674	173
3	27 April	432	400	32	<i>343</i>	230
4	28 April	623	481	142	410	227
5	29 April	480	326	154	<i>330</i>	232
6	30 April	400	326	74	281	233
Total (mg C m ⁻²)		7177	6360	817	2750	1262

Table 3. Concentrations of particulate (POC) and dissolved (DOC) organic carbon integrated over the euphotic zone and the upper twilight zone of the northwest Atlantic Ocean at the beginning (day 1) and the end (day 7) of a Lagrangian study of the decline of the spring bloom in 2003. The semi-labile (DOC_{SL}) and labile (DOC_L) fractions of the total DOC stock (DOC_T) are indicated. Minimum and maximum estimates of bacterial respiration on labile DOC (R_{DOC_L}) from days 1 to 7 were calculated based on bacterial growth efficiencies of 34% (Rivkin & Legendre 2001) and 5% (del Giorgio & Cole 2000), respectively. See Materials and Methods for more details on estimates of DOC fractions and bacterial respiration

	Day	POC	DOC _T	DOC _{SL}	DOC _L	R_{DOC_L}
Euphotic zone	1	19.21	42.73	17.13	1.28	0.66–0.95
	7	12.78	36.55	11.13	1.10	
Upper twilight zone	1	14.95	94.06	34.49	2.82	0.30–0.44
	7	14.45	78.48	19.38	2.35	

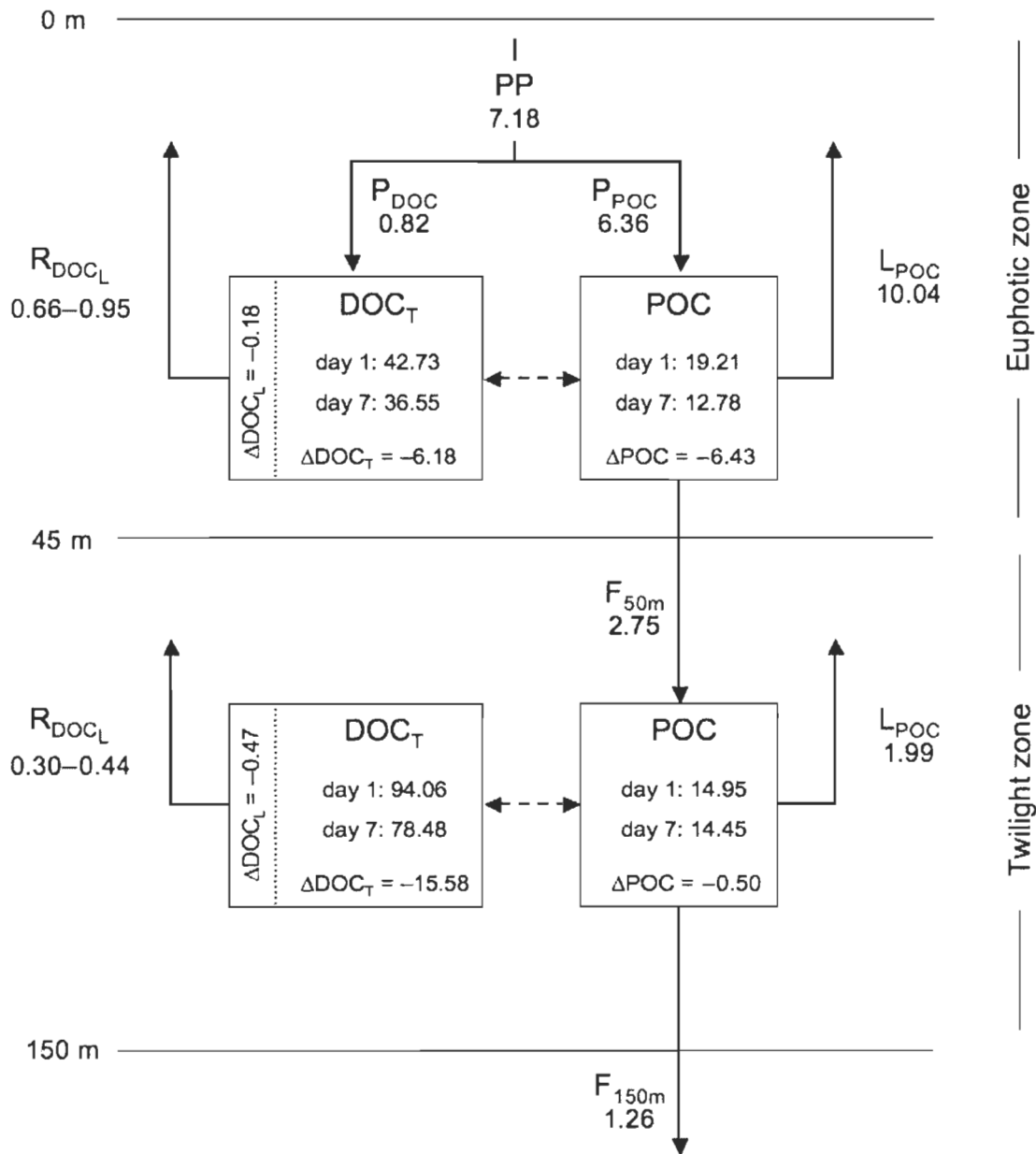


Fig. 2. Budget of dissolved and particulate organic carbon in the euphotic and upper twilight zones of the northwest Atlantic Ocean during a Lagrangian study conducted from 25 April (day 1) to 01 May 2003 (day 7).

Fig. 2. Cont'd. Rates of total primary production (PP), of particulate primary production (P_{POC}) and of phytoplankton dissolved organic carbon release (P_{DOC}) over the euphotic zone; vertical sinking fluxes of particulate organic carbon (POC) beneath the euphotic zone (F_{50m}) and at 150 m (F_{150m}); particulate organic carbon concentration (POC); total dissolved organic carbon concentration (DOC_T); variations in POC, DOC_T and labile DOC (DOC_L) concentrations from days 1 to 7 (ΔPOC , ΔDOC_T , ΔDOC_L , respectively); estimate of the loss of POC (L_{POC}); minimum and maximum estimates of bacterial respiration on labile DOC (R_{DOC_L}) based on bacterial growth efficiencies of 0.34 (Rivkin & Legendre 2001) and 0.05 (del Giorgio & Cole 2000), respectively. Units are in $g C m^{-2}$. Boxes and solid arrows represent carbon stocks and fluxes, respectively. Dashed arrows represent potential transfer of organic carbon between the dissolved and particulate phases

3.3.1 Carbon budget in the euphotic zone

In the euphotic zone, $7.18 g C m^{-2}$ were fixed as total primary production (PP) over the study period, of which $6.36 g C m^{-2}$ were fixed as particulate organic carbon (P_{POC}). During the study period, POC concentrations in the euphotic zone decreased by $6.43 g C m^{-2}$ (ΔPOC in the euphotic zone; Fig. 2). Given a total sinking flux of POC below the euphotic zone of $2.75 g C m^{-2}$ (F_{50m} ; Table 2, Fig. 2), we estimated that $10.04 g C m^{-2}$ were lost through zooplankton grazing, viral lysis and other solubilization processes within the euphotic zone (L_{POC} in the euphotic zone; Fig. 2). The total DOC (DOC_T) pool in the euphotic zone decreased by $6.18 g C m^{-2}$ over the study period (ΔDOC_T in the euphotic zone; Fig. 2). This decrease in DOC_T comprises a large decrease in DOC_{SL} ($6.00 g C m^{-2}$; Table 3) and a small decrease in DOC_L ($0.18 g C m^{-2}$; Table 3, Fig. 2). If one considers an input of labile DOC of $0.82 g C m^{-2}$ through P_{DOC} (Fig. 2), then DOC_L removal from the euphotic zone was actually $1.00 g C m^{-2}$ (i.e. $0.18 + 0.82 g C m^{-2}$) from days 1 to 7. Based on this latter value, we estimated that bacterial respiration on DOC_L in the euphotic zone ranged from 0.66 to $0.95 g C m^{-2}$ (R_{DOC_L} ; Table 3, Fig. 2).

3.3.2 Carbon budget in the upper twilight zone

In the upper twilight zone, POC stocks decreased by 0.50 g C m^{-2} from days 1 to 7 (ΔPOC in the upper twilight zone; Fig. 2). Given a POC input of 2.75 g C m^{-2} from the total POC sinking flux at 50 m and an output of 1.26 g C m^{-2} from the total POC sinking flux at 150 m (Table 2, Fig. 2), we estimated that 1.99 g C m^{-2} of POC were lost through zooplankton grazing, viral lysis and other solubilization processes within the upper twilight zone (L_{POC} in the upper twilight zone; Fig. 2). The DOC_T pool in the upper twilight zone decreased by 15.58 g C m^{-2} during the study period (Fig. 2). This decrease in DOC_T comprised a large decrease in DOC_{SL} (15.12 g C m^{-2} ; Table 3) and a small decrease in DOC_{L} (0.47 g C m^{-2} ; Table 3, Fig. 2). Based on the decrease in DOC_{L} in the upper twilight zone from days 1 to 7, we estimated that bacterial respiration on DOC_{L} in that zone ranged from 0.30 to 0.44 g C m^{-2} ($R_{\text{DOC}_{\text{L}}}$; Table 3, Fig. 2).

3.4 Discussion

3.4.1 POC budget

Throughout the study period, 12.03 g C m^{-2} of POC were estimated to be lost through zooplankton grazing, viral lysis and other solubilization processes in the upper 150 m (L_{POC} in the euphotic zone + L_{POC} in the upper twilight zone; Fig. 2). During the western North Atlantic Bloom Experiment at 45°N , Harrison et al. (1993) reported that springtime micro- and mesozooplankton grazing in the upper 100 m removed up to 88% and 9% of the particulate primary production, respectively. When applying these percentages to P_{POC}

(6.36 g C m^{-2} , Table 2), we estimated that micro- and mesozooplankton grazing on POC removed 5.60 and 0.57 g C m^{-2} , respectively, i.e. about 60% of the total POC loss calculated from our budget. Moreover, viruses are recognized to play an important role in the functioning of pelagic food webs and in biogeochemical cycling in the oceans (Fuhrman 1999, Wilhelm & Suttle 1999, Suttle 2005). Based on a simple food-web model, Wilhelm & Suttle (1999) estimated that an average of 16% (range: $6\text{-}26\%$) of the POC produced by primary production could be converted to DOC by viral lysis. When applying this average percent value to P_{POC} (6.36 g C m^{-2} , Table 2), we estimated that 1.02 g C m^{-2} were transferred from the particulate to the dissolved phase through viral lysis during our study. Finally, as 12.03 g C m^{-2} of POC were lost within the upper 150 m during the study period, 7.19 g C m^{-2} of which were related to grazing ($5.60 + 0.57 \text{ g C m}^{-2}$) and viral lysis (1.02 g C m^{-2}), we estimated that the remaining loss of 4.84 g C m^{-2} was due to other solubilization processes of the particulate organic matter. Through their activity, grazers, viruses and bacteria not only influenced the POC stock but also the DOC stock, as estimated below.

3.4.2 DOC budget

P_{DOC} was assumed to be the main input of DOC in our budget. However, while DOC production is ultimately constrained by the magnitude of the primary production, it potentially includes many other processes such as photorespiration; grazer-mediated release (mesozooplankton sloppy feeding, excretion and egestion; protozoan egestion; leaching from fecal pellets); spontaneous, bacterial and viral lysis of phytoplankton cells; and

solubilization of particles by bacterial hydrolytic exoenzymes (Valiela 1995, Nagata 2000, Carlson 2002). Nagata (2000) estimated that ~20% and ~15% of the particulate primary production can be converted to DOC through micro- and mesozooplankton grazing, respectively. Estimates using these values would yield a potential DOC production of 1.27 and 0.95 g C m^{-2} in the upper 150 m, through micro- and mesozooplankton grazing, respectively, during the study period. Møller et al. (2003) reported that DOC leaching from mesozooplankton fecal pellets can account for 28% of the pellets organic carbon content. During our study, the sinking flux of fecal pellets at 150 m averaged $0.04 \text{ g C m}^{-2} \text{ d}^{-1}$ (Pommier et al. ms-b, Chapitre II) which gives, when extrapolated to the study period, a total fecal-POC sinking flux of 0.28 g C m^{-2} . Hence, we estimated that DOC production through leaching from fecal pellets in the upper 150 m could have amounted 0.08 g C m^{-2} (i.e. $28\% \times 0.28 \text{ g C m}^{-2}$) for the study period. Given the viral and other solubilization processes involved in the transformation of POC into 5.86 g C m^{-2} of DOC ($1.02 + 4.84 \text{ g C m}^{-2}$; see previous section), then a total amount of 8.16 g C m^{-2} of DOC ($1.27 + 0.95 + 0.08 + 5.86 \text{ g C m}^{-2}$) was potentially released in the upper 150 m by grazers, leaching from fecal pellets, viral and other solubilization processes.

The decreases in labile DOC from days 1 to 7 in both the euphotic and upper twilight zones were attributed to bacterial consumption. While labile DOC has a rapid turnover rate of hours to days, the semi-labile fraction of DOC (DOC_{SL}) is biologically reactive over months to a year (Carlson 2002), i.e. on time scales much longer than our study period. Yet, Ducklow et al. (2002) reported that the semi-labile DOC that accumulates during the North Atlantic spring bloom could support bacterial metabolism. Therefore, occasional bacterial

consumption of DOC_{SL} may have occurred in our study and could at least partially explain the decrease in DOC_{SL} in the euphotic and upper twilight zones from days 1 to 7 (Table 3). Harrison et al. (1993) reported that bacterial production rates in the upper 100 m of the temperate northwest Atlantic can represent 12% to 39% of the total primary production. Given a total primary production rate of 7.18 g C m^{-2} throughout the study period (Fig. 2), we estimate an average bacterial production (BP) of 1.83 g C m^{-2} . Considering this latter estimate and a bacterial growth efficiency (BGE) ranging from 5% to 34% (see Materials and methods), then a bacterial carbon demand (BCD = BP/BGE) varying between 5.38 and 36.6 g C m^{-2} can be estimated for the study period. This range of values is in good agreement with the total decrease in DOC_{SL} (21.12 g C m^{-2} ; Table 3) observed in the euphotic and upper twilight zones during our study, thus suggesting that bacterial consumption on semi-labile DOC could explain, in part, the observed change. Heterotrophic flagellates have also been reported to take up dissolved and colloidal organic carbon (Sherr 1988, Tranvik et al. 1993), but their ecological significance regarding DOC cycling is though to be minor (Legendre & Rivkin 2002, 2005).

The formation of transparent exopolymer particles (TEP) could also have contributed to the observed decrease in DOC_{SL} in the euphotic and upper twilight zones. TEP formation is recognized as a major pathway through which dissolved organic matter is converted to particulate organic matter. TEP are gel-like particles composed of acidic polysaccharides and formed from dissolved precursors (fibrillar polymers) that coagulate to form aggregates (Passow 2002). Large concentrations of TEP can be associated with aggregate formation particularly as a function of nutrient depletion during the decline of diatom blooms (Passow

et al. 2001). Large amorphous aggregates were observed in the sediment traps as part of the collected material and $\geq 50\%$ of the POC sinking flux at 150 m was composed of unidentified material other than intact phytoplankton cells and fecal pellets (Pommier et al. ms-b, Chapitre II). These observations point to the potential importance of TEP during our study. Engel (2004) reported TEP-related POC accounting for 18% of the total POC concentration within the upper 70 m of the temperate northeast Atlantic Ocean. Based on this latter estimate and given a total POC stock of 40.52 g C m^{-2} in the upper 150 m ($P_{\text{POC}} + \text{POC}$ concentrations on day 1 in the euphotic and in the upper twilight zones; Fig. 2), we estimate a potential TEP-related carbon concentration of 7.29 g C m^{-2} .

Finally, photooxidation, i.e. the photochemical transformation of dissolved organic matter by UV radiation, may also be invoked to explain the loss of DOC_{SL} in the euphotic zone from days 1 to 7. Indeed, DOC photooxidation is considered to play an important role in the carbon cycle of aquatic systems either by the direct photoproduction of dissolved inorganic carbon and carbon monoxide or indirectly by the transformation of refractory compounds to more labile DOC that can be oxidized by heterotrophic bacteria (Mopper et al. 1991, Mopper & Kieber 2000). Photooxidation has mainly been investigated in freshwater and coastal ocean systems and its importance in the open ocean remains poorly quantified. Vodacek et al. (1997) estimated that photooxidation represented $\sim 10\%$ of the total DOC stock in the surface mixed layer of the Middle Atlantic Bight. Based on this latter estimation, and given an integrated concentration of DOC_{T} over the surface mixed layer (10–26 m) of 8.63 g C m^{-2} during our study (data not shown), then photooxidation would have yielded a DOC loss of 0.86 g C m^{-2} .

When combining our estimates of the bacterial carbon demand ($5.38\text{--}36.6 \text{ g C m}^{-2}$), TEP formation (7.29 g C m^{-2}) and photooxidation (0.86 g C m^{-2}), a total DOC loss ranging from 13.53 to 44.75 g C m^{-2} is obtained for the upper 150 m during the study period. This range of values is in fairly good agreement with the decrease in DOC_{SL} observed for the euphotic and upper twilight zones (21.12 g C m^{-2} ; Table 3) and suggests that bacterial consumption of DOC and TEP formation were the most important processes influencing the dynamics of the DOC pool during our study.

3.4.3 Heterotrophic community respiration

Based on the changes in labile DOC stocks from days 1 to 7 (Table 3), the bacterial respiration in the upper 150 m of the water column during the study period was estimated to range from 0.96 to 1.39 g C m^{-2} (Fig. 2). As mentioned in the previous section, micro- and mesozooplankton grazing, viral lysis and other solubilization processes of POC were estimated to yield a potential DOC supply of 8.16 g C m^{-2} in the upper 150 m . Of this amount, 3% (i.e. 0.24 g C m^{-2}) could have been constituted of labile compounds (Carlson 2002) and then directly taken up by heterotrophic bacteria. Taking into account the potential consumption of this additional source of DOC_{L} by heterotrophic bacteria and BGEs of 5 and 34% (see Materials and methods), we estimate a supplementary respiration rate varying between 0.16 and 0.23 g C m^{-2} . Hence, a total bacterial respiration of labile DOC ranging from 1.12 to 1.62 g C m^{-2} can be estimated for the upper 150 m during the study period. This range of values is lower than previous values reported for the temperate North Atlantic Ocean. Indeed, in the euphotic zone of the temperate northwest Atlantic

Ocean, Li et al. (1993) reported springtime bacterial production rates averaging 0.37 g C m⁻² d⁻¹ which, when extrapolated to the duration of our study and using a BGE of 34% (see Materials and methods), give a bacterial respiration rate of 5.03 g C m⁻². Similarly, springtime bacterial production rates of 0.21 g C m⁻² d⁻¹ have been reported in the euphotic zone of the temperate northeast Atlantic Ocean (Ducklow et al. 2002) which, when extrapolated to a 7-day period and using a BGE of 34%, would give a bacterial respiration rate of 2.85 g C m⁻². Nevertheless, the estimated range of bacterial respiration in our budget should be considered as lower estimates as it is based only on the labile fraction of DOC and that semi-labile DOC could also have supported bacterial metabolism throughout the study period (see previous section). In addition, based on our estimates of micro- and mésozooplancton grazing (5.60 and 0.57 g C m⁻², respectively), and assuming micro- and mésozooplancton assimilation efficiencies of 30% (Edwards et al. 2000) and 70% (Carlotti et al. 2000), respectively, POC respiration due to micro- and mésozooplancton grazing would be 3.92 and 0.17 g C m⁻², respectively. When combining our estimates of mésozooplancton, mésozooplancton and bacterial respiration, a constrained total respiration of the heterotrophic community ranging from 5.21 to 5.71 g C m⁻² is obtained for the upper 150 m during our study. Arístegui & Harrison (2002) reported a community respiration of ~60 mmol C m⁻² d⁻¹ for the upper 100 m of the temperate northwest Atlantic Ocean in fall 1992, which when extrapolated to a 7-day period gives a community respiration of 5.04 g C m⁻². This value is in close agreement with our community respiration estimate.

3.4.4 Ecological significance of the carbon budget

The primary production rate measured during our study (7.18 g C m^{-2}) represents only 2.4% of the annual primary production of 300 g C m^{-2} reported in that region of the World Ocean by Sarmiento & Gruber (2006). However, if one considers the preformed pool of POC on day 1 in the upper 150 m (i.e. 34.16 g C m^{-2} ; Fig. 2) as a conservative estimate of primary production prior to the study period, then the bloom investigated during our study contributed 41.34 g C m^{-2} or ~14% to the annual primary production at the sampling location.

The sum of the particulate primary production and of the POC concentration on day 1 in the euphotic zone (i.e. 25.57 g C m^{-2} ; Fig. 2) represents the total amount of POC in that zone that was potentially available for export through sinking (F_{50m} ; Fig. 2) and for grazing, viral lysis and other solubilization processes (L_{POC} in the euphotic zone; Fig. 2) during the study period. Of this total amount of available POC, ~50% remained suspended in the euphotic zone on day 7 (i.e. 12.78 g C m^{-2} ; Fig. 2), ~39% was channelled through L_{POC} (10.04 g C m^{-2} ; Fig. 2) and ~11% was exported through sinking at 50 m (2.75 g C m^{-2} ; Fig. 2). Similarly, the sum of the vertical sinking flux of POC at 50 m and of the concentration of POC on day 1 in the upper twilight zone (17.70 g C m^{-2} ; Fig. 2) represents the total amount of POC in that zone that was potentially available for export through sinking (F_{150m} ; Fig. 2) and for losses through grazing, viral lysis and other solubilization processes (L_{POC} in the upper twilight zone; Fig. 2), during the study period. Of this total amount of available POC, ~82% remained suspended in the twilight zone on day 7 (i.e. 14.45 g C m^{-2} ; Fig. 2), ~11% was channelled through L_{POC} (1.99 g C m^{-2} ; Fig. 2) and ~7%

was exported through sinking at 150 m (1.26 g C m^{-2} ; Fig. 2). These results indicate that a large amount of POC remained suspended in the upper 150 m during the study period rather than being exported or recycled *in-situ*. Indeed, the POC sinking flux at 150 m (1.26 g C m^{-2} ; Fig. 2) and the total loss of POC in the upper 150 m through grazing, viral lysis and other solubilization processes (12.03 g C m^{-2} ; Fig. 2) represented only 3% and 30% of the POC available in that layer (40.52 g C m^{-2}), respectively. The accumulation of suspended particulate organic matter in the upper 150 m could be related to the development of a deep chlorophyll *a* maximum, corresponding to maxima in phytoplankton biomass and in POC concentration, close to the base of the euphotic zone throughout the decline of the bloom (Pommier et al. ms-a, Chapitre I). Our results also highlight the relative incapacity of heterotrophs in making use of the large stock of suspended POC in the upper 150 m of the water column, particularly in the upper twilight zone. This may be related to the typical temporal lag between phytoplankton growth and mesozooplankton grazing in the temperate North Atlantic Ocean (Parsons & Lalli 1988). It is also possible that copepods avoided to feed on diatoms of the genera *Chaetoceros* and *Thalassiosira* (Irigoién et al. 2002) which were the most abundant phytoplankton throughout the study period (Pommier et al. ms-a, Chapitre I). Inefficient removal of suspended POC by heterotrophs during the northeast Atlantic spring bloom has already been reported by Bender et al. (1992).

Satellite imagery of the sampling area showed that only the first half of the decline of the spring bloom was captured during our study (Forget et al. 2007). The fate of the large amount of suspended POC in the euphotic and upper twilight zones later during the decline

of the bloom (i.e. whether it was recycled *in situ* and respired, or exported to depth) is unknown. It could have had profound implications in regard to the ocean biogeochemistry at our sampling location given that the respiration of organic matter in the euphotic and upper twilight zones releases dissolved inorganic carbon that could return to the atmosphere on short time-scales of days to weeks. Moreover, about as much DOC_{SL} as POC remained accumulated in the upper 150 m of the water column on day 7 (Table 3). The fate of this accumulated DOC_{SL} is also of great importance in regard to the ocean biogeochemistry at our sampling location. This semi-labile DOC may have fuelled bacterial metabolism over time scales longer than our sampling period (i.e. weeks to months) and/or may have eventually been exported to depth by convection at high latitudes on time scales relevant to the thermohaline circulation (Hansell 2002).

Using the total primary production rate measured in the euphotic zone (7.18 g C m^{-2}) and the respiration of the heterotrophic community estimated for the euphotic and upper twilight zones ($5.21\text{--}5.71 \text{ g C m}^{-2}$), we calculated a ratio of total primary production to community respiration ranging from 1.26 to 1.38. This provides evidences for net autotrophy of the marine system studied. We acknowledge that the accurate determination of the trophic balance of aquatic systems requires investigations over time scales much longer (i.e. over the seasonal cycle of production) than that considered in our study (del Giorgio & Williams 2005). Nevertheless, the range of production:respiration ratios estimated in our budget is in agreement with the general understanding that the spring bloom in the temperate North Atlantic acts as a net sink for atmospheric CO₂.

CONCLUSION GÉNÉRALE

La détermination des processus contrôlant l'efficacité de transfert du carbone organique particulaire (COP) vers l'océan profond est un prérequis essentiel à une meilleure compréhension du fonctionnement de la pompe biologique océanique de carbone. À cet égard, la zone mésopélagique est depuis longtemps reconnue comme une interface cruciale entre la zone euphotique et l'océan profond (Angel 1989, Tréguer et al. 2003). Cependant, les processus de transformations de la matière organique lors de son exportation dans la zone mésopélagique sont peu connus (Boyd & Trull 2007). Dans ce contexte, cette thèse a permis : (1) de décrire la variabilité de l'exportation de COP depuis la zone euphotique et ses transformations à travers la partie supérieure de la zone mésopélagique (50-150 m) lors du déclin d'un bloom printanier de l'océan Atlantique nord-ouest, (2) de relier cette variabilité aux changements des communautés phytoplanctoniques (production, biomasse, structure de taille, composition spécifique) au sein de la zone euphotique et (3) de calculer un budget des stocks et des flux de COD et de COP dans les 150 premiers mètres de la colonne d'eau.

Le premier chapitre de cette thèse a permis d'établir le contexte physique, chimique et biologique de cette étude. Ce travail décrit la première phase du déclin de l'une des floraisons phytoplanctoniques les plus productives rapportées pour les eaux ouvertes de l'océan Atlantique du nord-ouest, sous l'influence d'une limitation de la production primaire par la disponibilité en nitrates. Le déclin du bloom était associé à une diminution

de la production et de la biomasse de la communauté phytoplanctonique, laquelle était dominée par le phytoplancton de grande taille, majoritairement des diatomées centrales. Treize jours plus tard, le système étudié a été remplacé par un système productif dominé par des flagellés de petite taille et présentant des concentrations en chlorophylle *a* plus faibles que lors du déclin du bloom. L'analyse de la structure de taille de la production et de la biomasse phytoplanctonique, en utilisant l'approche de Tremblay & Legendre (1994), a permis de proposer que la biomasse du petit phytoplancton (0,7-5 µm) a été préférentiellement broutée par le microzooplancton tandis que celle du gros phytoplancton ($\geq 5 \mu\text{m}$) avait tendance à s'accumuler dans la zone euphotique. Cette accumulation de cellules phytoplanctoniques a été confirmée par la présence d'un maximum profond de chlorophylle *a* (MPC) au voisinage de la base de la zone euphotique, juste au-dessus de la nitracline, qui s'est maintenu pendant tout la durée de l'étude.

Le second chapitre examine pour la première fois la variabilité temporelle, à court terme, des flux verticaux de COP dans la zone mésopélagique de l'océan Atlantique nord-ouest. Les résultats de ce chapitre ont mis en évidence la diminution des flux verticaux de COP sous la base de la zone euphotique durant le déclin du bloom et sa transition vers des conditions de post-bloom. Cette décroissance des flux de COP était positivement corrélée à la diminution de la production du gros phytoplancton tout au long de la période d'étude. Ces résultats confirment l'importance du gros phytoplancton dans le contrôle du potentiel d'exportation verticale du COP en dehors de la zone euphotique (Boyd & Newton 1999). En revanche, les flux verticaux de COP à 150 m sont restés relativement constants tout au

long de la période d'étude en dépit de la forte diminution de l'exportation verticale de COP depuis la zone euphotique.

L'analyse des profils verticaux de décroissance du flux de COP avec la profondeur a mis en lumière la diminution temporelle du recyclage de la matière organique au sein de la partie supérieure de la zone mésopélagique (50-150 m). Il s'en suit que l'efficacité de transfert du COP à 150 m (i.e. la profondeur à laquelle se situait la thermocline permanente) a augmenté graduellement lors du déclin du bloom. L'hypothèse d'une compensation entre la réduction du flux de COP à la base de la zone euphotique et la diminution du recyclage de la matière organique dans la zone mésopélagique a été émise pour expliquer les faibles variations temporelles du flux de COP à 150 m.

Les résultats du second chapitre de cette thèse démontrent que les communautés hétérotrophes mésopélagiques sont capables de répondre rapidement et proportionnellement aux variations de l'apport de COP depuis la zone euphotique. En effet, le taux de recyclage du COP au sein de la zone mésopélagique était positivement corrélé au flux de COP sous la base de la zone euphotique durant la période d'étude. Ces résultats mettent en lumière le rôle déterminant des variations à court terme du recyclage du matériel organique par les organismes hétérotrophes au sein de la zone mésopélagique en regard à l'efficacité de transfert du COP en profondeur.

Cette étude n'a pas permis d'identifier la nature exacte des processus hétérotrophes de recyclage de la matière organique au sein de la zone mésopélagique. Néanmoins, la faible contribution des pelotes fécales et des cellules phytoplanctoniques au flux total de COP suggère que le broutage par le mésozooplancton a joué un rôle mineur en regard au recyclage de la matière organique au sein du système étudié. Ce résultat met l'accent sur l'importance potentielle des processus microbiens de recyclage de la matière organique (minéralisation bactérienne, broutage par le microzooplancton) durant notre étude, telle que précédemment rapportée aux latitudes tempérées de l'océan Atlantique Nord (Ducklow & Harris 1993, Karayanni et al. 2005, Reinthaler et al. 2006). Le rôle limité du mésozooplancton et la dominance des processus bactériens en regard au recyclage de la matière organique ont également été mis en évidence dans l'océan Pacifique subarctique lors du déclin d'un bloom de diatomées induit par un enrichissement en fer (Boyd et al. 2004, Sastri & Dower 2006).

Le budget de carbone présenté dans le troisième chapitre de cette thèse offre une vision globale et intégrée des stocks et des flux de carbone organique dans la zone euphotique et la zone mésopélagique pour la période du déclin du bloom. Ce budget a été établi pour une durée de sept jours avec les données recueillies pendant l'étude lagrangienne. Pendant cette période d'étude, la moitié (50 %) du COP de la zone euphotique est demeurée en suspension au sein de cette zone. Environ 40 % du COP a été recyclé par les hétérotrophes au sein de la zone euphotique tandis que 10 % a été exporté sous la zone euphotique (50 m). Dans la zone mésopélagique, environ 80 % du COP est

resté en suspension au sein de cette zone alors que 10 % a été recyclé par les hétérotrophes et 10 % ont été exportés en dessous de 150 m. Le maintien dans les 150 premiers mètres de la colonne d'eau d'une importante biomasse de COP reflète l'accumulation de cellules phytoplanctoniques au niveau du MPC mise en évidence dans le premier chapitre. Ces résultats témoignent également de l'incapacité des hétérotrophes à utiliser toute la biomasse de carbone organique disponible dans cette couche. Cette difficulté à transformer le carbone organique présent dans les eaux de surface est confirmée par la réduction du recyclage du COP dans la zone mésopélagique lors du déclin du bloom, laquelle a été mise en évidence dans le second chapitre. Ces résultats peuvent refléter le découplage entre la croissance du phytoplancton et le broutage du mésozooplancton qui caractérise le bloom printanier de l'océan Atlantique Nord.

Le devenir de l'importante biomasse de COP demeurée en suspension dans les 150 premiers mètres de la colonne d'eau (i.e. l'agrégation puis la sédimentation des particules ou bien le broutage par le zooplancton et la minéralisation bactérienne) revêt une importance cruciale en regard à la balance métabolique du système étudié (autotrophie *versus* hétérotrophie nette). L'étude réalisée au cours de cette thèse, bien que se déroulant durant une phase cruciale du bloom, est d'une durée trop restreinte pour établir convenablement cette balance métabolique. Néanmoins, les résultats du bilan de carbone présenté dans le troisième chapitre ont permis d'estimer un rapport entre la production primaire totale et la respiration par la communauté hétérotrophe en faveur de l'autotrophie

nette du système étudié. Ce bilan est en accord avec le consensus voulant que l'océan Atlantique Nord soit un puits de carbone.

Contributions de la thèse et perspectives de recherche

La connaissance des processus clés contrôlant le flux vertical de COP au sein d'écosystèmes pélagiques variés est un prérequis nécessaire à une meilleure compréhension du fonctionnement de la pompe biologique océanique et à l'amélioration des modèles du cycle biogéochimique du carbone (Boyd & Trull 2007). À cet égard, l'océan mondial demeure sous-échantillonné. Plus particulièrement, les eaux ouvertes très productives de l'océan Atlantique nord-ouest ont été peu étudiées jusqu'à présent en ce qui a trait aux flux verticaux de COP. Cette thèse a ainsi contribué à l'amélioration des connaissances concernant le fonctionnement de la pompe biologique océanique de carbone dans l'océan Atlantique nord-ouest.

De plus, il est reconnu qu'une meilleure compréhension de la pompe biologique océanique de carbone passe par le développement des connaissances relatives aux processus affectant la transformation de la matière organique dès son exportation en dehors de la zone euphotique (Boyd & Trull 2007, Buesseler et al. 2007b). Néanmoins, les flux verticaux de COP ont été, à ce jour, principalement décrits dans les eaux océaniques profondes. En décrivant la variabilité quasi journalière de l'exportation de COP depuis la zone euphotique jusqu'à la thermocline permanente, les résultats de cette thèse ont permis

d'améliorer les connaissances relatives à l'exportation initiale du COP dans les eaux de surface et de subsurface.

De nombreux modèles d'exportation de la matière organique utilisent le paramètre b développé par Martin et al. (1987) pour déterminer les flux verticaux de COP dans la colonne d'eau. Ce paramètre décrit l'atténuation du flux vertical de COP avec la profondeur. Cette approche assume que la pente de la décroissance du flux de COP avec la profondeur ne varie pas dans le temps et qu'elle est constante pour une région océanique donnée (Berelson 2001). Toutefois, les résultats de cette thèse ont démontré clairement que la valeur de cette pente varie à court terme. Ceci a des implications importantes sur notre compréhension, au sein d'une même région océanique, du recyclage de la matière organique et de l'efficacité de transfert du COP en profondeur. Cette variabilité temporelle devrait être considérée dans les prochains modèles de la pompe biologique océanique de carbone.

Les résultats présentés dans les différents chapitres de cette thèse constituent une base de données essentielles servant de soutien à l'ensemble des équipes de recherche qui étudient les interactions biogéochimiques entre l'océan et l'atmosphère dans le cadre du programme C-SOLAS/SABINA. De plus, les données de cette thèse participeront à l'effort de développement et d'amélioration des modèles de la biogéochimie océanique en général et de la pompe biologique de carbone dans l'Atlantique Nord en particulier.

Des études supplémentaires sont nécessaires afin de décrire la structure des communautés hétérotrophes mésopélagiques et l'importance relative des eubactéries, des archéobactéries, des virus, du micro- et du mésozooplancton (Herndl et al. 2005, Tanaka et al. 2005, Reinthaler et al. 2006, Fukuda et al. 2007) en regard au recyclage de la matière organique au sein de la zone mésopélagique. Il est également nécessaire de connaître la dynamique de ces communautés hétérotrophes mésopélagiques afin de mieux comprendre la variabilité temporelle du recyclage de la matière organique dans la zone mésopélagique et sa relation avec les changements dans l'exportation de matière organique provenant de la zone euphotique. À ma connaissance, les travaux de Buesseler et al. (2007b) dans le Pacifique subarctique et ceux du second chapitre de cette thèse sont les seuls rapportant que les communautés hétérotrophes mésopélagiques répondent rapidement et proportionnellement aux variations des apports de matière organique depuis la zone euphotique. Ces variations à court terme (de quelques heures à quelques jours) sont peu considérées bien qu'elles soient déterminantes pour la compréhension du cycle océanique du carbone. L'utilisation d'une approche lagrangienne, aussi longue que possible, permettrait de mieux comprendre cette variabilité à court terme et sa pertinence en regard à l'intensité de la pompe biologique océanique de carbone. Enfin, une meilleure caractérisation de la composition chimique et de la biodisponibilité (i.e. la nature labile ou réfractaire) de la matière organique particulaire et dissoute est essentielle à la compréhension des transformations du matériel organique transitant au sein de la zone mésopélagique (Lee 2004). De telles perspectives rejoignent les objectifs de recherche du

programme VERTIGO (Vertical Transport In the Global Ocean) et du réseau de recherche IMBER (Integrated Marine Biogeochemistry and Ecosystem Research).

RÉFÉRENCES

- Angel MV (1989) Does mesopelagic biology affect the vertical flux? In: Berger WH, Smetacek VS, Wefer G (eds) *Productivity in the ocean: present and past*. John Wiley and Sons, New York, p 155–173
- Antia AN, Koeve W, Fischer G, Blanz T, Schulz-Bull D, Scholten J, Neuer S, Kremling K, Kuss J, Peinert R, Hebbeln D, Bathmann U, Conte M, Fehner U, Zeitzschel B (2001) Basin-wide particulate carbon flux in the Atlantic Ocean: regional export patterns and potential for atmospheric CO₂ sequestration. *Global Biogeochem Cycles* 15:845–862.
- Arístegui J, Harrison WG (2002) Decoupling of primary production and community respiration in the ocean: implications for regional carbon studies. *Aquat Microb Ecol* 29:199–209
- Armstrong RA, Lee C Hedges JI, Honjo S, Wakeham SG (2002) A new, mechanistic model for organic carbon fluxes in the ocean based on the quantitative association of POC with mineral ballast materials. *Deep-Sea Res II* 49:219–236
- Aumont O, Bopp L (2006) Globalizing results from ocean in situ iron fertilization studies. *Global Biogeochem Cycles* 20, doi:10.1029/2005GB002591
- Azetsu-Scott K, Passow U (2004) Ascending marine particles: Significance of transparent exopolymer particles (TEP) in the upper ocean. *Limnol Oceanogr* 49:741–748
- Baker ET, Milburn HB, Tennant DA (1988) Field assessment of sediment trap efficiency under varying flow conditions. *J Mar Res* 46:573–592
- Båmstedt U, Gifford D J, Irigoien X, Atkinson A, Roman M (2000) Feeding. In: Harris R P, Wiebe P H , Lenz J, Skjoldal H R, Huntley M (eds) *ICES Zooplankton methodology manual*. Academic Press, San Diego, p 297–399
- Barnett T.P., Pierce D.W., Schnur R. (2001) Detection of anthropogenic climate change in the world's oceans. *Science* 292:270–274
- Bender M, Ducklow H, Kiddon J, Marra J, Martin J (1992) The carbon balance during the 1989 spring bloom in the North Atlantic Ocean, 47°N, 20°W. *Deep-Sea Res* 39:1707–1725
- Berelson W (2001) The flux of particulate organic carbon into the ocean interior: a comparison of four US-JGOFS regional studies. *Oceanography* 14:59–67

- Betzer PR, Showers WJ, Laws EA, Winn CD, DiTullio GR, Kroopnik PM (1984) Primary productivity and particulate fluxes on a transect of the equator at 153°W in the Pacific Ocean. *Deep-Sea Res* 31:1–11
- Bienfang PK (1981) SETCOL: a technologically simple and reliable method for measuring the phytoplankton sinking rates. *Can J Fish Aquat Sci* 38:1289–1294
- Bienfang PK, Harrison PJ (1984) Sinking rate response of natural assemblages of temperate and subtropical phytoplankton to nutrient depletion. *Mar Biol* 83:293–300
- Bienfang PK, Szyper J, Laws E (1983) Sinking rate and pigment responses to light limitation in a marine diatom: implications to dynamics of chlorophyll maximum layer. *Oceanol Acta* 6:55–62
- Bigg GR, Jickells TD, Liss PS, Osborn TJ (2003) The role of the oceans in climate. *Int J Climatol* 23:1127–1159
- Bishop JKB (1989) Regional extremes in particulate matter composition and flux: effects on the chemistry of the ocean interior. In: Berger WH, Smetacek VS, Wefer G (eds) *Productivity of the ocean: present and past*. J. Wiley & Sons, New York, p 117–138
- Blain S, Guieu C, Claustre H, Leblanc K, Moutin T, Quéguiner B, Ras J, Sarthou G (2004) Availability of iron and major nutrients for phytoplankton in the northeast Atlantic Ocean. *Limnol Oceanogr* 49:2095–2104
- Bopp L, Legendre L, Monfray P (2002) La pompe à carbone va-t-elle se gripper ? *Recherche* 355:48–51
- Boyd PW, Doney SC (2003) The impact of climate change and feedback processes on the ocean carbon cycle. In: Fasham MJR (ed) *Ocean biogeochemistry: The role of the ocean carbon cycle in global change*. Global Change-The IGBP series, Springer-Verlag, Berlin, p 157–193
- Boyd PW, Newton PP (1995) Evidence of the potential influence of planktonic community structure on the interannual variability of particulate organic carbon flux. *Deep-Sea Res II* 42:619–639
- Boyd PW, Newton PP (1999) Does planktonic community structure determine downward particulate organic carbon flux in different oceanic provinces? *Deep-Sea Res I* 46:63–91
- Boyd PW, Trull TW (2007) Understanding the export of biogenic particles in oceanic waters: Is there a consensus? *Prog Oceanogr* 72:276–312

- Boyd PW, Law CS, Wong CS, Nojiri Y, Tsuda A, Levasseur M, Takeda S, Rivkin R, Harrison PJ, Strzepek R, Gower J, McKay RM, Abraham E, Arychuk M, Barwell-Clarke J, Crawford W, Crawford D, Hale M, Harada K, Johnson K, Kiyosawa H, Kudo I, Marchetti A, Miller W, Needoba J, Nishioka J, Ogawa H, Page J, Robert M, Saito H, Sastri A, Sherry N, Soutar T, Sutherland N, Taira Y, Whitney F, Wong S-KE, Yoshimura T (2004) The decline and fate of an iron-induced subarctic phytoplankton bloom. *Nature* 428:549–553
- Bronk DA, See JH, Bradley P, Killberg L (2007) DON as a source of bioavailable nitrogen for phytoplankton. *Biogeosciences* 4:283–296
- Brzezinski MA (1985) The Si:C:N ratio of marine diatoms: inter-specific variability and the effect of some environmental variables. *J Phycol* 21:347–357
- Buesseler KO (1998) The de-coupling of production and particulate export in the surface ocean. *Global Biogeochem Cycles* 12:297–310
- Buesseler KO, Antia AN, Chen M, Fowler SW, Gardner WD, Gustaffson Ö, Harada K, Michaels AF, van der Looff MR, Sarin M, Steinberg DK, Trull T (2007a) An assessment of the use of sediment traps for estimating upper ocean particle fluxes. Accepted in *J Mar Res*
- Buesseler KO, Lamborg CH, Boyd PW, Lam PJ, Trull TW, Bidigare RR, Bishop JKB, Casciotti KL, Dehairs F, Elskens M, Honda M, Karl DM, Siegel DA, Silver MW, Steinberg DK, Valdes J, Mooy Van Mooy B, Wilson S (2007b) Revisiting carbon flux through the ocean's twilight zone. *Science* 316:567–570
- Buesseler KO, Bacon MP, Cochran JK, Livingston HD (1992) Carbon and nitrogen export during the JGOFS North Atlantic bloom experiment estimated from ^{234}Th : ^{238}U disequilibria. *Deep-Sea Res* 39:1115–1137
- Burdige DJ, Homstead J (1994) Fluxes of dissolved organic carbon from Chesapeake Bay sediments. *Geochim Cosmochim Acta* 58:3407–3424
- Burkill PH, Edwards ES, John AWG, Sleigh MA (1993) Microzooplankton and their herbivorous activity in the northeastern Atlantic Ocean. *Deep-Sea Res II* 40:479–493
- Bury SJ, Boyd PW, Preston T, Savidge G, Owens NJP (2001) Size-fractionated primary production and nitrogen uptake during a North Atlantic phytoplankton bloom: implications for carbon export estimates. *Deep-Sea Res I* 48:689–720
- Calbet A, Landry MR (2004) Phytoplankton growth, microzooplankton grazing and carbon cycling in marine systems. *Limnol Oceanogr* 49: 51–57

- Carlotti F, Giske J, Werner F (2000) Modeling zooplankton dynamics. In: Harris RP, Wiebe PH, Lenz J, Skjoldal H, Huntley ME (eds) ICES Zooplankton methodology manual. Academic Press, London, p 571–667
- Carlson CA (2002) Production and removal processes. In: Hansell DA, Carlson CA (eds) Biogeochemistry of marine dissolved organic matter. Academic Press, San Diego, p 91–151
- Carlson CA, Ducklow HW, Michaels AF (1994) Annual flux of dissolved organic carbon from the euphotic zone in the northwestern Sargasso Sea. *Nature* 371:405–408
- Caron G, Michel C, Gosselin M (2004) Seasonal contribution of phytoplankton and fecal pellets to the organic carbon sinking flux in the North Water (northern Baffin Bay). *Mar Ecol Prog Ser* 283:1–13
- Carpenter EJ, Romans K (1991) Major role of the cyanobacterium *Trichodesmium* in nutrient cycling in the North Atlantic Ocean. *Science* 254:1356–1358
- Cho BC, Azam F (1988) Major role of bacteria in biogeochemical fluxes in the ocean's interior. *Nature* 332:441–443
- Christian JR, Anderson TR (2002) Modelling DOM biogeochemistry. In: Hansell DA, Carlson CA (eds) Biogeochemistry of marine dissolved organic matter. Academic Press, San Diego, p 717–755
- Colebrook JM (1979) Continuous plankton records: seasonal cycles of phytoplankton and copepods in the North Atlantic Ocean and the North Sea. *Mar Biol* 51:23–32
- Colebrook JM (1982) Continuous plankton records: seasonal variations in the distribution and abundance of plankton in the North Atlantic Ocean and the North Sea. *J Plankton Res* 4:435–462
- Collos Y, Slawyk G (1980) Nitrogen uptake and assimilation by marine phytoplankton. In: Falkowski PG (ed) Primary production in the sea. Brookhaven Symposium in Biology No. 31, Plenum Press, New York, p 195–211
- Conkright ME, Garcia HE, O'Brien TD, Locarnini RA, Boyer TP, Stephens C, Antonov JI (2002) World Ocean Atlas 2001, Volume 4: Nutrients. In: Levitus S (ed) NOAA Atlas NESDIS 52. U.S. Government Printing Office, Wash DC, 392 p
- Cullen JJ (1982) The deep chlorophyll maximum: comparing vertical profiles of chlorophyll a. *Can J Fish Aquat Sci* 39:791–803

- Dam HG, Miller CA, Jonasdottir SH (1993) The trophic role of mesozooplankton at 47°N, 20°W during the North Atlantic Bloom Experiment. *Deep-Sea Res II* 40:197–212
- del Giorgio PA, Cole JJ (2000) Bacterial energetics and growth efficiency. In: Kirchman DL (ed) *Microbial ecology of the oceans*. Wiley-Liss, New York, p 289–325
- del Giorgio PA, Duarte CM (2002) Respiration in the open ocean. *Nature* 420:379–384
- del Giorgio PA, Williams PJ le B (2005) The global significance of respiration in aquatic ecosystems: from single cells to the biosphere. In: del Giorgio PA, le B Williams PJ (eds) *Respiration in aquatic ecosystems*. Oxford University Press, New York, p 267–303
- del Giorgio PA, Cole JJ, Cimbleris A (1997) Respiration rates in bacteria exceed phytoplankton production in unproductive aquatic systems. *Nature* 385:148–151
- Doney SC, Wallace DWR, Ducklow HW (2000) The North Atlantic carbon cycle: new perspectives from JGOFS and WOCE. In: Hanson RB, Ducklow HW, Field JG (eds) *The changing ocean carbon cycle: a midterm synthesis of the Joint Global Ocean Flux Study*. International Geosphere-Biosphere Programme Book series 5, Cambridge University Press, Cambridge, p 375–391
- Dortch Q, Clayton Jr JR, Thoresen SS, Ahmed SI (1984) Species differences in accumulation of nitrogen pools in phytoplankton. *Mar Biol* 81:237–250
- Duarte CM, Agusti S (1998) The CO₂ balance of unproductive aquatic ecosystems. *Science* 281:234–236
- Ducklow HW (1989) Joint Global Ocean Flux Study: The 1989 North Atlantic Bloom Experiment. *Oceanography* 2:1–8
- Ducklow HW (2000) Bacterial production and biomass in the ocean. In: Kirchman DL (ed) *Microbial ecology of the oceans*. Wiley-Liss, New York, p 85–120
- Ducklow HW, Harris RP (1993) Introduction to the JGOFS North Atlantic Bloom Experiment. *Deep-Sea Res II* 49:1–8
- Ducklow HW, Steinber DK, Buesseler KO (2001) Upper ocean carbon export and the biological pump. *Oceanography* 14:50–58
- Ducklow HW, Kirchman DL, Anderson TR (2002) The magnitude of the spring bacterial production in the North Atlantic Ocean. *Limnol Oceanogr* 47:1684–1693
- Dugdale RC (1967) Nutrient limitation in the sea: dynamics, identification and significance. *Limnol Oceanogr* 12:685–695

- Dugdale RC, Goering JJ (1967) Uptake of new and regenerated forms of nitrogen in primary production. *Limnol Oceanogr* 12:196–206
- Edwards CA, Batchelder HP, Powell TM (2000) Modeling microzooplankton and macrozooplankton dynamics within a coastal upwelling system. *J Plankton Res* 22:1619–1648
- Emerson S, Quay P, Karl D, Winn C, Tupas L, Landry M (1997) Experimental determination of the organic carbon flux from open-ocean surface waters. *Nature* 389:951–954
- Engel A (2004) Distribution of transparent exopolymer particles (TEP) in the northeast Atlantic Ocean and their potential significance for aggregation processes. *Deep-Sea Res I* 51:83–92
- Eppley RW, Peterson BJ (1979) Particulate organic matter flux and planktonic new production in the deep ocean. *Nature* 282:677–680
- Estrada M, Alcaraz M, Marrasé C (1987) Effect of turbulence on the composition of phytoplankton assemblages in marine microcosms. *Mar Ecol Prog Ser* 38:267–281
- Falkowski PG, Green RM, Geider RJ (1992) Physiological limitations on phytoplankton productivity in the ocean. *Oceanography* 5:64–91
- Falkowski PG, Barber RT, Smetacek V (1998) Biogeochemical controls and feedbacks on ocean primary production. *Science* 281:200–206
- Fernández CI, Raimbault P (2007) Nitrogen regeneration in the NE Atlantic Ocean and its impact on seasonal new, regenerated and export production. *Mar Ecol Prog Ser* 337:79–92
- Fileman ES, Leakey RJG (2005) Microzooplankton dynamics during the development of the spring bloom in the north-east Atlantic. *J Mar Biol Ass UK* 85:741–753
- Forget MH, Sathyendranath S, Platt T, Pommier J, Vis C, Kyewalyanga MS, Hudon C (2007) Extraction of photosynthesis-irradiance parameters from phytoplankton production data: demonstration in various aquatic systems. *J Plankton Res* 29:249–262
- Fortier L, Le Fèvre J, Legendre L (1994) Export of biogenic carbon to fish and to the deep ocean : The role of large planktonic micropahages. *J Plankton Res* 16:809–939
- Francois R, Honjo S, Krishfield R, Manganini S (2002) Factors controlling the flux of organic carbon to the bathypelagic zone of the ocean. *Global Biogeochem Cycles* 16, doi:10.1029/2001GB001722

- Fuhrman JA (1999) Marine viruses and their biogeochemical and ecological effects. *Nature* 399:541–548
- Fukuda H, Sohrin R, Nagata T, Koike I (2007) Size distribution and biomass of nanoflagellates in meso- and bathypelagic layers of the subarctic Pacific. *Aquat Microb Ecol* 46:203–207
- Gardner WD (2000) Sediment trap sampling in surface waters. In: Hanson RB, Ducklow HW, Field JG (eds) *The changing ocean carbon cycle: a midterm synthesis of the Joint Global Ocean Flux Study*. Cambridge University Press, Cambridge, p 240–281
- Gaul W, Antia A, Koeve W (1999) Microzooplankton grazing and nitrogen supply of phytoplankton growth in the temperate and subtropical northeast Atlantic. *Mar Ecol Prog Ser* 189:93–104
- Glover HE (1980) Assimilation numbers in cultures of marine phytoplankton. *J Plankton Res* 2:69–79
- González HE, González S, Brummer GJ (1994) Short-term sedimentation pattern of zooplankton, faeces and microplankton at a permanent station in the Bjørnafjorden (Norway) during April-May 1992. *Mar Ecol Prog Ser* 105:31–45
- González N, Anadón R, Marañón E (2002) Large-scale variability of planktonic net community metabolism in the Atlantic Ocean: importance of temporal changes in oligotrophic subtropical waters. *Mar Ecol Prog Ser* 233:21–30
- Gosselin M, Levasseur M, Wheeler PA, Horner RA, Booth BC (1997) New measurements of phytoplankton and ice algal production in the Arctic Ocean. *Deep-Sea Res II* 44:1623–1644
- Gruber N, Keeling CD, Bates NR (2002) Interannual variability in the North Atlantic Ocean carbon sink. *Science* 298:2374–2378
- Hansell DA (2002) DOC in the global ocean carbon cycle. In: Hansell DA, Carlson CA (eds) *Biogeochemistry of marine dissolved organic matter*. Academic Press, New York, p 685–715
- Hansell DA, Carlson CA (2001) Marine dissolved organic matter and the carbon cycle. *Oceanography* 14:41–49
- Harrison WG, Head EJH, Horne EPW, Irwin B, Li WKW, Longhurst AR, Paranjape MA, Platt T (1993) The Western North Atlantic Bloom Experiment. *Deep-Sea Res II* 40:279–305

- Herndl GJ, Reinhaler T, Teira E, Van Haken H, Veth C (2005) Contribution of archaea to total prokaryotic production in the deep Atlantic ocean. *Appl Environ Microbiol* 71:2303–2309
- Herring P (2002) Seeing in the dark. In: Crawley MJ, Little C, Southwood TRE, Ulfstrand S (eds) *Biology of habitats - The biology of the deep ocean*. Oxford University Press, Oxford, New York, p 161–187
- Hillebrand H, Dürselen C-D, Kirschtel D, Pollinger U, Zohary T (1999) Biovolume calculation for pelagic and benthic microalgae. *J Phycol* 35:403–424
- Honjo S (1996) Fluxes of particles to the interior of the open oceans. In: Ittekkot V, Shhäfer P, Honjo S, Depetris PJ (eds) *Particle flux in the ocean*. Wiley & Sons, Chichester, p 91–145
- Honjo S (1997) Marine snow and fecal pellets : The spring rain of food to the abyss. *Oceanus* 40:2–3
- Honjo S, Manganini SJ (1993) Annual biogenic particle fluxes to the interior of the North Atlantic Ocean; studied at 34°N 21°W and 48° N 21°W. *Deep-Sea Res II* 40:587–607
- IPCC-Intergovernmental Panel on Climate Change (2001) Climate change 2001-synthesis report: contribution of working groups I, II and III to the third assessment report of the Intergovernmental Panel on Climate Change. Cambridge University Press, Cambridge, 397 p
- IPCC-Intergovernmental Panel on Climate Change (2007) Summary for policymakers: contribution of working group I to the fourth assessment report of the Intergovernmental Panel on Climate Change, 18 p [En ligne: <http://ipcc-wg1.ucar.edu/wg1/wg1-report.html>, pages consultées le 04 mai 2007]
- Irigoién X, Harris RP, Verheyen HM, Joly P, Runge J, Starr M, Pond D, Campbell R, Shreeve R, Ward P, Smith AN, Dam HG, Peterson W, Tirelli V, Koski M, Smith T, Harbour D, Davidson R (2002) Copepod hatching success in marine ecosystems with high diatom concentrations. *Nature* 419:387–389
- Joint I, Pomroy A, Savidge G, Boyd P (1993) Size fractionated primary productivity in the northeast Atlantic in May June 1989. *Deep Sea Res II* 40:423–440
- Joint I, Wollast R, Chou L, Batten S, Elskens M, Edwards E, Hirst A, Burkhill P, Grooma S, Gibb S, Miller A, Hydes D, Dehairs F, Antia A, Barlow R, Rees A, Pomroy A, Brockmann U, Cummings D, Lampitt R, Loijens M, Mantoura F, Miller P, Raabeg T, Alvarez-Salgadoa X, Stelfox C, Woolfenden J (2001) Pelagic production at the Celtic Sea shelf break. *Deep Sea Res II* 48:3049–3081

- Kähler P, Bauerfeind E (2001) Organic particles in a shallow sediment trap: Substantial loss to the dissolved phase. *Limnol Oceanogr* 46:719–723
- Kähler P, Koeve W (2001) Marine dissolved organic matter: can its C:N ratio explain carbon overconsumption? *Deep-Sea Res I* 48:49–62
- Karayanni H, Christaki U, Van Wambeke F, Denis M, Moutin T (2005) Influence of ciliated protozoa and heterotrophic nanoflagellates on the fate of primary production in the northeast Atlantic Ocean. *J Geophys Res* 110:10.1029/2004JC002602
- Karl DM, Bates NR, Emerson S, Harrison PJ, Jeandel C, Llinás O, Liu K-K, Marty J-C, Michaels AF, Miquel JC, Nueur S, Nojiri Y, Wong CS (2003) Temporal studies of biogeochemical processes determined from ocean time-series observations during the JGOFS era. In: Fasham M.J.R (ed) *Ocean Biogeochemistry: The role of the ocean carbon cycle in global change*. Global Change-The IGBP series, Springer-Verlag, Berlin, p 239–267
- Kiørboe T, Tiselius P, Mitchell-Innes B, Hansen JLS, Visser AW, Mari X (1998) Intensive aggregate formation with low vertical flux during an upwelling-induced diatom bloom. *Limnol Oceanogr* 43:104–116
- Klaas C, Archer DE (2002) Association of sinking organic matter with various types of mineral ballast in the deep sea: Implications for the rain ratio. *Global Biogeochem Cycles* 16, doi:10.1029/2001GB001765
- Kleppel GS (1993) On the feeding behaviour of calanoid copepods. *Mar Ecol Prog Ser* 99:183–195
- Knap A, Michaels A, Close A, Ducklow H, Dickson A (1996) Protocols for the Joint Global Ocean Flux Study (JGOFS) Core Measurements. JGOFS Report Nr. 19, vi+170 pp. Reprint of the IOC Manuals and Guides No. 29, UNESCO 1994
- Knauer G, Asper V (1989) Sediment trap technology and sampling: report of the U.S. GOFS working group. U.S. GOFS Planning Report 10, 94 p
- Koeve W, Ducklow HW (2001) JGOFS synthesis and modeling: the North Atlantic Ocean. *Deep-Sea Res II* 48:2141–2154
- Körtzinger A, Koeve W, Kähler P, Mintrop L (2001) C:N ratios in the mixed layer during the productive season in the northeast Atlantic Ocean. *Deep-Sea Res I* 48:661–688
- Kudo I (2003) Change in the uptake and cellular Si:N ratio in diatoms responding to the ambient Si:N ratio and growth phase. *Mar Biol* 143:39–46

- Lancelot C, Billen G (1984) Activity of heterotrophic bacteria and its coupling to primary production during the spring phytoplankton bloom in the southern bight of the North Sea. *Limnol Oceanogr* 29:721–730
- Lean DRS, Burnison BK (1979) An evaluation of errors in the ^{14}C method of primary measurement. *Limnol Oceanogr* 24:917–928
- Leblanc K, Leynaert A, Fernandez C, Rimmelin P, Moutin T, Raimbault P, Ras J, Quéguiner B (2005) A seasonal study of diatom dynamics in the North Atlantic during the POMME experiment (2001): Evidence for Si limitation of the spring bloom. *J Geophys Res* 110, C07S14, doi:10.1029/2004JC002621
- Lee C (2004) Transformations in the “Twilight Zone” and beyond. *Mar Chem* 92:87–90
- Legendre L (1990) The significance of microalgal blooms for fisheries and for the export of particulate organic carbon in the oceans. *J Plankton Res* 12:681–699
- Legendre L, Gosselin M (1989) New production and export of organic matter to the deep ocean: Consequences of some recent discoveries. *Limnol Oceanogr* 34:1374–1380
- Legendre L, Le Fèvre J (1989) Hydrodynamical singularities as controls of recycled versus export production in oceans. In: Berger, WH, Smetacek, VS, Wefer G (eds) *Productivity of the ocean: present and past*. John Wiley and Sons, New York, p 49–63
- Legendre L, Le Fèvre J (1995) Microbial food webs and the export of biogenic carbon in oceans. *Aquat Microb Ecol* 9:69–77
- Legendre L, Rassoulzadegan F (1996) Food-web export of biogenic carbon in oceans: hydrodynamic control. *Mar Ecol Prog Ser* 145:179–193
- Legendre L, Rivkin RB (2002) Fluxes of carbon in the upper ocean: regulation by food web control nodes. *Mar Ecol Prog Ser* 242:95–109
- Legendre L, Rivkin RB (2005) Integrating functional diversity, food web processes, and biogeochemical carbon fluxes into a conceptual approach for modelling the upper ocean in a high- CO_2 world. *J Geophys Res* 110:10.1029/2004JC002530
- Legendre L, Demers S, Yentsch CM, Yentsch CS (1983) The ^{14}C method: patterns of dark CO_2 fixation and DCMU correction to replace the dark bottle. *Limnol Oceanogr* 28:996–1003
- Lenz J (1977) On detritus as a food source for pelagic filter-feeders. *Mar Biol* 41:39–48

- Levitus S, Antonov JI, Boyer TP, Stephens C (2000) Warming of the world ocean. *Science* 287:2225–2229
- Li WKW, Irwin BD, Dickie PM (1993) Dark fixation of ^{14}C : variations related to biomass and productivity of phytoplankton and bacteria. *Limnol Oceanogr* 38:483–494.
- Li WKW, Dickie PM, Harrison WG, Irwin BD (1993) Biomass and production of bacteria and phytoplankton during the spring bloom in the western North Atlantic Ocean. *Deep Sea Res II* 40:307–327
- Liebig J (1940) Chemistry in its application to agriculture and physiology. Taylor and Walton, London
- Lochte K, Ducklow HW, Fasham MJR, Stienen C (1993) Plankton succession and carbon cycling at 47°N 20°W during the JGOFS North Atlantic Bloom Experiment. *Deep-Sea Res II* 40:91–114
- Lohrenz SE, Redalje DG, Verity PG, Flagg CN, Matulewski KV (2002) Primary production on the continental shelf off Cape Hatteras, North Carolina. *Deep-Sea Res II* 49:4479–4509
- Longhurst AR (1991) Role of the marine biosphere in the global carbon cycle. *Limnol Oceanogr* 36:1507–1526
- Longhurst AR, Harrison WG (1989) The biological pump: profiles of plankton production and consumption in the upper ocean. *Prog Oceanogr* 22:47–123
- Lorbacher K, Dommelget D, Niiler PP, Köhl A (2006) Ocean mixed layer depth: a subsurface proxy of ocean-atmosphere variability. *J Geophys Res* 111:10.1029/2003JC002157
- Lorenzen, CJ (1968) Carbon/Chlorophyll relationships in an upwelling area. *Limnol Oceanogr* 13:202–204
- Lorenzen CJ, Welschmeyer NA (1983) The in situ sinking rates of herbivore fecal pellets. *J Plankton Res* 5:929–933
- Lund JWG, Kipling C, Le Cren ED (1958) The inverted microscope method of estimating algal numbers and the statistical analysis of estimations by counting. *Hydrobiologia* 11:143–170
- Mague TH, Friberg E, Hughes DJ, Morris I (1980) Extracellular release of carbon by marine phytoplankton; a physiological approach. *Limnol Oceanogr* 25:262–279

- Mann KH, Lazier JRN (1996) Dynamics of marine ecosystems: biological-physical interactions in the oceans, 2nd ed. Blackwell Science, Oxford, 394 p
- Mann ME, Jones PD (2003) Global surface temperature over the past two millennia. *Geophys Res Lett*, 30, 1820, doi:10.1029/2003GL017814
- Margalef R (1958) Temporal succession and spatial heterogeneity in phytoplankton. In: Buzzati-Traverso AA (ed) Perspective in marine biology. University of California Press, Berkeley & Los Angeles, p 323–349
- Margalef R (1997) Our biosphere. In: Kinne O (ed) Excellence in ecology 10. Ecology Institute, Oldendorf/Luhe, Germany, 176 p
- Marti O, Braconnot P, Bellier JHG, Benshila R, Bony S, Brockmann P, Cadule P, Knaueer A, Caubel A, Denvil S, Dufresne JL, Fairhead L, Filliberti MA, Foujols M-A, Fichefet T, Friedlingstein P, Goose H, Grandpeix JY, Hourdin F, Krinner G, Lévy C, Madec G, Musat I, deNoblet N, Plocher J, Talandier C (2005) The new IPSL climate system model: IPSL-CM4. Note du pôle de modélisation, 26, ISPL, Paris, France, ISSN 1288–1619
- Martin JH, Knauer GA, Karl DM, Broenkow WW (1987) VERTEX: carbon cycling in the northeast Pacific. *Deep-Sea Res* 34:267–285
- McCarthy JJ (1972) The uptake of urea by natural populations of marine phytoplankton. *Limnol Oceanogr* 17:738–748
- Menden-Deuer S, Lessard E (2000) Carbon to volume relationships for dinoflagellates, diatoms, and other protist plankton. *Limnol Oceanogr* 45:568–579
- Michaels AF, Karl DM, Capone DG (2001) Element stoichiometry, new production and nitrogen fixation. *Oceanography* 14:68–77
- Michel C, Gosselin M, Nozais C (2002) Preferential sinking export of biogenic silica during the spring and summer in the North Water Polynya (northern Baffin Bay): temperature or biological control? *J Geophys Res C* 107:10.1029/2000JC000408
- Mills MM, Ridame C, Davey M, La Roche J, Geider RJ (2004) Iron and phosphorus co-limit nitrogen fixation in the eastern tropical North Atlantic. *Nature* 429:292–294
- Møller EF, Thor P, Nielsen TG (2003) Production of DOC by *Calanus finmarchicus*, *C. glacialis* and *C. hyperboreus* through sloppy feeding and leakage from fecal pellets. *Mar Ecol Prog Ser* 262:185–191

- Mopper K, Kieber DJ (2000) Marine photochemistry and its impact on carbon cycling. In: de Mora S, Demers S, Vernet M (eds) *The effects of UV radiation in the marine environment*, Cambridge Environmental Chemistry Series 10, Cambridge University Press, Cambridge, p 101–129
- Mopper K, Zhou X, Kieber RJ, Kieber DJ, Sikorski RJ, Jones RD (1991) Photochemical degradation of dissolved organic carbon and its impact on the oceanic carbon cycle. *Nature* 353:60–62
- Morales C (1999) Carbon and nitrogen fluxes in the oceans: the contribution by zooplankton migrants to active transport in the North Atlantic during the Joint Global Ocean Flux Study. *J Plankton Res* 21:1799–1808
- Nagata T (2000) Production mechanisms of dissolved organic matter. In: Kirchman DL (ed) *Microbial ecology of the oceans*. John Wiley & Sons, New York, p 121–152
- Nelson DM, Tréguer P, Brzezinski MA, Leynaert A, Quéguiner B (1995) Production and dissolution of biogenic silica in the ocean: revised global estimates, comparison with regional data and relationship to biogenic sedimentation. *Global Biogeochem Cycles* 9:359–372
- Ohman MD, Runge JA (1994) Sustained fecundity when phytoplankton resources are in short supply - omnivory by *Calanus finmarchicus* in the Gulf of St. Lawrence. *Limnol Oceanogr* 39:21–36.
- Pace ML, Knauer GA, Karl DM, Martin JH (1987) Primary production, new production and vertical flux in the eastern Pacific Ocean. *Nature* 325:803–804
- Paerl HW (1985) Enhancement of marine primary production by nitrogen-enriched acid rain. *Nature* 315:747–749
- Parsons TR, Lalli CM (1988) Comparative oceanic ecology of the plankton communities of the subarctic Atlantic and Pacific oceans. *Oceanogr Mar Biol Annu Rev* 26:317–359
- Parsons TR, Maita Y, Lalli CM (1984) *A manual of chemical and biological methods for seawater analysis*. Pergamon Press, Toronto, 173 p
- Passow U (2002) Transparent exopolymer particles (TEP) in aquatic environments. *Prog Oceanogr* 55:287–333
- Passow U, Shipe RF, Murray A, Pak DK, Brzezinski MA, Alldredge AL (2001) The origin of transparent exopolymer particles (TEP) and their role in the sedimentation of particulate organic matter. *Cont Shelf Res* 21:327–346

- Petit JR, Jouzel J, Raynaud D, Barkov NI, Barnola J-M, Basile I, Bender M, Chappellaz J, Davis M, Delaygue G, Delmotte M, Kotlyakov VM, Legrand M, Lipenkov VY, Lorius C, Pépin L, Ritz C, Saltzman E, Stievenard M (1999) Climate and atmospheric history of the past 420,000 years from the Vostok ice core, Antarctica. *Nature* 399:429–436
- Platt T, Sathyendranath S, Ulloa O, Harrison WG, Hoepffner N, Goes J (1992) Nutrient control of phytoplankton photosynthesis in the Western North Atlantic. *Nature* 356:229–231
- Pommier J, Gosselin M, Michel C (ms-a) Size-fractionnated phytoplankton production and biomass during the decline of the Northwest Atlantic spring bloom. Submitted to Mar Ecol Prog Ser
- Pommier J, Michel C, Gosselin M (ms-b) Particulate organic carbon export in the upper twilight zone of the Northwest Atlantic Ocean during the decline of the spring bloom. Submitted to Mar Ecol Prog Ser
- Prézelin BB (1981) Light reactions in photosynthesis. In: Platt T (ed) Physiological bases of phytoplankton ecology. Can Bull Fish. Aquat Sci 210:1–43
- Primeau F (2006) On the variability of the exponent in the power law depth dependence of POC flux estimated from sediment traps. *Deep-Sea Res I* 53:1335–1343
- Prospero JM, Barrett K, Church T, Dentener F, Duce RA, Galloway JN, Levy II H, Moody J, Quinn P 91996) Atmospheric deposition of nutrient to the North Atlantic Basin. *Biogeochemistry* 35:27–73
- Raven JA, Falkowski PG (1999) Oceanic sinks for atmospheric CO₂. *Plant Cell Environ* 22:741–755
- Redfield AC, Ketchum BH, Richards FA (1963) The influence of organisms on the composition of seawater. In: Hill M.N. (ed) The sea: ideas and observations on progress in the study of the seas. Interscience, John Wiley and Sons, New-York, p 26–77
- Reigstad M, Wexels Risser C, Svensen C (2005) Fate of copepod faecal pellets and the role of *Oithona* spp. *Mar Ecol Prog Ser* 304:265–270
- Reinthalter T, van Aken H, Veth C, Arístegui J, Robinson C, le B. Williams PJ, Lebaron P, Herndl GJ (2006) Prokaryotic respiration and production in the meso- and bathypelagic realm of the eastern and western North Atlantic basin. *Limnol Oceanogr* 51:1262–1273

- Riley GA, Stommel H, Bumpus DF (1949) Quantitative ecology of the plankton of the Western North Atlantic. Bull Bingham Oceanogr Collect 12:1–169
- Rivkin R, Legendre L (2001) Biogenic carbon cycling in the upper ocean: Effects of microbial respiration. Science 291:2398–2400
- Roux R, Gosselin M, Desrosiers G, Nozais C (2002) Effects of reduced UV radiation on a microbenthic community during a microcosm experiment. Mar Ecol Prog Ser 225:29–43
- Sarmiento JL, Gruber N (2002) Sinks for anthropogenic carbon. Physics Today 55:30–36
- Sarmiento JL, Gruber N (2006) Ocean biogeochemical dynamics. Princeton University Press, Princeton, 503 p
- Sarmiento JL, Dunne J, Armstrong RA (2004) Do we now understand the ocean's biological pump? U.S. JGOFS News 12:1–5
- Sarmiento JL, Monfray P, Maier-Reimer E, Aumont O, Murnane RJ, Orr JC (2000) Sea-air CO₂ fluxes and carbon transport: a comparison of three ocean general circulation models. Global Biogeochem Cycles 14:1267–1281
- Sastri AR, Dower JF (2006) Mesozooplankton community response during the SERIES iron enrichment experiment in the subarctic NE Pacific. Deep-Sea Res II 53:2268–2280
- Sathyendranath S, Longhurst A, Caverhill CM, Platt T (1995) Regionally and seasonally differentiated primary production in the North Atlantic. Deep-Sea Res I 42:1773–1802
- Sherr EB (1988) Direct use of high molecular weight polysaccharide by heterotrophic flagellates. Nature 335:348–351
- Siegenthaler U, Sarmiento JL (1993) Atmospheric carbon dioxide and the ocean. Nature 365:119–125
- Sieracki ME, Verity PG, Stoecker D (1993) Plankton community response to sequential silicate and nitrate depletion during the 1989 North Atlantic spring bloom. Deep-Sea Res II 40:213–225
- Smayda TJ (1970) The suspension and sinking of phytoplankton in the sea. Oceanogr Mar Biol Annu Rev 8:353–414

- Smayda TJ (2002) Turbulence, watermass stratification and harmful algal blooms: an alternative view and frontal zones as “pelagic seed banks”. *Harmful Algae* 1:95–112
- Smetacek V, Passow U (1990) Spring bloom initiation and Sverdrup’s critical-depth model. *Limnol Oceanogr* 35 :228–234
- Sokal RR, Rohlf FJ (1995) Biometry: the principles and practice of statistics in biological research, 3rd ed. Freeman WH, New York, 887 p
- Solórzano L (1969) Determination of ammonia in natural waters by the phenolhypochlorite method. *Limnol Oceanogr* 14:799–801
- Suess E (1980) Particulate organic carbon flux in the oceans—surface productivity and oxygen utilization. *Nature* 288:260–263
- Shuttle CA (2005) Viruses in the sea. *Nature* 437:356–361
- Sverdrup HU (1953) On conditions for the vernal blooming of phytoplankton. *J Cons Int Explor Mer* 18:287–295
- Takahashi T (1989) The carbon dioxide puzzle. *Oceanus* 32:22–29
- Tanaka T, Rassoulzadegan F, Thingstad TF (2005) Analyzing the trophic link between the mesopelagic microbial loop and zooplankton from observed depth profiles of bacteria and protozoa. *Biogeosciences* 2:9–13
- Tans PP, Fung IY, Takahashi T (1990) Observational constraints on the global atmospheric CO₂ budget. *Science* 247:1431–1438
- Thronsdæsen J (1978) Preservation and storage. In: Sournia A (ed) *Phytoplankton manual*. UNESCO, Paris, p 69–74
- Tranvik LJ, Sherr EB, Sherr BF (1993) Uptake and utilization of ‘colloidal DOM’ by heterotrophic flagellates in seawater. *Mar Ecol Prog Ser* 92:301–309
- Tréguer P, Nelson DM, Van Bennekom AJ, DeMaster DJ, Leynaert A, Quéguiner B (1995) The silica balance in the world ocean: a reestimate. *Science* 268:375–379
- Tréguer P, Legendre L, Rivkin RB, Ragueneau O, Dittert N (2003) Water column biogeochemistry below the euphotic zone. In: Fasham MJR (ed) *Ocean biogeochemistry: The role of the ocean carbon cycle in global change*. Global Change-The IGBP series, Springer-Verlag, Berlin, p 145–156

- Tremblay J-É, Legendre L (1994) A model for the size fractionated biomass and production of marine phytoplankton. Limnol Oceanogr 39:2004–2014
- Tremblay J-É, Klein B, Legendre L, Rivkin RB, Therriault J-C (1997) Estimation of *f*-ratios in the oceans based on phytoplankton size structure. Limnol Oceanogr 42:595–601
- Tremblay J-É, Hattori H, Michel C, Ringuette M, Mei Z-P, Lovejoy C, Fortier L, Hobson KA, Amiel D, Cochran K (2006) Trophic structure and pathways of biogenic carbon flow in the eastern North Water Polynya. Progr Oceanogr 71:402–425
- Turner JF (2002) Zooplankton fecal pellets, marine snow and sinking phytoplankton blooms. Aquat Microb Ecol 27:57–102
- Urban JL, Deibel D, Schwinghamer P (1993) Seasonal variations in the densities of fecal pellets produced by *Oikopleura vanhoeffeni* (C. Larvacea) and *Calanus finmarchicus* (C. Copepoda). Mar Biol 117:607–613
- Utermöhl von H (1931) Neue Wege in der quantitativen Erfassung des Planktons (Mit besondere Berücksichtigung des Ultraplanktons). Verh Int Verein Theor Angew Limnol 5:567–595
- Valiela I (1995) The carbon cycle: production and transformations of organic matter. In: Valiela I (ed) Marine ecological processes, 2nd ed. Springer-Verlag, New York, p 385–423
- Varela MM, Bode A, Fernández E, Gonzales N, Kitidis V, Varela M, Woodward EMS (2005) Nitrogen uptake and dissolved organic nitrogen release in planktonic communities characterised by phytoplankton size structure in the Central Atlantic Ocean. Deep Sea Res I 52:1637–1661
- Vodacek A, Blough NV, DeGrandpre MD, Peltzer ET, Nelson RK (1997) Seasonal variation of CDOM and DOC in the Middle Atlantic Bight: Terrestrial inputs and photooxidation. Limnol Oceanogr 42:674–686
- Volk T, Hoffert MI (1985) Ocean carbon pumps: analysis of relative strengths and efficiencies in ocean-driven circulation atmospheric CO₂ changes. In: Sundquist ET, Broecker WS (eds) The carbon cycle and atmospheric CO₂: natural variations archean to present. AGU monograph 32, American Geophysical Union, Washington DC, p 99–110
- Ward BB (2000) Nitrification and the marine nitrogen cycle. In: Kirchman DL (ed) Microbial ecology of the oceans. Wiley-Liss, New York, p 427–453

- Ward BB, Kilpatrick KA, Renger EH, Eppley RW (1989) Biological nitrogen cycling at the nitracline. *Limnol Oceanogr* 34:493–513
- Warrant E (2000) The eyes of deep-sea fishes and the changing nature of visual scenes with depth. *Philos Trans R Soc Lond B* 355:1155–1159
- Wassmann P (1990) Relationship between primary and export production in the boreal coastal zone of the North Atlantic. *Limnol Oceanogr* 35:464–471
- Wassmann P (1998) Retention versus export food chains: processes controlling sinking loss from marine pelagic systems. *Hydrobiologia* 363:29–57
- Watson AJ, Orr JC (2003) Carbon dioxide fluxes in the global ocean. In: Fasham MJR (ed) *Ocean biogeochemistry: The role of the ocean carbon cycle in global change. Global Change-The IGBP series*, Springer-Verlag, Berlin, p 123–143
- Wefer G (1989) Particle flux in the ocean: effects of episodic production. In: Berger WH, Smetacek VS, Wefer G (eds) *Productivity in the ocean: present and past*. John Wiley and Sons, New York, p 139–154
- Whitehead RF, de Mora S, Demers S, Gosselin M, Monfort P, Mostajir B (2000) Interactions of ultraviolet-B radiation, mixing, and biological activity on photobleaching of natural chromophoric dissolved organic matter: a mesocosm study. *Limnol Oceanogr* 45:278–291
- Wilhelm SW, Suttle CA (1999) Virus and nutrient cycles in the sea – Viruses play critical roles in the structure and function of aquatic food webs. *Biogeoscience* 49:781–788
- Williams PJ le B (1998) The balance of plankton respiration and photosynthesis in the open oceans. *Nature* 394:55–57
- Williams PJ le B (2000) Heterotrophic bacteria and the dynamics of dissolved organic matter. In: Kirchman DL (ed) *Microbial ecology of the oceans*. John Wiley & Sons, New York, p 153–200
- Williams PJ le B, Bowers DG (1999) Regional carbon imbalances in the oceans. *Science* 284:1735b
- Zehr JP, Ward BB (2002) Nitrogen cycling in the ocean: New perspectives on processes and paradigms. *Appl Env Microbiol* 68:1015–1024